Characterising *Plasmodium falciparum* cyclin dependent like kinase 1 (P*f*CLK1) as a potential antimalarial target

OLANIYAN NINIOLA

BSc, MSc

Submitted in fulfilment of the requirements for the Degree of

Doctor of Philosophy

School of Molecular Biosciences

College of Medical, Veterinary & Life Sciences

University of Glasgow

August 2024

Abstract

The widespread and indiscriminate use of antimalarial drugs has contributed to recurring parasite resistance that threatens a global resurgence of malaria with increasing morbidity and mortality rate towards the verge of endemicity. The dual specificity protein kinase family, CLKs, play crucial roles in the regulation of transcript splicing by phosphorylating SR proteins. Global phospho-proteomic studies of the *Plasmodium* kinome have shown such splicing events to be an essential process across developmental stages of the parasite life cycle. Thus, members of the CLK family have been considered as potential therapeutic targets in present antimalarial drug development pipelines for new molecules which demonstrate the required efficacy and selective toxicity to the parasite without the propensity to induce parasite resistance. A member kinase P*f*CLK3 was validated as a cross species multistage drug target in a previous study by our group using a selective and specific small drug like inhibitor TCMDC-135051. However, to achieve poly-pharmacology or develop drugs for combination therapy as an approach to circumvent potential drug resistance, a second target P*f*CLK1 with similar therapeutic potential was identified. This thesis aimed to extend the previous study by characterising potent selective inhibitors for P*f*CLK1 and explore the role of the kinase in *Plasmodium falciparum*. The primary screen at GlaxoSmithKline from the previous study yielded four distinct chemical series of small molecule inhibitors with specific nanomolar activity towards P*f*CLK1. In this study, two potent members JZ208105-178D1 and HGC-0017530023-NX-1 were further characterised through enzymatic and cellular analyses to investigate their mode of inhibition and determine their interaction with the target kinase.

First, the enzymatic parameters of the biochemical assays were determined using recombinant P*f*CLK3 and kinase domain P*f*CLK1 proteins. In addition, a robust assay measuring ATP consumption was developed that proved suitable for high throughput screening. Substrates that were recognised and efficiently phosphorylated by both kinases were identified and used to establish optimal concentrations of protein and ATP for inhibition assay conditions. Second, a detailed analysis of the inhibition mechanism, target specificity, timing of peak activity during life cycle and the rate of parasite reduction was completed to identify the most potent inhibitor that could be optimised to the status of lead

compound through further *in vitro* and *in vivo* studies. *In vitro* inhibition results showed that both compounds displayed low nanomolar inhibition of kinase domain P*f*CLK1 and further demonstrated selective inhibition towards P*f*CLK3 suggestive of an affinity for the highly conserved domain between both kinases. Additionally, JZ208105-178D1 demonstrated a mode of binding suggestive of ATP competitive inhibition, in contrast to the non-ATP competitive inhibition observed for HGC-0017530023-NX-1. Both inhibitors emerged effective at high nanomolar to low micromolar concentrations against asexual blood stages of *P. falciparum* 3D7 wild type. For chemical validation, a P*f*CLK1-like P*f*CLK3 mutant parasite, G449P demonstrated the same sensitivity as wild type parasites to both inhibitors suggesting P*f*CLK1 inhibition is linked to their parasitical activity.

Susceptibility profiling of *P. falciparum* 3D7 asexual blood stages to both inhibitors revealed a variety of stage-specific profiles that differentiated the modes of action including TCMDC-135051 and identified trophozoite-specific peak activity for JZ208105-178D1 and TCMDC-135051. Given that JZ208105-178D1 conferred higher inhibitory effect *in vitro* and *in vivo*, further investigations were carried without HGC-0017530023-NX-1. The morphological analysis of asexual blood stages following treatment with JZ208105-178D1 confirmed that parasite development was completely arrested at the early trophozoite stage. This contrasted with the progression of untreated parasites to late trophozoites at comparable time points. In addition, JZ208105-178D1 impaired the maturation of *P. falciparum* NF54 gametocytes, stages responsible for transmission, by an ~11-fold reduction in gametocyte number at 1x EC_{50} concentration.

The parasite reduction rate assay was used to quantify the speed of therapeutic capacity, JZ208105-178D1 demonstrated activity levels similarly to TCMDC-135051 and standard antimalarial artemisinin. The combined data in this study suggests the malaria parasite's response to JZ208105-178D1 inhibition are P*f*CLK1 dependent and corroborate previous functional characterisation studies relating to P*f*CLK1 expression in the parasites. Thus, pointing to the P*f*CLK1 kinase as a promising target for antimalarial and transmission blocking chemotherapy strategies.

Table of Contents

List of Tables

List of Figures

List of Publications

Brettell S, Janha O, Begen A, Cann G, Sharma S, **Olaniyan N**, et al.Targeting P*f*CLK3 with Covalent Inhibitors: A Novel Strategy for Malaria Treatment. J Med Chem.2024 Nov 14;67(21):18895-18910. doi:10.1021/acs.jmedchem.4c01300.Epub 2024 Oct 23.

Omar Janha, **Niniola Olaniyan**, Andrew G. Jamieson, Dario Beraldi, Andrew B. Tobin, and Katarzyna Modrzynska. Inhibition of *Pf*CLK3 directly affects RNA splicing and influence the splicing machinery.2024 (Unpublished).

Acknowledgements

I am finally here! It took a whole village, and I am beyond fortunate I did not have to get through this journey without them.

Firstly, I would like to thank God for giving me life, strength, and fast recovery to good health particularly in the last months of my PhD. The warmest thank you goes to my parents Olayiwole Olaniyan, Omolara Olaniyan and brother Temiloluwa Olaniyan for their unwavering support in all my academic and personal endeavours up to and including this PhD; Ọpẹ́ olóore, àdáàdátán ni.

I would like to express my deepest and sincerest gratitude to my supervisory team; Professors Andrew Tobin, Matthias Marti and Dr Omar Janha. My experience under your invaluable guidance during this PhD programme has shaped and defined not only my growth as a scientist but also my personal development. It was a wonderful opportunity to have learnt from such outstanding scientists. Special thanks to Dr Gonzalo who under no official obligation, kept me grounded as a mentor, friend and kept me fed at work! To the rest of the Tobin lab and CTP, thank you for lending your expertise whenever I needed it.

I consider myself very fortunate to have gained a community of people during this journey. In particular Jose, Eloise, Miriam, Woroud, Lola, Arvin, Marwa and Wandiahyel for your warm embrace and consistent support when I felt at my lowest, you are forever a part of the best experiences of the start of my life in Glasgow. Lastly, a huge thank you goes to my friends from home Ugonnaya, Yewande, Idokua, Damilare - who remained my biggest cheerleaders despite 2900 miles of physical distance – thank you for never not believing in and always encouraging me.

Author's Declaration

"I declare that, except where explicit reference is made to the contribution of others, this thesis is the result of my own work and has not been submitted for any

other degree at the University of Glasgow or any other institution."

Olaniyan Niniola

August 2024

Definitions/Abbreviations

ACT	Artemisinin combination therapy
AMA1	Apical membrane antigen 1
ANOVA	Analysis of variance
AS	Alternative splicing
BSA	Bovine serum albumin
BTO	Benzothiazinone
BPS	Branch point sequence
CDK	Cylin-dependent protein kinase
CDPK1	Calcium dependent protein kinase 1
cDNA	Complementary DNA
CK1	Casein Kinase 1
CLK	Cyclin dependent kinase like kinases
CpCDPK1	Cryptosporidium parvum CDPK1
CO_2	Carbon dioxide
CSA	Chondroitin-4- sulphate
CSP	Circumsporozoite protein
DHFR	Dihydrofolate reductase
DHPS	Dihydropteroate synthetase
DMSO	Dimethyl sulfoxide
DNA	Deoxyribonucleic acid
DTT	1,4-dithiothreitol
DV	Digestive vacoule
DYRK	Dual-specificity tyrosine-regulated kinase
EBL	Erythrocyte binding like

EC_{50}	Concentration of drug that gives half maximal response
EDTA	Ethylenediaminetetraacetic acid
EGTA tetraacetic	Ethylene glycol-bis(ß-aminoethyl ether)- N,N,N′,N′- acid tetrasodium salt
EMP1	Erythrocyte membrane protein 1
ePK	eukaryotic protein kinase
ER	Endoplasmic reticulum
HEPES	4-(2-hydroxyethyl)-1-piperazineethanesulfonic acid)
ICAM1	Intracellular adhesion molecule 1
IC_{50}	Concentration of an inhibitor where the response is reduced by half 50% inhibition)
IPTG	Isopropyl ß-D-1-thiogalactopyranoside
IP3	Inositol 1,4,5-trisphosphate
Kb	Kilobase
$ATPK_m$	Michelis menton constant for ATP
KCl	Potassium Chloride
LB	Lauria Broth
MAPK	Mitogen activated protein kinase
MBP	Myelin Basic Protein
$MgCl_2$	Magnesium Chloride
MgSO4	Magnesium Sulphate
$NaCl_2$	Sodium Chloride
PBS	Phosphate Buffered Saline
P*f*CDPK1	*Plasmodium falciparum* Calcium dependent protein

	kinase 1
P*f*CLK3	*Plasmodium falciparum* cyclin dependent kinase like kinase 3
P*f*CLK1	*Plasmodium falciparum* cyclin dependent kinase like kinase 1
P*f*PKG	*Plasmodium falciparum* Protein Kinase G
PK	Protein kinase
PKA	Protein kinase A
PKC	Protein kinase C
PKG	Protein kinase G
PVM	Parasitophorous vacuole membrane
RH	Reticulocyte-binding homologue
RNA	Ribonucleic acid
RPM	Rotation per minute
RT	Room temperature
SDS	Sodium dodecyl sulphate
SDS-PAGE	Sodium dodecyl sulfate polyacrylamide gel electrophoresis
S.E.M	Standard error of the mean
SEA	South East Asia
SERA1	Serine-rich antigen 1
SF1	Splicing factor 1
snRNP	small nuclear ribonucleoprotein particles
SRPK	Serine Arginine Protein Kinases
SR-B1	Scavenger receptor type B class I
SS	Splice site

SSA	Sub-Saharan Africa
TEMED	N,N,N′,N′-Tetramethylethylenediamine (1,2 Bis(dimethylamino) ethane
TLK	Tyrosine like kinase
TR-FRET	Time-resolved fluorescence energy transfer
U2AF	U2 auxiliary factor
U*Light*-MBP	U*Light*-Myelin Basic Protein
VSA	Variant surface antigen
WHO	World Health Orginisation
WT	Wild type

Chapter 1. Introduction

1.1 Malaria History

Firm scientific understanding of malaria might have begun 140years ago, but theories of wet ground associated fevers dates to early Greeks in 600BC, spanning across 1400 years, malaria-like cases were reported in Mesopotamia clay tablets from 2000 BC, ancient Egyptian papyri from 1507 BC and Chinese documentations around 2700BC (Cox, 2010). And for over two millennia swampland miasmas were thought to be the causative agents of disease, therefore coined the word malaria from Italian mal'aria meaning “bad air” (Boualam et al., 2021). However, progressive scientific discovery of bacteria, microorganisms in relation to infectious diseases and the germ theory in the 19th century disproved the miasmas theory(Casanova & Abel, 2013), led to the first identification of malaria parasite in the blood of infected patients by French army officer Charles Louis Alphonse Laveran in 1880 (Dagen, 2020)and the subsequent vector incrimination of mosquitoes to malaria parasites by British officer Ronald Ross in 1897(Cox, 2010). The vector disease link discovery resulted in the first effectual control efforts towards malaria, from the combined use of insecticides with swamp treatment, good drainage system, widespread disease campaign during the two world wars to investments in antimalarial drug development, malaria burden was vastly suppressed through the 20th century (Tizifa et al., 2018). Notwithstanding, the highly infectious disease continues to impose a tremendous burden on global public health till present day (WHO, 2023).

1.1.1. Global Health Burden

With the exception of Antarctica, malaria's geographic prevalence in tropical and subtropical areas of the world risks half the world's population making it a huge global health issue. According to World Health Organization report 2023, 247 million global cases and 619 000 malaria deaths were reported in 2022. Endemic regions like Southeast Asia, Eastern Mediterranean Region hold the majority percentage of infected individuals with 95% of malaria cases and 96% of malaria death concentrated in Africa, 80% of total death accounted for children under the age of 5 (WHO 2023). With the dawn of the millennium, health initiatives and development strategies towards global effort to reduce overall malaria burden and achieve malaria eradication has progressed substantially. Decline trends in malaria case incidences by 40% and mortality rate by 48% since the 2000s (Figure 1.1) can be credited to the strategies outlined in preventative and control methods using insecticide beds, indoor sprays, improved diagnostic tests and development of novel malaria treatments and vaccines(Weiss et al., 2019).

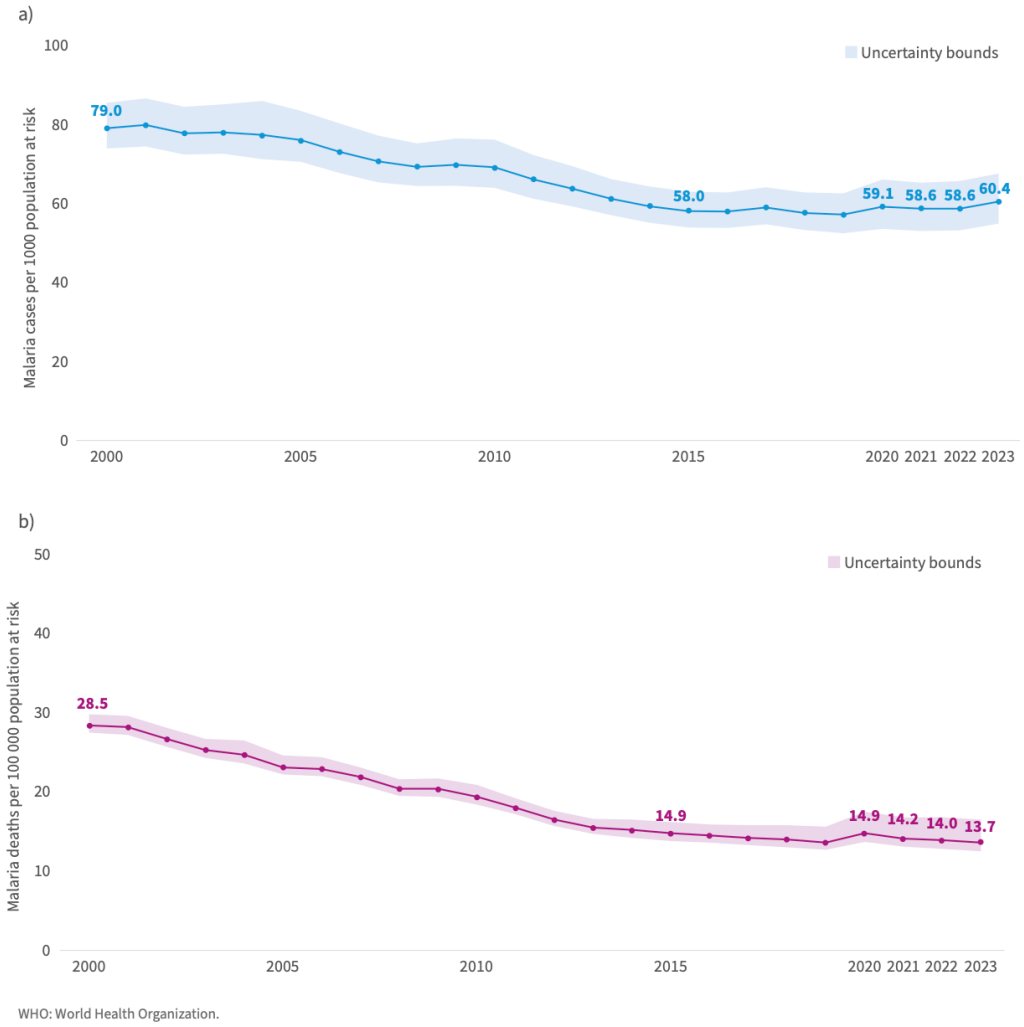

Figure 1.1 Global trends in malaria case incidence and mortality rate 2000–2023.
(A) Malaria case incidence declined 79.0 to 60.4 cases per 1000 population at risk. (B) mortality rate declined 28.5 to 13.7 deaths per 100 000 population at risk, 2000–2023. Source: WHO database (World Health Organization, 2024).

1.2 Malaria Transmission

Mosquitoes are indisputably the most medically important vectors on a global scale(Yee et al., 2022). In majority of mosquito species, females feed on vertebrate blood to obtain proteins, iron and amino acids for egg production. Feeding and reproduction occurs repeatedly every 3-4-days. This cyclic feeding behavior is exploited by *Plasmodium* for transmission between vector and host(Harrison et al., 2021). Therefore vector-borne transmission of human malaria requires the host, vector and parasite triad. Other important routes of non-entomological inoculation in humans can occur via transplacental or

peripartum congenital infection, blood transfusion, organ-tissue transplantation and needle or syringe contamination (Niederhauser & Galel, 2022).

1.2.1 Malaria vector

There are 465 species of *Anopheles* with over 50 unnamed globally recognized species complexes, approximately 70 are most relevant in human malaria transmission(Pimenta et al., 2015). Of which 41 are classified as dominant vector species/species complexes (DVS) distributed across the contemporary geographic regions (Americas (9); Africa, Europe, and Middle East (13); Asia-Pacific region (19)) with the capacity to transmit high severity malaria(van de Straat et al., 2021)(Figure 1.2). Vectoral capacity has a direct correlation to transmission intensity of human malaria. It is the quantitative cumulative influence of vector density, longevity and competence factors on vector-to-pathogen-to-host association mediated by decisive determinants like behavioural and environmental factors (Tusting et al., 2014).

The variety of unique transmission patterns with specific definitions like forest, urban, and frontier malaria mapped across the DVS biogeographical regions are a consequence of any or combinations of variable species behavioural traits such as host preferences (anthrophilic/zoophilic), feeding propensity (exophagic/endophagic) and resting habits (exophilic/endophilic) (Sinka et al., 2012). Sub-Sahara Africa (SSA) is endemic to the four most efficient and effective DVS complexes, *Anopheles gambiae*, *An.funestus* , *An.nili* and *An.moucheti* (Kyalo et al., 2017). Sibling species of the *Gambiae* complex have different host preferences, *An.gambiae* feeds on human hosts and *An.arabiensis* on animals, preferentially cattle (Mlacha et al., 2020). On the other hand, host feeding in *An.funestus* of the *funestus* complex is opportunistic, they are reported to be anthropophilic in western Senegal and zoophilic in eastern Senegal (Bouafou et al., 2024). Similarly, a prevalent member of the *Minimus* Complex in Southeast Asia (SEA), *An.minimus*, is facultatively anthropophilic/zoophilic depending on host availability. The feeding and resting habits vary across SEA, endophagy and endophilia in india, exophagy and exophilia in Cambodia, southern China, Thailand and Vietnam(Dev & Manguin, 2016). Knowledge of these behavioral variabilities can inform the effectiveness of malaria vector control strategies across geographic regions. For

example, *An.funestus* behavior characteristics makes it an ideal candidate for indoor insecticide controls like indoor residual spraying (IRS) that target indoor resting mosquitoes or long-lasting insecticide-treated nets (LLINs) that target nocturnal human indoor feeding mosquitoes as opposed to zoophilic, exophagic and exophilic *An.arabiensis* (Okumu & Finda, 2021).

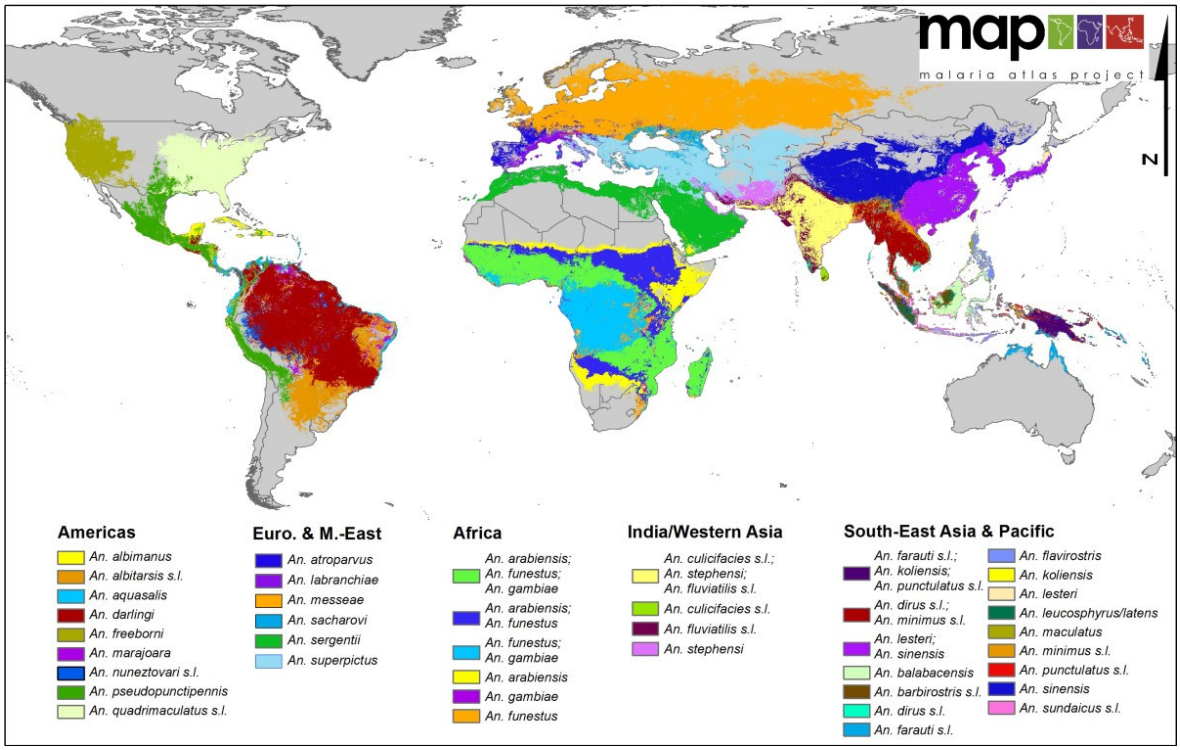

Figure 1.2 A global distribution of dominant malaria vector species (DVS).
Indicating the distribution of 34 DVS and highlights the variability in the complexity of the malaria vector species communities.(Sinka et al., 2012).

1.2.2 Malaria parasite

Single- celled, obligate intracellular tissue and blood protozoan parasites of the order hematozoa in the apicomplexa phylum, characterised by their transmission via hematophagous arthropod vectors with aquatic and aerial environment life stages are known to infect a broad diversity of vertebrate hosts(Cozzarolo et al., 2020). The most encountered human infective disease-causing genera are *Trypanosoma spp.*, *Leishmania spp.*, *Plasmodium spp.* and *microfilaria*(Seeber & Steinfelder, 2016). The most clinically significant blood parasite is the *Plasmodium* genus which produces malaria, a disease characterized by cyclical bouts of chills, fever, anaemia(Phillips et al., 2017) . There are over 200 species of *Plasmodium* out of which only five are human infecting, they include

malariae, *ovale*, *knowlesi*, the two most prevalent forms, *vivax* and *falciparum* risking infection of approximately 2.5 million people globally (Sato, 2021).

Although *P.falciparum* remains the most virulent strain causing high severity and fatality malaria incidences and deaths in endemic regions like sub-Saharan Africa where *P.vivax* infection overlaps although rarer and milder(Howes et al., 2016). However *P.vivax* malaria is globally more geographically pervasive estimating over 4 million worldwide as at 2020 with a significant proportion of incidence cases at 0.3% in Africa,36.3% in South-East Asia and 30.1% in Western Pacific (WHO, 2023). Duffy glycoproteins expressed on the surface of human red blood cells are generally believed to mediate reticulocyte invasion by *P.vivax* merozoites (Barnwell et al., 1989). Thus, Duffy blood group negativity in sub-Saharan Africa has been hypothesized as a proxy of the population's natural resistance to *vivax* malaria to explain the lower prevalence of the disease in that region. Recent molecular studies have challenged the paradigm with evidence of *P.vivax* infection in Duffy negative indigenes of sub-Saharan African countries and raised the possibility of a widely distributed alternate receptor to Duffy for *P.vivax* invasion mechanism (Bouyssou et al., 2023; Mendes et al., 2011; Ryan et al., 2006).

For decades, the lack of knowledge and neglected research on *P.vivax* pathophysiology under-represented the extent and burden of this malaria form, classifying the infectivity as "benign" in comparison to the "malignant" tertian form of *P. falciparum* (Bassat et al., 2016). Recent findings have challenged this misconception,revealing tha *vivax* malaria can be severe, life threatening and fatal, particularly in high endemic regions (WHO, 2024). The disparity between true and observed prevalence of of *P.vivax* is further explained by its distinct biological features including low parasitaemia, early gametocyte emergence, and dormant liver stages. These adaptations enable continuous survival under unconducive conditions, extending beyond the geographic restrictions of *P.falciparum* into temperate climates that are inhospitable to anopheline mosquito (Adams & Mueller, 2017; Mueller et al., 2009).

Hypnozoites are dormant liver stage forms characteristic to relapsing species like *P.vivax*, *P.ovale*, simian malaria *P.cynomolgi* , *P.fieldi*,

P.simiovale and *P.schwetzi* infections(FB Cogswell, 1992; Howes et al., 2016). Relapse periodicities differ between tropical (3-4 weeks post treatment) and temperate (circa 9 months) regions. However recurrent vivax malaria cycles are not limited to relapse by hypnozoite reactivation but can be activated by recrudescence from blood stage treatment failure or re-infection from new mosquito inoculation, all of which are un-distinguishable and uniquely complicate the biological understanding to develop control measures for vivax malaria(Flannery et al., 2022; Taylor et al., 2019).

Prior to Stephens identification as a distinct species in 1922, benign tertian form of malaria *P.ovale* was initially mis-classified as a variant of *P.vivax* based on morphological and clinical pattern fever similarities between both species. Unlike in *P.vivax*, relapse periodicity in *ovale* malaria is not controlled by Duffy-mediated blood invasion rather it occurs as a result of secondary infections generated from latent liver parasites. To circumvent the challenges of microscopic detection due to low parasite density and morphological resemblance to *P.vivax*, molecular methods were developed to differentiate *P.ovale* from other *Plasmodium* species(Gimenez et al., 2021). However, Subunit ribosomal RNA gene SSUrRNA found in PCR amplified isolates are un-detectable in other microscopically identified isolates due to dimorphism in *P.ovale* species (R. H. Miller et al., 2015). Sequence variation in other genes like the mitochondrial locus cytochrome b, cysteine encoding protease genes and the ookinete surface antigens differentiate the two distinct forms as globally prevalent and nonrecombining sympatric species, *P.ovale curtisi* and *P.ovale wallikeri*. Geographical prevalence is primarily in sub-Saharan Africa and western pacific islands, with recent migration reports to Asian mainland (Zaw & Lin, 2017).

Another causative species of benign malaria in humans is P.*malariae*, also considered to be the New World monkey infecting species, *Plasmodium brasilianum*(Sato, 2021). Italian biologist and pathologist, Camillo Golgi postulated a direct correlation between recurrent bouts of fever at approximately three days interval to the quartan multiplication cycle of schizogony and merogony in *P.malariae* lifecycle (Simoiu et al., 2023). Low parasitemia and co-infection with are commonly observed for *P.malariae*

infection contributing to the substantial underestimation and variation of species prevalence distribution in endemic regions. In addition, there is a paucity of data on malariae biology and disease burden largely attributed to challenges with using non-sensitive methods to detect *P.malariae* in wide ranging levels of blood stage infection for diagnostic and epidemiology studies(Oriero et al., 2021) .

Contrary to other human infecting *Plasmodium* species, *P. knowlesi* naturally parasitize simians, however, experimental human infections by intradermal and subcutaneous inoculation were demonstrated by Knowles and Das Gutpa(Raja et al., 2020). With human-to-human blood transfusion as a tool, the experimental discovery facilitated the brief use of *P.knowlesi* as a pyretic agent in malaria therapy to induce high fever for neurosyphilis treatment in the early 20th century(Anstey et al., 2021). On the other hand, natural human infections by *P.knowlesi* zoonosis were first reported in a US national working in Malaysia as at 1965, two years later experimental data demonstrated the transimission of *P.knowlesi* from monkey to human by *Anopheles balabacencis* (Chin et al., 1965) In 2004, an initial misdiagnosis of *P.malariae* infection by routine microscopy on the island of Borneo Malaysia was conclusively found to be prevalent *P.knowlesi* malaria by PCR amplification and DNA sequencing of ssrRNA genes and circumsporozoite protein (csp) . Characterised by quotidian cycle with high fatality the same frequency as, *P.knowlesi* is now the major cause of malaria morbidity and mortality in Malaysia (Ramasamy, 2014; B. Singh et al., 2004).

1.2.3 Malaria lifecycle

The conserved life cycle features of malaria parasites across all vertebrate infecting *Plasmodium* lineages are characterized by two phases, sporogony cycle in *Anopheles* mosquito (exogenous sexual phase) and schizogony cycle in the vertebrate host (endogenous asexual phase) (Figure 3)(Venugopal et al., 2020). The sexual cycle is concluded when a biologically suitable female anopheline ingests an infective blood meal, averagely 2-3µL that contains at least one male and female gametocyte(Sato, 2021). The ingested gametocytes then undergo the process of gametogenesis, which can take up to 15 minutes in the mosquito midgut to produce sporozoites that migrate to the salivary gland making the

mosquito infective. Facilitated by an infective mosquito bite, sporozoites are injected into the vertebrate host bloodstream and initiate the parasite's asexual cycle (Dash et al., 2022). Sporozoites in the bloodstream replicate asexually in liver cells (exo-erythrocytic schizogony) and multiplication in erythrocytes (erythrocytic schizogony). Here, merozoites invade red blood cells in a continuous cycle or differentiate into gametocytes for mosquito infection(Venugopal et al., 2020).

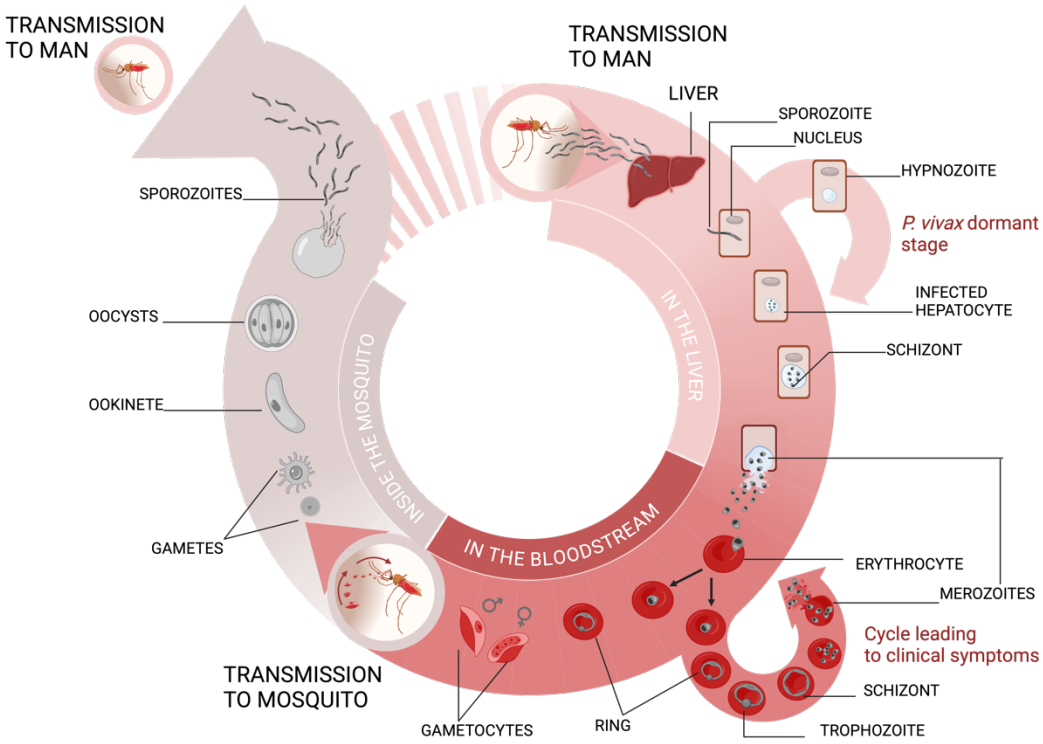

Figure 1.3 The *Plasmodium* parasite life cycle.
In the human host, malaria infection cycle begins with the injection of infective stages called sporozoites into the bloodstream by a female anopheline mosquito during a blood meal. The sporozoites migrate to the liver, invade hepatocytes and multiply asexually to form schizonts which then rupture and release erythrocyte infective merozoites that are released into bloodstream. Clinical systems develop from subsequent rounds of merozoite invasion, replication and multiplication in the blood. Some merozoites differentiate into sexual stages-gametocytes. In the mosquito gut, male and female gametocytes fuse to form a zygote. The zygote develops into an ookinete which invades the mosquito's gut wall and forms an oocyst. Inside the oocyst, sporozoites develop. Oocyst then rupture to release Mature sporozoites that migrate to the mosquito's salivary glands and are taken up on subsequent blood meal to infect another host, repeating the cycle. Created with https://biorender.com/.

1.2.3.1 Gametogenesis

Gametogenesis is an intricate process that involves cell division, differentiation and morphological changes that are facilitated by multiple biochemical pathways. As a stress response, sexual parasite stages called gametocytes develop through morphological stages I-V. Mature gametocytes (stage V) circulate in the human bloodstream for several days, while immature stages (I-IV) are generally sequestered in other tissues(Usui & Williamson, 2021). Once ingested during blood meal, mature stage V gametocytes migrate to the mosquito midgut lumen where they undergo two stage conversions, gamete activation and ookinete formation. In the first midgut phase, gametogenesis is initiated when gametocytes are activated for gamete formation by signaling cascades such as decrease in temperature by approximately 5˚C, the release of mosquito-derived molecule xanthurenic acid (XA) and additionally a shift in pH from 7.4 to 8.0 (Bennink et al., 2016). While XA is shown to trigger signaling pathways of guanylyl cyclase GCα activity in gametocyte membrane however the binding receptor remains unknown. During gametocyte activation male and female gametocytes exit the enveloping host erythrocyte and differentiate into microgametes and macrogamete respectively. Once activated, female gametocytes mature, round off and egress into a fertile macrogamete(Usui & Williamson, 2021). Micro gametogenesis on the other hand involves endomitosis, egress and ex-flagellation to release male microgametes within a timeframe of 8-10 minutes post activation (mpa) (Venugopal et al., 2020).

During endomitosis, haploid (1N) microgametocytes arrested at the G_0-like cell cycle stage undergo rapid nuclear division (karyokinesis) with three rounds of spindle formation and genomic replication (Mitosis I – III) assembling eight basal bodies in a single time frame without concomitant cytokinesis (Dash et al., 2022). During the first round of genome replication, mitosis I spindle is formed simultaneously with one axoneme nucleation per basal body from cytoplasmic tubulins for flagella formation. At 6 mpa, four mitosis III spindles undergo chromatin condensation and cytokinesis into octoploid (8N) genome microgametocytes that concurrently egress from the host cell via ex-flagellation(Guttery et al., 2024). During ex-flagellation, a process mediated by E3 ubiquitin ligase, anaphase-promoting complex 3 (APC3) through proteolysis of

securin and cyclin B cell cycle regulators, motile axoneme swim out of the main cellular body and incorporate residual haploid genome from basal bodies still attached to the mitotic spindle into ex-flagellated microgametes(Wall et al., 2018).

The process of gametocyte and gamete egress from host erythrocyte and gametocyte body respectively, involves osmiophilic body (OB) mediated rupturing of the erythrocyte membrane (EM) and the parasitophorous vacuole membrane (PVM)(Tachibana et al., 2018). Although unclear, the directionality of membrane rupture in the above egress mechanisms are proposed in two models: the inside-out model, in which the PVM is degraded before the EM, and the outside-in model, in which the EM ruptures first. The former is the presently more favored model (Usui & Williamson, 2021). Osmiophilic bodies (OBs) are membrane bound organelles unique to gametocytes with phenotypically distinctive sex specific features, oval-shaped in female gametocytes, three times the size and density of the club shaped OBs in male gametocytes. Consequently, OBs are co-localized with sex specific proteins such as P*f*G377, actin II, perforin-like proteins 2 (PPLP2) and resident proteins that play dual sex functions like male development-1/protein of early gametocyte 3 (MDV1/PEG3), gamete egress and sporozoite traversal (GEST) and merozoite TRAP-like protein (MTRAP) to facilitate molecular mechanisms implied in egress of gametocytes(Dash et al., 2022,Tachibana et al., 2018). The secretory proteins clubbed beneath the plasma membrane in intracellular vesicles are transported through OBs migrated to the parasite surface and release their content via exocytosis into the parasitophorous vacuolar space, meditating the break-down of the PVM and EM (D. E. Goldberg & Zimmerberg, 2020).

Ex-flagellation is an exclusive phenomenon to micro gametogenesis, induced by XA triggered signaling cascades that increase intracellular calcium and cGMP. Increased cGMP triggers the downstream activation of cGMP-dependent protein kinase (PKG) that induces male gametocyte differentiation from crescent shape to spherical in a process termed rounding up(Sharma et al., 2021). Additional triggers of ex-flagellation include phosphoinositide-specific phospholipase C (PI-PLC) activity by-products of phosphatidylinositol-(4,5) -bisphosphate (PIP_2) hydrolysis into diacylglycerol (DAG) and inositol-(1,4,5) -trisphosphate (IP_3). The

latter mediates the rapid mobilization of Ca^{2+} from cellular stores like the endoplasmic reticulum into the cytoplasm (Ouologuem et al., 2023).

Evidence suggests a crosstalk and interdependency between secondary messengers in what appears to be a calcium-regulated feedback mechanism where PI-PLC stimulation is impaired by Ca^{2+} ionophore and cytoplasmic levels of Ca^{2+} is further dependent on PKG activation(Sharma et al., 2021). Inhibiting PKG phosphorylation dysregulates phosphatidylinositol-4-kinase (PI4K) and phosphoatidlyinositol-4-phosphate-5-kinase (PIP5K) metabolism during PIP2 conversion from the synthesis of phosphatidylinositol 4-phosphate (PI4P) via phosphatidyl-1D-myo-inositol (PI) (Sharma et al., 2021,de Oliveira et al., 2021). A cascade of calcium-dependent protein kinases (CDPKs) is activated by signals from increased intracellular Ca^{2+} for translational cellular responses during gametogenesis. CDPK1 depletion causes a defect in male and female gametocyte egress whereas CDPK2's significant implication in flagella development and erythrocyte membrane lysis is specific to male gametogenesis (Ghartey-Kwansah et al., 2020a)

Motile octoploid microgametes and haploid macrogametes fertilize in a 1:1 ratio. During fertilization male and female gamete plasma membranes bind allowing the axoneme and residual haploid male nucleus to enter the female cytoplasm for nuclear fusion followed by 3 hours of meiotic division(Kumar et al., 2022). Here, diploid spherical zygotes differentiate into elongated ookinetes with tetraploid genome that remains persistent through to sporozoite budding in oocyst before returning to haploid state. The zygote stage parasites undergo a round of genomic recombination that concludes 19-36 hours after blood meal and transform into motile, tissue traversing invasive ookinetes(Zeeshan et al., 2020). Using motility microneme proteins like CDPK3 and CTRP (circumsporozoite and TRAP-related protein), ookinetes exit the blood meal bolus then breach the peritrophic matric layer and transmigrate epithelial cells of the mosquito midgut lumen in cell traversal mode before exiting through the basal side of the mid-gut epithelium in sessile mode (Currà et al., 2019). Exposure to toxic intracellular factors like the midgut microbial flora, human and mosquito immune response molecules, between the migration end point and initiation of oocyst transformation decreases parasite abundance by 300-

fold(Smith & Barillas-Mury, 2016). Following egress from the basal side epithelium few surviving ookinetes rest beneath the basal lamina and bind to the conserved components, laminin and collagen IV for subsequent oocyst development. Within 14 days, the small oocyst syncytium progressively enlarges and simultaneously undertakes a dozen uncoupling nuclear and cellular divisions followed by a series of complex differentiation from solid to vacuolated phase until the cytoplasm is segregated into sporoblasts (Klaus et al., 2022). Mature sporozoites become crescent shaped upon completion of budding from the sporoblast and acquire motility prior to release from the oocyst into the mosquito hemolymph (Vlachou et al., 2006). Here, the mosquito becomes infective with motile sporozoites that invade and remain in the salivary gland to be injected with saliva into the mammalian host skin during a blood meal.

1.2.3.2 Exo-erythrocytic schizogony

Once in the blood circulation, infecting hepatic cells is the first obligatory step initiated by *Plasmodium* sporozoites in the mammalian host following dermal inoculation(Ménard et al., 2013). Larva looking sporozoites cross the sinusoidal cellular layer separating the blood and the liver parenchyma to infect hepatocytes, here, intrahepatic development can either remain dormant in hypnozoite forms or proliferate and differentiate to culminate in merozoite liberation for blood stage infection(Vantaux et al., 2022).

When sporozoites traverse cells into the liver in migratory mode, signalling cascades involving CDPK6 and other kinases are initiated by parasite and host molecular interactions that aid endothelium adhesion, trigger sporozoite retention in the hepatic sinusoid and finally results in the switch to invasion mode(Loubens et al., 2021). Constituent proteins of sporozoite invasive organelles such as micronemes and rhoptries when exocytosed into the Disse space mediate the binding of circumsporozoite surface protein (CSP) to heparan sulfate proteoglycans (HSPGs) receptors on the basolateral cell surface of hepatocytes. However, sporozoites do not invade on first contact but rather transmigrate the endothelium and numerous kupffer cells until reaching one last

hepatocyte and induces plasma membrane invagination of the host cell(Zheng et al., 2022). The final hepatocyte invasion concludes with the formation of the parasitophorous vacuole membrane (PVM) around the parasite. At 20h post invasion, sporozoites undergo comparative morphological changes in the apicoplast and mitochondrion that transform the elongated PVM into a small round trophozoite(Jayabalasingham et al., 2010). Simultaneously, the uninucleate trophozoites undergo rapid repetitive nuclear division spanning about 35 hours, generating up to 30,000 nuclei within a singular hepatocyte during merozoite formation(Roques et al., 2023). Hepatocyte-derived merozoites re-enter the bloodstream in a well-orchestrated, multi-step process. First the PVM ruptures by action of *Plasmodium* proteases, then the merozoites contained in merosomes egress into the host cytoplasm and enter the lung capillaries via blood vessel transportation to initiate erythrocyte infection(Scheiner et al., 2023).

In certain *Plasmodium* species like *P.vivax* and *P.ovale* , post invasion sporogony can take a detour route from the sequential progression explained above and instead develop into non-replicating liver stages called hypnozoites that remain dormant for various periods of time and activate after primary infection causing relapse episodes. The underlying biology of sporozoite commitment to hypnozoite formation remains unclear(Flannery et al., 2022).

1.2.3.3 Erythrocytic schizogony

The erythrocytic cycle is initiated when hepatocytes rupture to release merozoite for egress and invasion (Tan & Blackman, 2021). Here the merozoites released into the hepatic circulation rapidly invade red blood cells (RBCs) within 2mins. The pre-invasion phase is characterized by weak host-parasite interactions that are mediated by a family of Merozoite Surface Proteins (MSPs) following the initial contact between the parasite surface and circulating erythrocyte. For subsequent binding, the merozoite is reorientated such that the apical pole irreversibly interacts with the erythrocyte membrane leading to formation of the parasite-host cell junction and as invasion proceeds, merozoites actively glide the stationary ring of the tight junction for internalisation to link the host cytoskeleton using submembrane actin-myosin motors(Beeson et al., 2016). During this apical interaction, rhoptry proteins like the reticulocyte binding protein homologue (RH) are released to facilitate invasion by forming the parasitophorous vacuole (PV) for merozoite replication while adhesins such as the erythrocyte binding like proteins (EBL) and apical membrane antigen-1(AMA-1) stored in micronemes are secreted for erythroid interactions with parasite ligands in a number of alternative pathways(Sherling et al., 2019).Rhoptries have a dual club shape made-up of the neck, bulb and base. During invasion, rhoptry neck proteins like RON2 are first released to initiate and form interactions with AMA1 as central architectural features of the tight junction(Lamarque et al., 2011). Following the formation of the tight junction, proteins from the rhoptry bulb and base are released next to establish the parasitophorous vacuole and maintain subsequent internalisation within the invaginated erythrocyte membrane bilayer.

Parasitized erythrocytes adopt an echinocyte shape, undergoing substantial morphological changes and lose deformability as the engulfed parasite grows through the transformative stages of the asexual lifecycle(Molina-Franky et al., 2022a). First asexual stage is dormant, having low metabolism the parasite adopts a ring form for the next 12 hours of the life cycle before progressing into the feeding trophozoite stage with increased metabolic activity and rapid growth, undergoing multiple rounds of DNA synthesis, mitotic and nuclear division into segmented schizont containing 16 to 22 nuclei and finally concludes

with the rupture of the PV membrane(PVM) and RBC membrane (RBCM) in a process known as egress, to release the newly formed daughter merozoites back into the blood stream for continuous invasion of fresh RBC(MacRae et al., 2013; Matthews et al., 2020; Molina-Franky et al., 2022b). The highly synchronised asexual growth cycle in a human host takes 48hours to complete and is accompanied by pathological manifestations of malaria that has been classified as mild or severe malaria by the WHO based on the occurrence of complications. Severe malaria is characterised by multiple complications as a direct consequence of falciparum asexual parasitaemia, this includes cerebral malaria, with abnormal behaviour, impaired consciousness, multiple seizures, neurologic abnormalities, haemolysis induced haemoglobinuria and severe anaemia(Thomas et al., 2018). Symptoms of mild malaria on the other hand are often periodic and flu like lasting about 2 days in infected individuals(Baird et al., 2019).

Meanwhile, a small percentage of ring stage parasites, about 1% do not stay through the intraerythrocytic asexual stages but are driven into gametocytogenesis. The intraerythrocytic sexual forms known as gametocytes formed within the RBC are obligatory for parasite transmission from an infected human host to the next stage of the lifecycle in a female *Anopheles* mosquito(Liu et al., 2011).

1.2.3.4 Gametocytogenesis

After much debate on the actual point of sexual commitment in *P.falciparum* in the last decade, advances in molecular studies have elucidated a combination of genetic, epigenetic and environmental factors determining the rate of commitment to sexual development between *Plasmodium* species(Josling et al., 2018). It has been shown that a small proportion of trophozoite stages of the preceding asexual generation emerged from a single schizont make the irreversible differentiation into either macrogametocytes (female gametocytes) or microgametocytes (male gametocytes). Gametocytes typically develop within erythrocytes through five distinctive stages (I-V) and reach full morphological maturity in 8- 12 days. Unlike most *Plasmodium* species, late-stage *P. falciparum* gametocytes adopt a characteristic crescent shape created by the emergence of a pellicular complex consisting of a sub-pellicular membrane vacuole and a microtubule-based cytoskeleton underneath the gametocyte plasma membrane(Liu et al., 2011).

Morphological sex dimorphism is apparent in maturing stages II-IV, here macrogametocytes are characterised by concentrated pigment pattern that is stained blue with Giemsa and a relatively small nucleus with a nucleolus; by contrast microgametocytes possess a larger nucleus lacking a nucleolus with diffused pigmentation that stains pink (Tadesse et al., 2019). Developing gametocytes stage II-IV are predominantly sequestered to the spleen and bone marrow by cytoadherence to glycoprotein CD36 expressing endothelial cells via P*f*EMP1 similarly to asexual parasites (Day et al., 1998). On the other hand, only mature stage V gametocytes appear in peripheral blood circulation for transmission to the mosquito during a blood meal(Messina et al., 2018).

1.3 Malaria Control

1.3.1 Vector Control

The discovery of how mosquito plays a role in malaria transmission-initiated strategy developments for vector control (Duffy, 2021). According to vector biologists malaria these control strategies cover three main point of attacks namely environmental management, human habit influence on transmission dynamics, and vector-stage parasite development(Meibalan & Marti, 2017). First attempt involved rolling out bed nets which were soon found limiting, then the removal or modification of mosquito breeding sites, for example releasing predatory mosquito-eating fish in rice fields and draining mosquito-breeding site swamps in part of the famous anti-malaria programme at the Panama Canal and management methods of surrounding environments in Malaysia and Indonesia(Imbahale et al., 2011).

Paris Green developed an inorganic insecticide containing copper acetoarsenite in the 1920s, used in Brazil for the successful eradication of *Anopheles arabiensis* (*Anopheles gambiae sensu lato*) it was later implemented for controlling malaria in Italy on a large scale(Takken, 2021). Following the wide scale trial, a novel synthetic compound dichlorodiphenyltrichloroethane (DDT) with added capacity of proofing houses and stables that serve as resting sites for the adult mosquitoes, was introduced as a more effective control tool. The success in initial results of DDT insecticide used in tandem with synthetic anti-malarial chloroquine prompted the launch of WHO's 1955 global malaria eradication campaign which ended in 1969 following the rapid emergence of DDT resistant mosquitoes and funds scarcity(Nájera et al., 2011). In the 1970s, synthetic pyrethroid insecticide-treated bed nets reoriented anti-vector measures towards reducing human–mosquito contact by deterring and killing mosquitoes that land of them(Killeen et al., 2017). This new class of Insecticide-Treated Nets (ITNs) tested successfully in African large-scale trials and were therefore included in a new global eradication campaign by the WHO termed Roll Back Malaria programme. The campaign estimated a 50% global reduction in malaria-related morbidity and mortality with ITN vector control accounting for 78% of 663 million malaria cases in 2000, however, a repeat development of

rapidly widespread anopheline insecticide resistance by 2015 drew a halt in the campaign progress(Bhatt et al., 2015).

In response to the recurring insecticide resistance, the WHO in 2017 adopted the Global Vector Control Response (GVCR) framework for Integrated Vector Management (IVM), a rational decision-making platform designed with a toolbox to suppress or eliminate anopheline vectors using a range of new vector control approaches listed as follows; Environmental management conduct intermittent irrigation, aquatic body drainage , small puddle removal, to prevent and control egg-laying and larval development at such potential sites (WHO., 2017). Housing improvements such as door, window screen installation limit the risk of malaria by preventing the entry of highly anthropophilic mosquitoes that feed and rest indoors during nocturnal hours(Agyemang-Badu et al., 2023). Biological control introduces predatory and pathogenic agents that kill mosquitoes such as larvivorous fishes, fungi and bacteria into breeding sites. Bio-rationale methods implement control approaches such as insect growth regulators (IGRs) that mimic juvenile hormones and common larvicides methoprene (Altosid®), pyriproxyfen and diflubenzuron (Dimilin®) to disrupt mosquito growth, development and communication systems(Huang et al., 2017). Chemical control albeit challenged with mosquito resistance to current insecticides remain very effective in reducing malaria transmission during a blood meal, particularly the use of insecticide-impregnated bed nets(Lindsay et al., 2021). Behavioural control can reduce vector density and potentially eradicate vectors by manipulating the mosquito's response to visual, acoustic and chemical cues aimed at feeding behaviour, biting intensity and general intra and interspecific interactions(Gatton et al., 2013). Genetic control involves the identification and manipulation of specific genetic regulatory traits, made possible by advancements in molecular biology. Genes implied in mosquito reproduction are knocked out to sterilise vector population density as well as mosquitoes rendered vulnerable to parasite infection that can impede *Plasmodium* transmission and lastly, the introduction of regulating genes for host seeking in mosquito rendering a preferred blood host unrecognizable(McLean & Jacobs-Lorena, 2016). Community engagement in the last decade has become one of the four significant pillars of the GVCR framework (WHO, 2020).

1.3.2 Vaccine Development

The malaria vaccine development pipeline has been a work in progress for over 60 years (El-Moamly & El-Sweify, 2023). The research was started by Dr. Ruth Nussenzweig in 1965, an immunologist inspired by by the remarkable success of vaccines developed for other diseases such as polio, measles, diphtheria, tetanus and rabies etc. Unfortunately, successful malaria vaccination has been challenging for medical science, hindered by multifactorial limitations such as the extreme complexity in pathophysiology and intricate nature of the life cycle, genome diversity and immune evasion mechanisms of the human system contributing to extensive antigen variability within each stage (El-Moamly & El-Sweify, 2023). Malaria vaccine targets are considered according to the targeted developmental stage of the parasite: pre-erythrocytic, erythrocytic stages and transmission-blocking vaccines (TBVs).

1.3.2.1 Pre-Erythrocytic Vaccines (Liver Stage)

The pre-erythrocytic vaccines (PEV) are designed to prevent the clinically silent forms, sporozoites and liver stages from initiating human infection after sporozoite inoculation into the skin from a mosquito blood meal. PEVs act by inducing antibodies to surface antigens that attack sporozoites contained in skin and bloodstream or by blocking subsequent liver cell invasion and inducing T-cell responses to clear infected hepatocyte. High efficacy PEVs also referred to as anti-infection vaccines (AIV), have a window of attack during the one-week development of infectious sporozoite invading liver cells and aim to completely clear hepatic pre-erythrocytic stages prior to release into the bloodstream(Duffy & Patrick Gorres, 2020).

The PEV vaccines employ two approaches to developing potential candidates, either by inducing immune responses to antigenic circumsporozoite protein (CSP) subunits or whole sporozoite exposure(C. A. Long & Zavala, 2016). Whole sporozoite vaccine (WSV) are managed by delivering irradiated parasites or genetically modified parasites or infection in conjunction with chemoprophylaxis (called chemoprophylaxis vaccination or CVac) to the vaccinee by mosquito bites(Sahu et al., 2021).Circumsporozoite protein (CSP) is an immunogen on the

surface of the malaria sporozoite that is represented early on in the liver phase of infection and continues to be a main focus in developing protein subunit vaccine (Almeida et al., 2021). The leading pre-erythrocytic malaria vaccine, RTS,S is a monovalent recombinant protein vaccine based on the CSP antigen(Wilder et al., 2022). Based on the safety and efficacy results across multiple clinical studies both RTS,S/AS01 (MosquirixTM) and R21/Matrix-M were approved as a prequalified vaccines by the WHO and are now approved for widespread use in malaria-endemic African countries(Laurens, 2020). Other candidate for PE vaccines is being developed based on other approaches such as the sprorozoite liver stage CSP antigens, liver stage antigen 1 (LSA-1), malaria exported protein 1 (Exp1), cell-traversal protein for *Plasmodium* ookinetes and sporozoites (CelTOS) and sporozoite surface protein 2/thrombospondin-related adhesion protein (SSP2/TRAP)(Schussek et al., 2017).

1.3.2.2 Erythrocytic Vaccines (Blood Stage)

The rationale for blood stage malaria vaccine research is based on semi-immune adults with naturally acquired immunity, residing in high-transmission areas that can passively transfer antibodies to relatively naive individuals with clinical disease and subsequently significant declined blood stage infection. BSVs block merozoites from invading erythrocytes to limit the parasite's asexual replication when released from the liver and induce anti-invasion and anti-disease responses. These vaccines also induce antibodies to infected erythrocyte surface proteins and against RBC membrane variant antigens(C. A. Long & Zavala, 2016).

Several clinical trials have evaluated P. falciparum merozoite antigens as vaccine candidates, however, developing anti-merozoite vaccines faces many challenges such as the brief window when merozoites are outside the erythrocytes and accessible to induced antibodies. extensive antigenic polymorphism; functionally redundant sialic acid-dependent and sialic acid-independent merozoite invasion pathways; a large merozoites ratio to low sporozoite number attacked in the PEVs; and difficulties in correct protein conformation expression(Takashima et al., 2024). Despite these disappointments, candidate vaccines are being developed with refined

approaches, in particular RH5 and the AMA1-RON2 complex are based on addressing the limitations of redundant invasion pathways.

1.3.2.3 Transmission Blocking Vaccines (Mosquito Stage)

Transmission blocking vaccines (TBVs) target sexual stages (gametes and zygotes) or sporogonic-specific surface antigens with the aim to induce antibodies against functionally important proteins inside the mosquito thereby reducing infectivity and preventing the spread of the disease. Leading vaccine candidate antigens being targeted by TBVs are categorised into two groups, pre and post fertilization(Patel & Tolia, 2021). The Pre-fertilization candidates include Pfs48/45, Pfs47 and Pfs230 , these are gamete surface cysteine rich proteins that are expressed by gametocyte in humans. The vaccines induces antibodies with transmission blocking activity against gametocyte in malaria exposed individuals with naturally acquired immunity. Post-fertilization antigens considered for TBV are zygote and ookinete surface proteins, Pfs25 and Pfs28, expressed in the mosquito midgut. In particular, the Pfs25 vaccine trials have reported durable immunogenicity and less antigenic polymorphism with some local and adverse systemic safety issues, however, Pfs25 remains a focus candidate for trails published to date.

Current limitations of TBV development is that they do confer protection to the recipient from new infections. TBVs might be helpful in maintaining high levels of antibodies in the long run following widespread coverage to accomplish mass immunization. Another important challenge is low efficacy that requires an immunity booster, this is due to human immune mechanisms not naturally exposed to antigens with transmission-blocking activity. As such future vaccine strategies can combine TBVs and PEVs to impede the human infection and mosquito transmission route or in combination with BSVs to reduce transmission(Duffy, 2021).

1.3.3 Drug Development

History of malaria drug development

The first effective antimalarial and prophylactic agents were traditionally developed unrefined products from natural sources. Prior to the first chemical purification of quinine in 1820 as the first pharmaceutical malaria treatment, indigenous south Americans unknowingly harnessed the power of quinine by using ground bark from cinchona (quina-quina) tree to treat malaria in the 1600s (Dagen, 2020). French chemists Pierre Joseph Pelletier and Joseph Bienaime Caventou stimulated the beginnings of modern pharmacology by isolating and extracting cinchona alkaloids; quinine, quinidine, cinchonine, and cinchonidine from the cinchona bark in small dispensable volumes of predictable potency(L. H. Miller et al., 2023).

Qunine synthesis constituted a strategic elusive asset as the mainline of defense with 98% efficacy above cure rate against malaria endemic amongst military of all belligerent nations during the 20th century war. The resulting near monopolisation of cinchona plantations and Japanese military conquest in Java (Indonesia) in 1942 imposed a supply scarcity that incentivised the race to develop synthetic alternatives to quinine between the first and second world wars(L. H. Miller et al., 2023). Parasite resistance to chloroquine initiated further research into new drugs. The discovery of proguanil (agents targeting folate producing enzymes) for human malaria treatment led to the development of pyrimethamine both of which were displaced by the emergence of parasite resistance within a year of introduction. The first effort to forestall potential drug resistance involved the unsuccessful combination therapy of proguanil with sulfones and sulfonamides and then consequent development of mefloquine that within a decade ended in the same pile of parasite resistance (Ippolito et al., 2021).

Frontline therapies used in recent times for malaria treatment are based on a group of semisynthetic derivatives generically known as ‘artemisinins’ that are derived from Artemisia annua, a sweet wormwood tree native to temperate northern parts of China(Siqueira-Neto et al., 2023). Despite being used to treat fever for over 2000 years, the active ingredient of the herb extract was first

identified as artemisinin (qinghaosu) in 1971, and antimalarial activity was first experimented in primate subjects (Dagen, 2020). In 1972, Chinese scientists through a collaborative effort on 'Project 523', first described and prepared the chemical structure of artemisinins by isolating the crystalline form of artemisinin from the Artemisia plant and derivatives dihydroartemisinin (DHA), artemether, artesunate and arteether and artelinic acid. Tu You You was awarded the Nobel Prize in Physiology or Medicine in 2015 as the scientist behind the discove(Su & Miller, 2015)test subject(Su & Miller, 2015). However, like predescessor antimalarial drugs, the emergence of artemisinin resistance has been reported, first in Southeast Asia and now widespread to other malaria endemic regions across the world putting millions of lives at risk (Woodrow & White, 2017).

Understanding the parasite's developmental biology continues to prove essential and similarly to antimalarial vaccines, chemo therapeutical intervention can be distinguished into three categories that represent the point of attack across *P. falciparum* life cycle; Chemoprophylaxis (asymptomatic liver stages), curative (schizonticidal) and transmission blocking (gametocytes and sporozoites)(Siqueira-Neto et al., 2023).

1.3.3.1 Molecular markers of drug resistance

Two main mechanisms of resistance drive *Plasmodium* resistance to antimalarial drugs; (i) Effluxes of the drug away from the site of action due to transporter gene mutations; and (ii) mutations in corresponding genes that modify the drug target (Ouji et al., 2018). The WHO now recommends the use of antimalarial drugs in combination therapy to curb the emergence of parasite resistant strains to mono therapy strategies. Particularly, to mitigate the emerged artemisinin resistance, fast acting artemisinin derivatives are combined with the other classes of drugs, quinoline-related compounds and anti-folates to create a new line of antimalarials, artemisinin-based combination therapy (ACT). Partner drugs include lumefantrine, mefloquine, amodiaquine, sulfadoxine/pyrimethamine, piperaquine and chlorproguanil/dapsone(Ouji et al., 2018). Recent advances in next-generation sequencing (NGS) technologies have made possible new and effective methods of tracking markers of resistance

across the diversity and the prevalence of *Plasmodium falciparum* (Suresh & Haldar, 2018).

The K76T mutation in the *P. falciparum* chloroquine resistance transporter (P*f*CRT) gene plays a primary role in determining the CQ resistance and susceptibility(Pirahmadi et al., 2013). The mutation occurs when positively charged lysine residue located in the first transmembrane domain of P*f*CRT protein is replaced by neutrally charged threonine residue at position 76 causing diprotonated CQ to efflux out of the digestive vacuole by active transport. The P*f*CRT mutations at 72–76 codons confers cross-resistance with quinine, amodiaquine (AQ), piperaquine, and lumefantrine(Foguim et al., 2020). The *P.falciparum* multidrug resistance protein 1 (P*f*mdr1) gene mutation at the following position (N86Y, Y184F, S1034C, N1042D, and D1246Y) has been linked to higher level of resistance to quinine, MQ, halofantrine, lumefantrine, and artemisinin. Mutations at position Y191H and A437S in *P.falciparum* multidrug resistance-associated protein (P*f*mrp) gene were found to be involved in varying the antimalarial response to CQ and quinine resistance(Pirahmadi et al., 2013). Point mutation at S108D codon in the P*f*DHFR is linked with resistance to Pyrimethamine whereas Double mutation at positions A16V and S108T are associated with *P.falciparum* resistance of to cycloguanil(Pirahmadi et al., 2013). Resistance to sulfadoxine in *P.falciparum* has been linked to five mutations in the P*f*DHPS protein (S436A/F, A437G, L540E, A581G, and A613T/S), hence the recommendation for sulfadoxine in combination therapy with pyrimethamine known as SP or Fansidar, which also has reduced drug susceptibility in association P*f*dhps and P*f*dhfr gene mutations(Zhao et al., 2020). Single mutation at Y268N/S/C codon in the Cytochrome b (cytb) gene at ubiquinol binding site for atovaquone confers resistance in field isolate *P.falciparum*(Suresh & Haldar, 2018). Whole genome sequencing of the artemisinin-resistant *P.falciparum* clinical and field isolates revealed several point mutations (F446I, N458Y, M476I, Y493H, R539T, I543T, P553L, R561H, P574L and C580Y) in Kelch 13 (K13) propeller region as a key determinant for artemisinin resistance(Ouji et al., 2018).

New criteria for developing next generation antimalarial are defined by a set of candidate characteristics and product combinations that ensure effectiveness beyond the present standards of care(Dechering et al., 2022). The target

candidate profile (TCP) which refers to an individual molecule in pre-clinical or clinical assessment and the target product profile (TPP) for two or more active candidates in the appropriate formulation for a final product, are strategic tools proposed by the medicines for malaria venture (MMV) to guide malaria drug discovery. Both profiles are summarised in Figure 1.4 below (Siqueira-Neto et al., 2023).

Antimalarial drugs that act on the asexual blood stage are categorized as target candidate profile 1 (TCP-1), whereas molecules active against liver-stage hypnozoites (*P.vivax*) or hepatic schizonts are in categories TCP-3 and TCP-4, respectively. Drugs that block transmission to the mosquito by inhibiting gametocytes are TCP-5 compounds, and those that block transmission by targeting the insect vector are TCP-6 (endectocides) There are two general categories of TPPs and multiple use cases: TPP-1 focuses on new drugs combinations for chemotherapeutic treatment of acute uncomplicated malaria in children or adults; TPP-2 focuses on chemoprevention, (giving a full treatment dose to individuals in high-transmission areas or during epidemics to control transmission, as some individuals can be asymptomatic carriers) and prophylaxis (administering a drug to asymptomatic individuals at risk of infection) (Siqueira-Neto et al., 2023; Umumararungu et al., 2023).

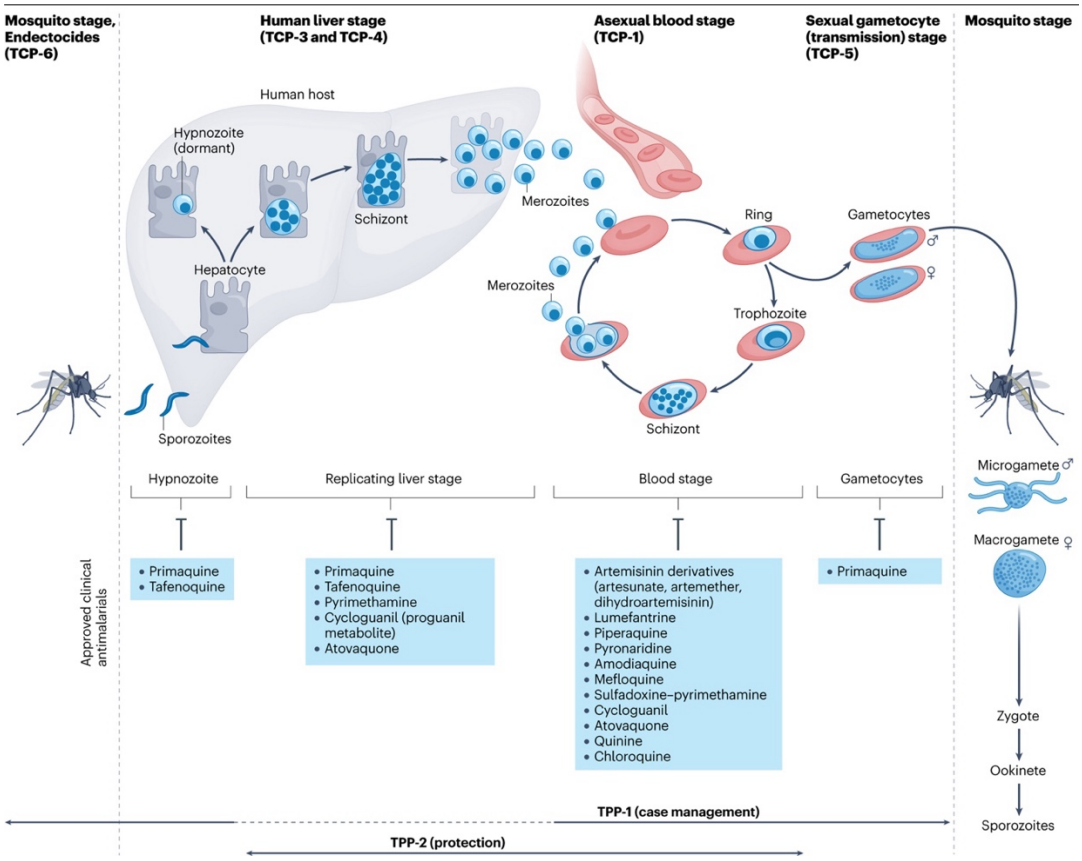

Figure 1.4 Malaria therapies in the context of the parasite life cycle.
Antimalarial drugs that act on the asexual blood stage are categorized as target candidate profile 1 (TCP-1), whereas molecules active against liver-stage hypnozoites (P. vivax) or hepatic schizonts are in categories TCP-3 and TCP-4, respectively. Drugs that block transmission to the mosquito by inhibiting gametocytes are TCP-5 compounds, and those that block transmission by targeting the insect vector are TCP-6(Siqueira-Neto et al., 2023) .

1.4 Protein kinases

Protein kinases (PKs) are a kind of phosphotransferase belonging to the great family of kinases that can selectively modify other proteins by covalent transfer of γ-phosphate from adenosine triphosphate (ATP) to specific amino acid residues on target proteins(substrate) in a reversible and dynamic process known as phosphorylation (Figure 1.5a)(Kanev et al., 2019). The phosphate addition is an ideal molecular "switch" that affects complex signalling network through protein conformational changes from hydrophobic apolar to hydrophilic polar allowing the direct the formation and reorganisation of protein complexes(Turnham & Scott, 2016).

Protein phosphorylation is one of the most common, important post-translational modifications (PTMs) and chemically stable under physiological conditions, regulate biological functions such as enzyme activity, cellular localization, or association with other proteins (Ardito et al., 2017). Recent phosphoproteomic studies have listed 760,000 potential phosphosites and over 200,000 known phosphorylated sites in the human proteome. While majority of the human phospho complexes contain only few phosphorylation sites, about 21,000 phosphorylation events have been described for 7000 human proteins with potentially more than 90% subjected to phosphorylation PTM. More than one-third of these protein are phosphorylated at serine (Ser or S), threonine (Thr or T), and tyrosine sites (Tyr or Y), in asymmetrically distribution on 85% serine, 11.8% threonine, and 1.8% tyrosine residues (Nishi et al., 2011).

Protein phosphorylation abundance and specificity as a regulatory mechanism in cellular processes such as protein synthesis, cell division, signal transduction, cell growth, development and aging are evident from the large number of protein kinase encoding genes, constituting almost 2% of the human genome, that are activated and deactivated via phosphorylation/dephosphorylation events(Pang et al., 2022). On the other hand, phosphatases number make up almost ten times smaller of the human genome. About 50 distinct kinase families that mediate a diversity of essential functions are conserved between yeast, invertebrate and mammalian kinomes(Stanford & Bottini, 2023). Approximately

568 protein kinases and 156 protein phosphatases in the human genome regulate phosphorylation events for the control of biological processes such as proliferation, differentiation and apoptosis. Of which 478 of these kinases belonging to a single superfamily, have catalytic domains that are related in primary sequences (Ardito et al., 2017).

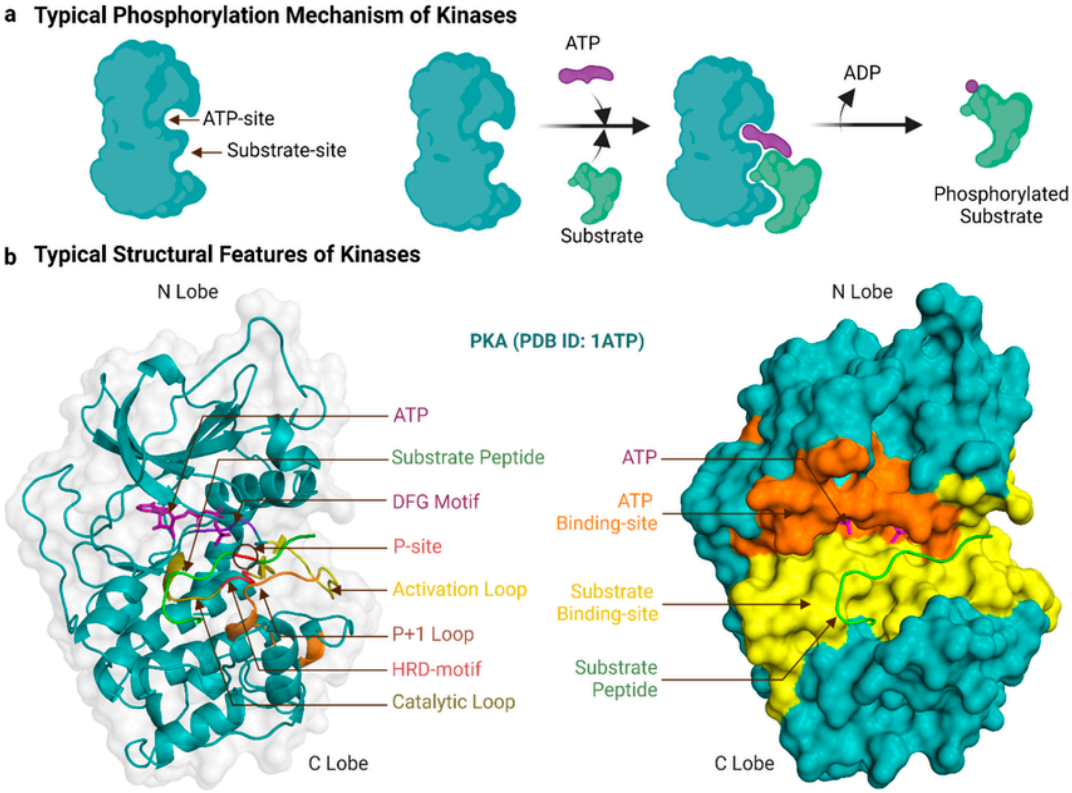

Figure 1.5 Typical phosphorylation mechanism and structural features of protein kinases. (A) shows the typical catalytic reaction carried out by kinases and (B) shows the essential structural features of the enzyme's kinase domain. Created with https://BioRender.com.

Eukaryotic protein kinases (ePKs) are characterized by a highly conserved catalytic domain, which adopts a similar three-dimensional structure across different ePKs (Kanev et al., 2019). The domain is subdivided into eleven subdomains with conserved motifs that conform to the classification system by Hanks and Quinn, in which ePKs are distributed into eight major groups, namely; i) the AGC group: protein kinases A, G, and C; (ii) CAMK group: Ca+/CAM-dependent kinases; (iii) CMGC group: Cyclin Dependent Kinase (CDK), Mitogen Activated Protein Kinase (MAPK), Glycogen Synthase 3 Kinase (GSK3), and CDC-like kinase (CLK); (iv) CK1 group: Casein kinase 1 (CK1); (v) STE group:

homologues of yeast sterile 7, 11, and 20 (STE7, STE11, STE20, respectively); (vi) RGC group: receptor guanylate cyclase; (vii) TK group: tyrosine kinase; and (viii) TKL group: tyrosine kinase like. In addition to the "typical" ePKs, several proteins possessing only weak sequence homology with any of these major ePK groups have been identified and classified as “OTHER” group and ‘atypical protein kinases ’(aPKs) (Hanks, 2003).

Beyond the conserved catalytic core, the canonical kinase catalytic domain fold is constituted of two major subdomains, a larger primarily α-helical, C-terminal lobe consisting of 250 to 300 amino acids and a smaller five strand ß-sheet with a single αC-helix, N-terminal lobe(Aubol et al., 2014). The N-and C-terminus are connected by a peptide scaffold (the hinge) forming a deep groove with a front and hydrophobic pocket (rear pocket) between the subdomains that constitutes the active site. The front pocket groove consists of catalytic residues that enable the binding of the peptide substrate and an ATP molecule while the back pocket supports regulatory functions under the control of a conserved lysine residue and a residue ‘gatekeeper’ (Biswas et al., 2024). Protein kinase crystal structures have revealed that the evolutionary conservation and conformational plasticity of the catalytic domain allow for a dynamic equilibrium between closely related active and highly specific inactive forms of kinases which can facilitate the regulation of the catalytic activity. Interestingly, about 10% of all human kinases are considered catalytically deficient and have been classified as pseudo kinases(Lim et al., 2015). Although sharing a typical kinase domain fold, pseudo kinases have been reported to lack at least one catalytic residue which is required for canonical protein kinase functions and instead maintain essential function by acting as scaffolding proteins to nucleate assembly and/or localisation of signalling complexes, allosteric regulators of conventionally active kinases and molecular switches of signalling complex assembly(Rauch et al., 2011).

1.4.1 *Plasmodium* kinome

The ensemble of protein kinases of an organism's genome is called kinome. With the advent of genome-sequencing projects, the genomic era made available databases such as PlasmoDB that have permitted the systematic analysis of eukaryotic protein kinases (ePKs) encoded in the *Plasmodium* kinome, thereby setting an important milestone in the study of *Plasmodium* biology. The malaria kinome of the most well studied species, *P.falciparum* encodes 91 protein kinase genes, with distinguishing sequences that constitute structural features similarly to the mammalian kinome and behave as expected in terms of their functional categories from their homologues in other organisms(Borba et al., 2022).

However structural data of the *Plasmodium* kinome demonstrate exploitable divergencies between parasite and mammalian hosts such as differences in parasite phosphosignalling pathways to hosts, atypical parasite PKs clustered within the ePK groups/families but have no sequence similarity to typical mammalian kinases and malarial protein kinases not classifiable into established families characterised in the human kinome.

Many of the sequences that constitute the *P. falciparum* kinome cluster within seven out of the nine major mammalian ePK groups, as follows AGC, CAMK, CMGC, CK1, NEK, TKL, OTHER in addition to a *Plasmodium*-specific group FIKK that do not cluster within the established groups found in the human kinome making a total of eight major groups in (Adderley & Doerig, 2022).

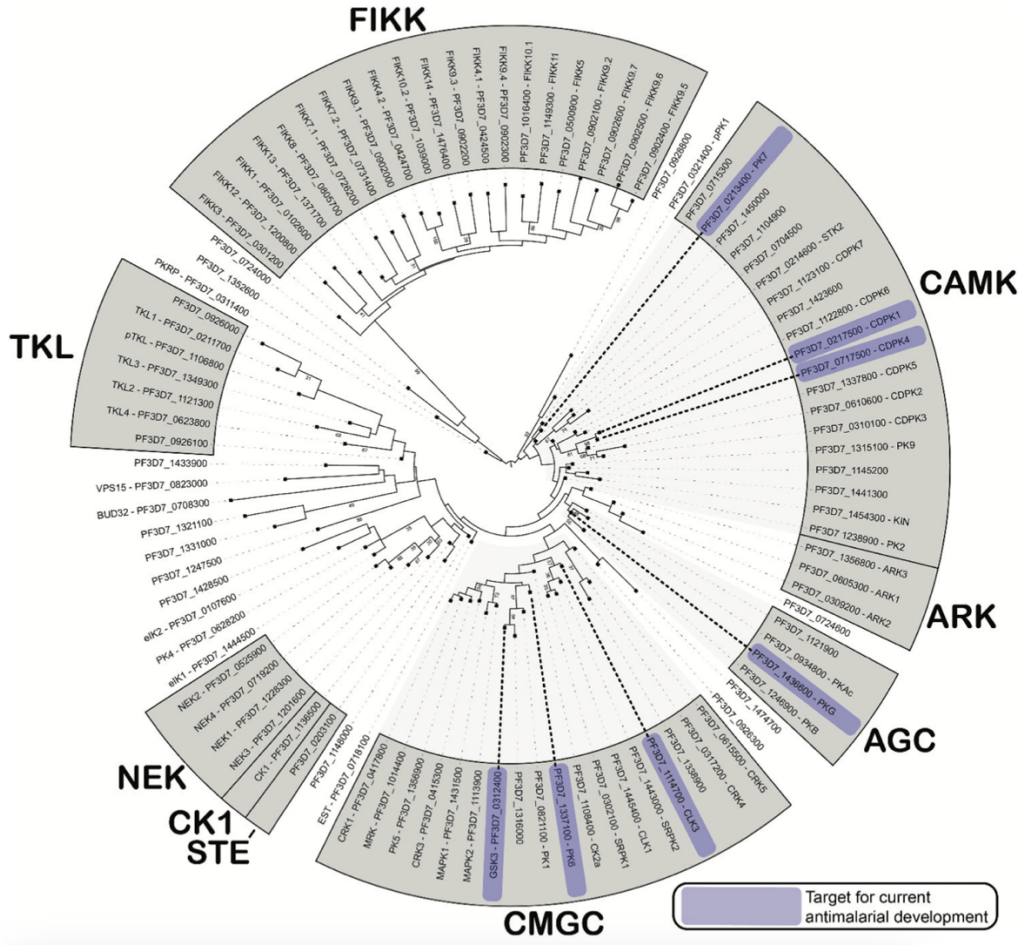

Figure 1.6 Phylogenetic tree of the *Plasmodium falciparum* kinome.
Highlighting kinases that are targets of ongoing drug discovery. Highlighted in blue are the parasite kinases discussed as ongoing targets for drug discovery (Ong et al., 2023).

AGC group

The cyclic-nucleotide & calcium/phospholipid-dependent kinase group (AGC) is represented by total of 33 proteins across 8 *Plasmodium* spp. With five malarial kinases found in falciparum, three of which have been characterised as the cAMP-dependent P*f*PKA [PFI1685w], the cGMP-dependent P*f*PKG [PF14_0346] and P*f*PKB [PFL2250c]. These kinases are implied in cAMP and calcium-dependent signalling pathways that regulate microneme exocytosis and are required for the sporozoite invasion of hepatocytes (Adderley & Doerig, 2022).

CamK group

The results of a bioinformatics pipeline to elucidate the kinome across eight *Plasmodium* species namely *falciparum*, *vivax*, *ovale*, *yoelii*, *berghei*, *chabaudi*, *knowlesi* and *malariae* report CAMK as the second prominent group containing 156 proteins (Borba et al., 2022). This is evident of CamK activity for ookinete motility in the mosquito, microgamete formation, and hepatocyte invasion in the host. The main branch of the tree anchored by the human CamKs also clusters 13 falciparum kinases, four of which which share the overall structure of the calcium-dependent protein kinases (CDPKs); P*f*CDPK1 [PF3D7_0217500], P*f*CDPK2 [PF3D7_0610600], P*f*CDKP3 [PF3D7_0310100] and P*f*CDPK4 [PF3D7_0717500]. Two sequence clusters P*f*CDPK5 [PF3D7_1337800] and PF3D7_1123100 appear to CDPK related and the other 6 form a sister branch (Ghartey-Kwansah et al., 2020; Govindasamy & Bhanot, 2020).

CMGC group

The CMGC is the largest group in the *Plasmodium* kinome comprising of 18 plasmodial genes from four kinase families: i) the cyclin-dependent kinase family (CDKs) ii) mitogen-activated protein kinases (MAPKs) iii) Glycogen synthase kinase 3 (GSK3) and iv) the Cdc2-like kinases (CLKs). Although well established in eukaryotes, only five CDK related members which are major regulators of cell-cycle progression have been described in *P.falciparum*(Alam et al., 2015). MAPKs are crucial transducers of cell cycle control or transcription factors. Two members of MAPK, P*f*map-1 and P*f*map-2 have been characterised in addition to two other kinases, P*f*PK6 and P*f*crk-4, with features from both CDKs and MAPKs. Member P*f*CK2 belonging to the Casein kinase 2 (CK2)-type subfamily in the GSK3 family is identified to be likely involved in the chromatin assembly pathway. Four P*f*CLK kinases play important roles in RNA metabolism and are investigated in detail in this study (Adderley & Doerig, 2022; Borba et al., 2022).

CK1 group

Bioinformatics pipeline updated the kinomes of eight *Plasmodium* species and classified only one malarial kinase in, P*f*CK1 [PF11_0377] for the Casein kinase 1 (CK1) group. Characterisation studies suggest interaction between P*f*CK1 and Rab GTPases that play a role in malaria parasite early and late endosome function (Borba et al., 2022).

TKL group

Five malarial enzymes clustered within the human TKL group play biological roles in protein co-localisation with cytoskeleton microtubules and asexual parasite proliferation in human erythrocytes (Borba et al., 2022).

OTHERS group

So far four members in the *P.falciparum* kinome are classified in the NIMA-related kinase (Nek) family, which play central roles in mitosis and meiosis in asexuals and gametocytes (Guttery et al., 2014).

Atypical kinases

This group consists of protein kinases that do not cluster clearly within the defined ePK groups . An example is the composite enzyme P*f*PK7 (classified under CAMK in Figure 1.6), a current target for malaria drug development, displays a unique structural homology to both MAPKKs (C-terminal region) and fungal PKAs (N-terminal region). Disruption of the P*f*PK7 gene in *P.falciparum* impairs schizogony and sporogony (Dorin-Semblat et al., 2008). Another atypical kinase P*f*PK9 (Figure 1.6) is implicated in proteasome regulation and cell cycle progression via phosphorylation of E2 ubiquitin-conjugating enzyme 13 (*Pf*UBC13) (Philip & Haystead, 2007).The FIKKs are a unique family of orphan kinases characterized by a conserved FIKK (Phenylalanine (F) – Isoleucine (I) – Lysine (K) – Lysine (K)) motif in the N-termianl region. This family constitutes distinctive

clusters of 21 members in *P.falciparum* (Figure 1.6) and 1 each in *P.berghei* , *P.yoelii* , *P.knowlesi* , *P.vivax* but none in *P.chabaudi* or *P.reichenowi*. Recent studies have characterized 5 FIKK members as critical for parasite survival within erythrocyte cells, 3 of these (FIKK9.1, FIKK10, FIKK10.2) are known to be exported into the cytoplasm of the infected RBCs via Maurer's clefts (Kats et al., 2014; Nunes et al., 2007, 2010). The other 2 namely, FIKK3 and FIKK9.5 are localized to the apical rhoptry and parasite nuclei respectfully. Some essential FIKK members are in implied in trafficking, adhesion and antigenic variation roles for the parasite lifecycle, for example FIKK9.4 and FIKK9.7 transcribed in trophozoite stages mediate both the rigidification of the cytoskeleton in infected erythrocytes and cytoadhering to host cell surface (Davies et al., 2020; Nunes et al., 2007; Scherf et al., 2008).

1.4.1.1 Cyclin dependent like kinase family in *P. falciparum*

The Cdc2-like kinase family (CLKs) are dual-specificity protein kinases belonging to the CMGC group that share the same ATP co-factor and phosphorylate downstream substrate proteins on the serine, threonine, and tyrosine residues(Aubol et al., 2014). Collectively denoted as the "LAMMER" kinase family due to the common "EHLAMMERILG" motif shared between the conserved catalytic domains located at the C-terminus of members 1-3 and the N-terminus of CLK-4. The EHLAMMERILG motif is located in an α-helix below the substrate-binding region which is important for kinase activity, substrate recognition, and subcellular localization (Figure 1.7) (Song et al., 2023).

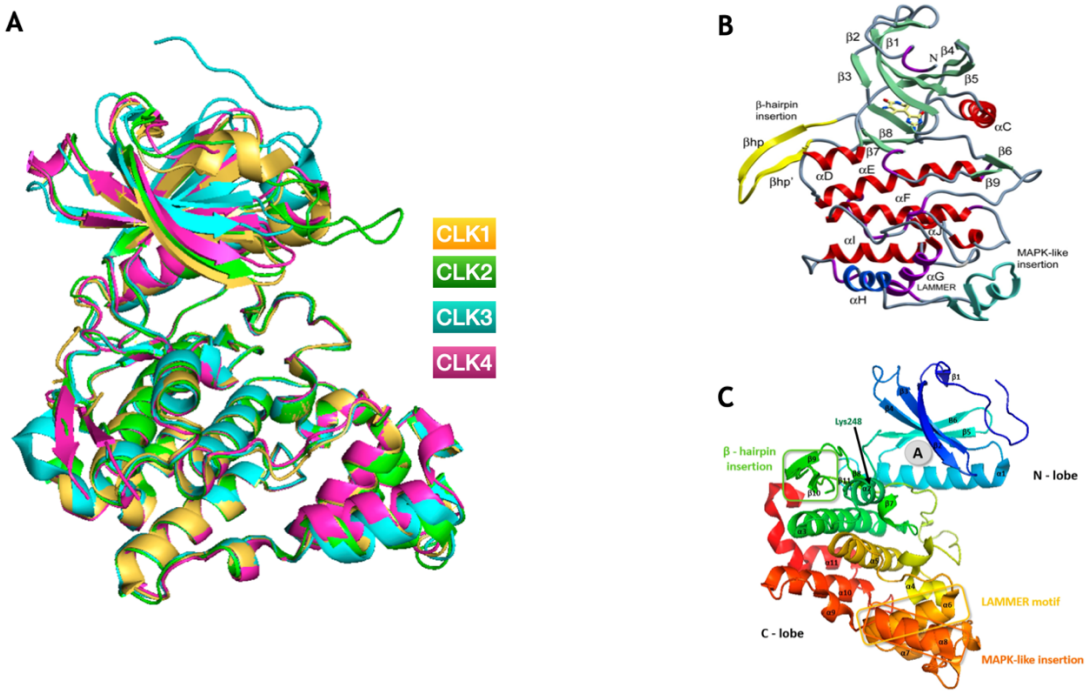

Figure 1.7 Structural alignment of human CLK1- 4.
(A) Overlay of X-ray crystal structures: CLK1 (yellow, ligand:12h, PDB: 6I5H), CLK2 (green, PDB: 3NR9), CLK3 (blue, PDB: 6YTW , CLK4 (pink, ligand: CX4945, PDB: 6FYV) (Martín Moyano et al., 2020) (B) Structure of the CLK1 kinase domain. Specific structural insertions defining the LAMMER kinases are highlighted by different colours and are labelled. The inhibitor debromohymenialdisine is shown in stick representation (Bullock et al., 2009) (C) CLK3 crystal structure. The grey circle (A) represents the most common binding pocket for small-molecule inhibitors. PDB: 2EU9 (Martín Moyano et al., 2020).

The CLKs in *Plasmodium falciparum* include four homologous enzymes (P*f*CLK1, P*f*CLK2, P*f*CLK3 and P*f*CLK 4) that regulate transcript splicing in the nuclear compartment via serine-arginine-rich protein phosphorylation, activity modulation and catalysing spliceosome molecular machinery within the nucleus and cytoplasm of the parasite. Localisation studies show the presence of P*f*CLK1 at the trophozoite stage in the nucleus, at schizont and gametocyte stages in the nucleus and cytoplasm. Similarly, P*f*CLK3 localises in the nucleus of trophozoites however in schizonts and gametocytes, is predominantly present in the cytoplasm (Kern et al., 2014).

Nuclear localization signals upstream of the C-terminal catalytic domain in member kinases P*f*CLK1 and P*f*CLK2, have been shown by in silico studies to be homologous to the non-essential serine-arginine (SR) protein kinase Sky1p known to be involved in splicing and transport of mRNA in budding yeast Saccharomyces cerevisiae (Agarwal et al., 2011). Similarly, P*f*CLK4 interacts with the alternative

splicing factor P*f*SR-1 required for parasite proliferation which also exhibits homologies to Sky1p specific substrate, Npl3p and mammalian SF2/ASF(Agarwal et al., 2011). On this basis, CLKs are implied in pre-mRNA splicing, a crucial process for cell growth and survival. Evidence of splicing processes in erythrocytic schizonogy, gametocyte differentiation, and gametogenesis emphasizes a possible therapeutic targeting of P*f*CLK kinases particularly P*f*CLK1 and P*f*CLK3 kinases which are expressed profusely in both asexual stages and in gametocytes(Kern et al., 2014).

1.4.1.2 Splicing in *Plasmodium*

Genomic sequencing revealed that quantity and quality of gene expression in humans and virtually all model organisms is subject to complex regulation by a multitude of post-transcriptional mechanisms, one of the most important being the splicing machinery(Zhan et al., 2018). In addition, 30 to 50% of protein-coding genes in higher eukaryotes are affected by another level of complexity in splicing known as the occurrence of alternative splicing. These vast majority of cells in response to splice signals can change alternative splicing patterns allowing the creation of protein isoforms with varying biological properties from a singular gene(Yeoh et al., 2019). The alternative splice sites are recognized and selected based on the dynamic formation of protein complexes on the processed pre-messenger RNA (pre-mRNA). Specific splicing regulatory proteins bound to different pre-mRNAs generate "messenger ribonucleoprotein code" also known as "splicing code" that determines exon recognition(Baralle & Giudice, 2017). Variant proteins generated from individual genes have different biological properties such as protein-protein and protein-RNA interactions influenced by reversible protein phosphorylation that modulate how regulatory protein assemble on pre-mRNAs, thus contributing to the coding potential of the genome(Aubol et al., 2016).

Pre-mRNA splicing is executed by a multimegadalton ribonucleoprotein (RNP) complex known as the spliceosome composed of five different RNP subunits and other associated protein cofactors tasked to remove introns from pre-mRNA post nuclear transcription(R. Wan et al., 2016). Spliceosomal subunits are made of Uridine-rich (U-rich) small nuclear RNPs (snRNPs) known individually as U1, U2,

U4, U5 and U6. Each snRNP spliceosomal subunit consists of one or more RNA components termed small nuclear RNAs (snRNAs), and a group of eight small polypeptides proteins (B/B′, D3, D2, D1, E, F, and G) known either as "Sm"or"core" proteins together with a variable number of complex-specific proteins(Didychuk et al., 2018).

The classic model for spliceosome assembly on pre-mRNA substrates is described as the ordered stepwise interaction of discrete spliceosomal snRNPs and other non-snRNP splicing factors to form the cross-intron spliceosomal complex, early complex (complex E) where U1 snRNP binds to the 5' end splice site (Zhan et al., 2018). Following the commitment to complex E, the 3′ splice site bind the pre-mRNA branch region by the branch-point-binding protein and interact with the complex component U2 snRNP auxiliary factor (U2AF) thereby establishing a duplex between the 5′ and 3′ splice sites for the first transesterification through the intron and/or the exon. Subsequently, the U2 snRNP recruits the branch point sequence (BPS) in an ATP-dependent manner to form a prespliceosome also known as complex A(Black et al., 2023).

The remaining snRNPs, U4, U5, and U6, pre-assemble in the tri-snRNP and bind complex A to be recruited to the assembling spliceosome that generates the pre-catalytic B complex. Undergoing a series of rearrangements in protein–protein, RNA–protein and RNA–RNA interactions results in U6 snRNA replacement of U1 snRNA, destabilization and release of U4 to subsequent catalytically activated spliceosome B* complex which catalyzes the first transesterification reaction to yield the C complex(Nguyen et al., 2015). The second of the two steps of splicing is catalysed by the C complex resulting in the post-catalytic P complex, finally the spliceosome dissociates and with additional remodelling that releases the mRNA which take part in additional rounds of spliceosome assembly and catalysis pathway. COcoa Supplement and Multivitamin Outcomes Study (COSMOS) revealed an alternate spliceosome assembly pathway, where U1 is recruited after U2(R. Wan et al., 2016). However, additional experiments showed both the U1-first and U2-first pathways during the first stage of spliceosome assembly bear no binding requisite and therefore will form U1·U2·pre-mRNA prespliceosomal complexes that are functionally equivalent for both tri-snRNP recruitment and intron excision(Black et al., 2023).

A highly regulated widespread phenomenon, alternative pre-mRNA splicing contributes to proteome diversity in higher eukaryotes. Many factors are involved in AS, one of which, the serine- and arginine-rich proteins (SR proteins) family plays a pivotal role in spliceosome assembly by interacting with multiple cofactors and the RNA regulatory sequences on the mRNA(Gehring & Roignant, 2021). The reversible phosphorylation of the SR protein family along with their capacity to recruit multiple RNA sequences at high specificity facilitates regulating pathways that influence alternative splice site selection. The RS domain with repeated Arg/Ser sequences in SR proteins is subject to kinase specific phosphorylation. There are two kinase families that specifically phosphorylate SR proteins at distinct sub-cellular localisations, namely the serine-arginine protein kinases (SRPK1–3) located in both in the cytoplasm and nucleus whereas CLKs are co-localised in nuclear speckles with SR proteins(Aubol et al., 2016). Furthermore, both SR kinase systems also differ in substrate specificity and recognition, SRPKs docks groove in the catalytic domain on the C-terminal lobe to phosphorylate Arg-Ser dipeptides, CLKs on the other hand bind SR proteins with very high affinity and phosphorylate Arg-Ser and Ser-Pro dipeptides using a disordered N-terminal domain(Y. Long et al., 2019).

In contrast to mammalian, yeast, and trypanosome systems, splicing and splicing factors are largely unexplored in P. falciparum although ~54 % of the parasite genes are predicted to possess introns and >30 % of these genes possess at least two introns(McHugh et al., 2023). Since the first reports of a conserved AS event in *Plasmodium* species that gives rise to variable isoforms of blood stage antigenic P41-3 precursor (Knapp B., 1991) and the adenylyl cyclase (Muhia et al., 2003), over 100 more AS events have been reported. In addition, genome wide study for several *Plasmodium* genes implied AS as a stage-specific phenomenon required for cellular differentiation into varying cell types (Yeoh et al., 2019). Recently in *P.falciparum* full length transcriptome analysis, 393 AS events were identified in 4% of the parasite genome, 200 of which occur during blood stage replication. Subsequently, RNA decay experiments showed that RNA rapidly turn over during the early hours of post-invasion and then transcript half-lives progressively elongate during the remainder of the blood stage cycle(Yang et al., 2021).

Sequencing technologies identified five basic events that mediate alternative splicing strategies in *Plasmodium*: cassette-exon inclusion or skipping, mutually exclusive exon, alternative 5′ splice-site, alternative 3′ splice-site, and intron retention (Otto et al., 2010). Mutually exclusive exons occur during exonic splicing when only one of the two exons involves the retention of only one of a set of two exons retains in mature mRNAs and the other is spliced out (Gehring & Roignant, 2021). Alternative 3 ’and 5 ’splice site selection within exon sequences may result in subtlLe changes such as the coding sequence being extended or kinase and an additional layer of complexity arises with mutually exclusive alternative exon (Otto et al., 2010). Intron retention in lower metazoans is the most prevalent alternative splicing pattern, occurring when an intron sequence is simply retained in the transcript and not spliced out(Li et al., 2023). Introns in *P.falciparum* are comparatively short averaging 179 nucleotides (nt) and extremely AT rich at 86.5%. In human transcripts Intron retention is positioned primarily in the untranslated regions (UTRs) and involves weaker splice sites, short length introns and cis-regulatory element regulation. Intron retention occurs when an intron is included and not spliced out of the transcript. Exon skipping or cassette exon on the other hand, at 30% is the most alternative splicing prevalent pattern in vertebrates and invertebrates(Jacob & Smith, 2017). Here exons are either end up in mature mRNA or spliced out of the primary transcript and the exons maintained in mature mRNA during alternative splicing are entirely regulated by the cis-acting elements that are bound by trans-acting factors. Cis-acting elements such as exonic splicing enhancers (ESEs), intronic splicing enhancers (ISE) interact with positive trans-acting factors, such as SR proteins and exonic splicing silencers (ESSs) and intronic splicing silencers interact with negative acting factors, like heterogeneous nuclear ribo-nucleoproteins (hnRNPs)(Yeoh et al., 2019). Lastly, alternative 3′ splice-site involve exon extension or truncation at alternate 3’ end due the occurrence of an alternate splice site at either end and vice versa for alternative 5′ splicing(Hurtig et al., 2020) .

1.5 Kinase Inhibitors

Protein and lipid kinases have emerged as promising targets for therapeutic intervention, more than 500 protein kinases and about 20 lipid kinases are present in the human kinome(Grossman & Adler, 2021). Reversible kinase phosphorylation plays key regulatory roles in a number of biological processes involved in cell growth, differentiation, proliferation, angiogenesis, apoptosis, cytoskeletal rearrangement, and metabolism. Activating mutations in kinases have been linked to dysfunctions in cellular signaling pathways that drive the pathophysiology of a number of diseases and disorders such as diabetes, cancer, cardiovascular, neurodegenerative, developmental, immune, and behavioral disorders(Li et al., 2024).

Most protein kinases share a highly conserved domain which contains the ATP and substrate-binding pockets that can be clinically exploited for the development of small molecule inhibitors that reversibly or irreversibly bind the ATP binding site in a competitive but mostly not an exclusively selective manner(Olivieri et al., 2022). Based on the activation state of the target kinase, particularly the active in, inactive out dispositions of DFG-Asp, the C-helix, and the active linear, inactive distorted disposition of the regulatory spine, kinase inhibitors are be classified into six categories, Type I - VI inhibitors (Breen & Soellner, 2015).

1.5.1 Type I Inhibitor

Type I inhibitors such as “baricitinib” are ATP competitive inhibitors that not only occupy the ATP adenine binding pocket but also bind the active kinase conformation (DFG-Asp in, αC-helix in) in an ATP-like manner (Figure 1.8)(Martinez et al., 2020a). Interaction with the target kinase functions based on hydrogen bond formation between the heterocyclic motif in the inhibitor and the hinge region separating the N- and C-lobe in the kinase. The conformation of the flexible activation loop which typically holds the Asp-Phe-Gly (DFG) motif is a common control mechanism at the molecular level in most but not all kinases, that determines access to the ATP active or inactive site(Beck et al., 2022). This requirement for this conformation in addition to structural studies suggest that type I inhibitor binders are generally in-sensitive to A-loop phosphorylation and

are therefore compatible with multiple kinase A-loop conformations which is believed to translate into significant therapeutic efficacy(Tomlinson et al., 2022) . However, the presence of substrate and high intracellular levels of ATP that compete for selective binding in the highly conserved domain could contribute to discrepancies in binding profiles observed *in vitro*/*in vivo*.

Type I inhibitors are further divided into two subtypes, A and B. Subtype A inhibitors bind within minutes to hours (long residence time) and extend into different proximal regions; the front pocket region, the hydrophobic pocket region, near the gatekeeper residue, all within the region connecting the small and large lobes(Cook & Cook, 2021). Subtype B inhibitors on the other hand bind the front pocket region and gatekeeper area but not extended to the back cleft within a short residence time (seconds to minutes)(Zhong et al., 2021).

1.5.2 Type II Inhibitor

In 2001, the first kinase inhibitor, imatinib, received FDA approval. Type II kinase inhibitors, such as imatinib, do not only bind the hydrophobic pocket adjacent to the ATP binding pocket in the DFG-Asp out inactive kinase conformation but also elongate past the "gatekeeper" of the adjacent allosteric site and form hydrogen bonds with the "hinge" residues in the adenine pocket (Figure 1.8)(Mohanan et al., 2022). Structural requirements that defines a type II inhibitor binding mode include the head, hinge binder, linker, hydrogen bond, and tail. The heterocyclic head group with a hydrophobic or hydrophilic moiety recognizes the kinase hinge region. The amido linkage or urea bridge bond that traverses across the α-helix gatekeeper residues and DFG motif by hydrogen bond formation(Vijayan et al., 2015) (Keszei et al., 2023). Lastly, the tail scaffold contains a hydrophobic moiety occupies the allosteric pocket created by the flip of the "DFG" motif . Conformational analysis of the DFG-Out kinase motif and chemical structure profiling suggest the possible contribution of the DFG-out conformational reorganization to enhanced selectivity in type II inhibitors. Type IIB drugs occur within the front cleft and gate area while the type IIA drugs occur in the front cleft, gate area, and extend into the back cleft. Based upon this conserved binding mode and the available biochemical data, type II inhibitor

binding is believed to be sensitive to A-loop phosphorylation(Vijayan et al., 2015).

1.5.3 Type III Inhibitor

Type III inhibitors regulate kinase activity by binding to the allosteric site close to the neighbouring inducible pocket or rear pocket such as with the MEK inhibitor “cobimetinib”, but do not interact with the hinge region and include molecules that bind in the hydrophobic pocket formed in the enzymatically inactive DFG-out confirmation (Figure 1.8)(Martinez et al., 2020a). Allosteric kinase inhibitors are mechanistically diverse as they may inhibit different protein–protein interactions targets outside the highly conserved ATP pocket and have been proposed to often give high kinome selectivity (Roskoski 2016). These can be further divided into two subtypes, namely Type IIIA and Type IIIB. MEK1/2 inhibitors, which bind at a particular cavity close to the ATP-binding site, are some of the well-studied type III inhibitors. Trametinib, Selumetinib, Binimetinib, and Cobimetinib are allosteric inhibitors of MEK and are among the MEK inhibitors currently approved by the FDA(P. Y. Lee et al., 2023).

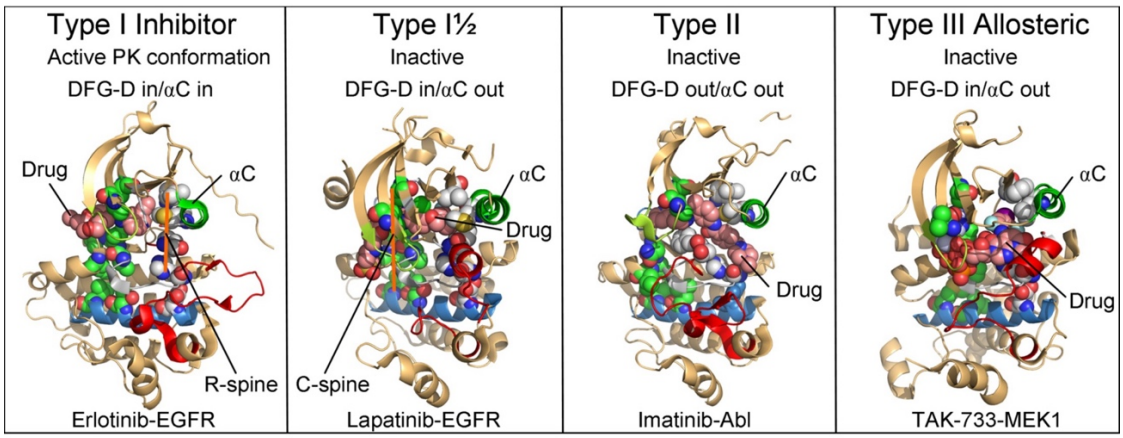

Figure 1.8 Classification of small molecule protein kinase inhibitors.
This is based upon the structures of their drug-enzyme complexes. Robert Roskoski (2016).

1.5.4 Type IV Inhibitor

A relatively new area in the development of selective kinase inhibitors has focused on targeting regions distant from the ATP-binding site, such as the allosteric pockets at the C-lobe, on the surface of the kinase domain, or at the N-lobe, which are binding targets for type IV inhibitors (Das et al., 2022). Also

known as substrate-directed inhibitors, type IV inhibitors do not bind to the ATP or peptide substrate binding sites but can instead alter enzymatic activity by disrupting the access to upstream activators or by preventing the phosphorylation of select downstream substrates. The pleiotropic effect of type IV kinase inhibitors may be exploited to selectively disrupt phosphorylation functions associated with a particular disease without blocking other beneficial kinase functions (Martinez et al., 2020).

1.5.5 Type V, VI and VII Inhibitors

Type V inhibitors are bivalent or bisubstrate compounds that target two different regions of the protein kinase domain, both the ATP-binding site and a unique structural feature found on a specific protein kinase (Nishal et al., 2022a). Several MAP kinases that specifically target the cSrc tyrosine kinase are currently being investigated to circumvent the challenge of developing inhibitors that can potentially block kinases through type I or II mechanisms of action irrespective of the highly conserved kinase domains(Martinez et al., 2020a).

Type VI such as afatinib, neratinib, ibrutinib, and dacomitinib are covalent inhibitors with the ability to interact with the cysteine nucleophiles in the pivot area of the ATP-pockets and through a Michael addition reaction, forms a covalent adduct (Martinez et al., 2020; Serafimova et al., 2012). Although reactions with lysine, aspartic acid, and tyrosine residues can be used to form covalent interactions, however what makes the type VI protein kinase inhibitors unique is the inclusion of reactive electrophilic acrylamide groups or warheads that primarily favor interactions with nucleophilic cysteines. Similarly to other drug discovery approaches, type VI inhibitors are designed with structure-guided approaches that exploit noncovalent interactions with the targeted kinase to increase specificity bias and position the warhead component to lock the inhibitor in place for targeted covalent interaction(Yoshimori et al., 2022) .

The Type VII inhibitors are classified as non-classical allosteric inhibitors that specifically target a receptor tyrosine kinase's extracellular domain(P. Y. Lee et al., 2023). These inhibitors are less potent than other types of inhibitors and do not directly prevent binding at the kinase domain/ligand-polypeptide binding site. SSR128129E and WRG-28 are two examples of this type of kinase inhibitor,

which inhibits the FGFR (extracellular domain of fibroblast growth factor receptor) family and DDRs (discoidin domain receptors), respectively(Nishal et al., 2022) .

1.6 Thesis Aims

History has demonstrated the inevitable emergence of *P. falciparum* resistance-associated mutations to nearly all antimalarials poses an ongoing dynamic challenge to malaria control and eradication strategies (Ippolito et al., 2021). Therefore, there is an urgent need to identify and validate drug targets for the development of new therapeutic agents or drug combinations with different modes of action and the capability to treat parasite strains resistant to present frontline antimalarials. This ambitious goal necessitates an in-depth understanding of the parasite's biology that is required for antimalarial drug discovery to make the shift from phenotypic screening toward target-based approaches(Forte et al., 2021).

Using whole genome sequence technology and reverse genetics, our group has established key phospho-signalling pathways in parasite development mediated by short listed 36 protein kinases, with focus on the role of *P. falciparum* CLK (cyclin-dependent–like kinase) family in RNA splicing processes required at all stages of the life cycle(Alam et al., 2015).

The work presented here builds upon the work of my supervisor in Mahmood M. Alam et al. 2019, "Validation of the protein kinase P*f*CLK3 as a multistage cross-species malarial drug target". To successfully accomplish the study on developing small drug like molecules as potential kinase inhibitors, this present study is conducted to characterise the role of another member kinase of the parasite CLK family, P*f*CLK1 in the context of development. Firstly, establishing the protein expression profile and biochemical characterisation of both kinases by means of Western blot analyses and TR-FRET assays. Both kinase genes were isolated in recombinant bacterial systems with histidine residues at the C-terminal for protein expression. Further separation strategies exploited the His-Tag for affinity chromatography to purify target proteins from whole bacterial cells. Given the chemistries for the phosphotransfer reactions catalyzed by P*f*CLKs on donator or acceptor protein substrates, subsequent phosphorylation

studies evaluated the in vitro enzyme activity by quantifying FRET dependent signals of the phosphorylated substrate. Findings show a direct proportion in increased kinase concentration to emission wavelength of the phosphorylated substrate. Preliminary investigations were undertaken into the interaction between inhibitor molecules JZ208105-178D1, HGC-001753 0023-NX-1 (Figure 1.9) and the conserved catalytic domain of both CLKs. Inhibitory effects of both compounds *in vitro*, is characterized by an ATP-dependent decrease in previously established substrate levels required for activity in both member kinases. Lastly, for the purpose of defining specific inhibition *in vivo*, a combination of viability, stage susceptibility and gametocyte toxicity assays were used on the asexual stages and gametocyte development.

Three results chapters cover the data gathered during the period of study: Protein expression and catalytic characterizations of the CLKs are covered in Chapter 3, inhibitory characterization is covered in Chapter 4, and data pertaining to plasmodial stage specificity in Chapter 5. Discussion of the results will take place primarily in the context of the results chapters, with a general discussion and conclusion chapter (Chapter 6) at the end.

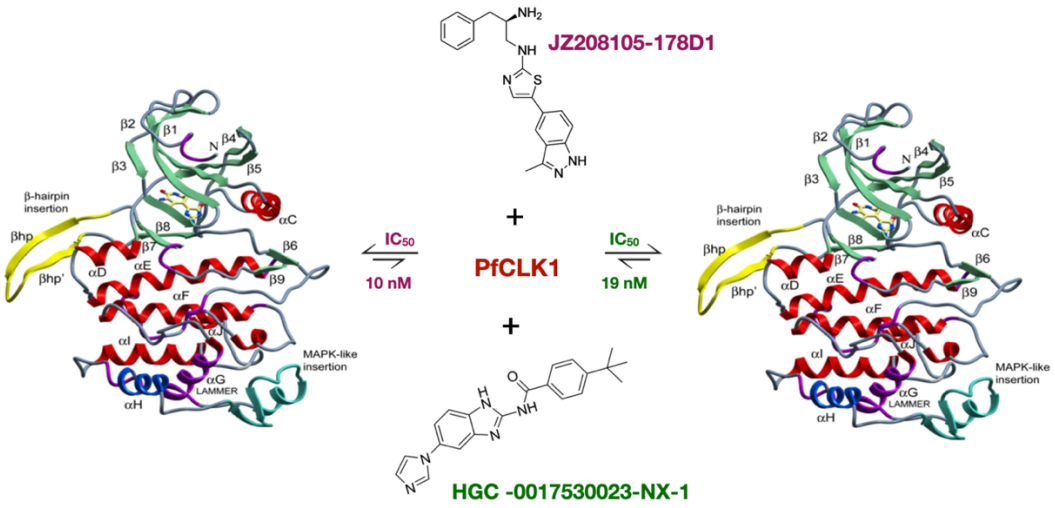

Figure 1.9 Graphical abstract.
Showing the structures of hit molecules and their respective potency towards P*f*CLK1.

Chapter 2 Materials and Methods

2.1 Materials

2.1.1 Pharmacological compounds

JZ208105-178D1- synthesised by The Jamieson group, University of Glasgow.

TCMDC-135051 - synthesised by The Jamieson group, University of Glasgow.

HGC-0017530023-NX-1- synthesised by HitGen, Cambridge England.

Artemisinin – gift from Keltic Pharma Therapeutics, University of Glasgow.

Chloroquine- gift from Keltic Pharma Therapeutics, University of Glasgow.

2.1.2 General Materials and Reagents

Acrylamide Bis-Acrylamide Stock Solution, 30% Acrylamide (w/v) Ratio 37.5:1 (Severn Biotech Ltd) .

Albumax II (Thermo Fisher Scientific).

Ampicillin (Sigma-Aldrich).

Brilliant III Ultra-Fast SYBR Green (Agilent) .

Calcium chloride solution (Sigma) .

cOmplete™, Mini, EDTA-free Protease Inhibitor Cocktail (Sigma-Aldrich) .

Dulbecco's Phosphate Buffered Saline (PBS) (Thermo Fisher Scientific).

EDTA 0.5M, pH 8.0 (Invitrogen).

Isopropyl B-D-1 thiogalactopyranoside (IPTG) (Sigma-Aldrich).

LANCE anti-P-MBP (Revvity Inc).

LANCE anti-P-Creptide (Revvity Inc).

LANCE Ultra U*Light* myelin basic protein (MBP) (Sequence: CFFKNIVTPRTPPPSQGK-amide) peptide (Revvity Inc).

LANCE *Ultra* U*Light*™- Creptide peptide (sequence: CKRREILSRRPSYRK) (Revvity Inc).

LANCE detection buffer (Revvity IncS).

Nickel-nitro acetic (Ni-NTA) beads (Sigma-Aldrich).

Precision Plus Protein All Blue Prestained Protein Standards (Bio-Rad)).

Sodium chloride (Sigma-Aldrich).

Tryptone (Sigma-Aldrich).

Yeast extract (Sigma-Aldrich).

2.1.3 Kits

High pure plasmid isolation mini kit (Roche Applied Science).

QIAfilter® maxiprep kit (Qiagen).

2.1.4 Recipes for buffers and solutions

Bradford reagent - 30 mg/ml Coomassie Brilliant Blue, 5.0% (v/v) orthophosphoric acid.

Coomassie Brilliant Blue solution -1 g/l Coomassie Brilliant Blue, 50% (v/v) methanol, 10% (v/v) acetic acid.

DNA loading dye 6X - Bromophenol Blue 0.25% (w/v) xylene cyanol FF and 30% (v/v) glycerol.

L-Broth Medium (LB) - 10g Tryptone, 5g Yeast extract, 10g NaCl.

Lysis Buffer - 20mM Tris pH 8, 150mM NaCl2, 25mM imidazole.

Elution Buffer - 20mM Tris pH 7.4, 150mM NaCl2 ,350mM imidazole.

Dialysis Buffer - 20mM Tris pH 7.4, 150mM NaCl2 , 1mM MgCL2, 1mM DTT.

PBS -140mM NaCl 3mM KCl, 1.5mM KH_2HPO_4, 8mM Na_2HPO_4 .

SDS-PAGE gel resolving buffer - 75mM Tris-HCl, pH 8.8, 0.2% (w/v) SDS.

SDS-PAGE gel stacking buffer - 25mM Tris-HCl, pH 6.8, 0.2% (w/v) SDS.

Tris-Glycine SDS Running buffer - 5 mM Tris-Cl, 250 mM glycine, 0.1% SDS.

2.1.5 Parasite culture

A summary of materials used in parasite culture are listed in table 2.1

Table 2.1- Parasite culture materials.

Materials	Supplier
RPMI 1640 medium Gentamycin sulphate Albumax ii HEPES free acid Sodium bicarbonate Glutamax Hypoxanthine D glucose Dulbecco's phosphate buffered saline (PBS)	Thermo Fisher Scientific
Sorbitol	Merck Life Science
Percoll	Cytiva Life Sciences
Giemsa stain solution	Sigma-Aldrich

2.1.6 Bioinformatic tools and online applications

Plasmodb database (http://plasmodb.org/plasmo/)

Clustal Omega (https://www.ebi.ac.uk/Tools/msa/clustalo/).

NCBI database (https://www.ncbi.nlm.nih.gov).

2.1.7 Specialised equipments

CLARIOstar microplate reader (BMG-Labtech).

ImageJ software (Version *1.54j, National Institutes of Health).*

EVOS™ 5000 Imaging system (Thermo Fisher Scientific).

Zeiss Labscope Microscope software (Zeiss).

2.1.8 Bacterial strains

XL-1 Blue competent cells (Agilent Technologies).

BL21 (DE3) Competent *E. coli (New England Biolabs).*

2.1.9 DNA and plasmid constructs

A summary of plasmid vector DNA constructs used during this research are listed in table 2.2.

Table 2.2- Plasmid vector DNA constructs.

Plasmid vector description	Supplier
PfCLK3 pLEICS-05 vector – 6x Histidine + Ampicillin resistance. Kinase domain P*f*CLK1 pLEICS-05 vector – 6x Histidine tag + Ampicillin resistance.	PROTEX, (Protein Expression Laboratory) department, University of Leicester.
Full length P*f*CLK1 pET-21a – 6x Histidine tag + Ampicillin resistance.	GenScript.
P*f*CLK3_G449P	Dr Mahmood Alam, University of Glasgow.

2.2 Molecular and Biochemical Methods

2.2.1 Bacterial growth

Transformed *Escherichia coli* (*E. coli*) cells were maintained at 37˚C on Luria broth (LB) agar plates (1% w/v sodium chloride, 1% w/v tryptone, 0.5% yeast extract and 1.5% agar) containing the appropriate antibiotics concentrations overnight. After overnight incubation, presence of bacterial colonies indicates growth of the respective cells with the transformed plasmid. LB media (1% w/v sodium chloride, 1% w/v tryptone and 0.5% yeast extract) was used for expression of large volumes of bacteria shaking at 220- 250 rotations per minute (rpm). The cells are initially grown at 37˚C until an optical density (OD) of between 0.6-0.8 before they are induced with IPTG. For induction, cells were incubated with 100 µM of IPTG either at 37˚C for the CLK3 kinases and at 22^0C for CLK1 4 hours.

2.2.2. Bacterial Transformation

Plasmids of the target sequence were transformed into chemically competent BL21-CodonPlus (DE3)-RIPL cells . These cells increase the supply of rare *E. coli* tRNA that corresponds to codons used more frequently by other organisms; they contain extra copies of the *argU*, *ileY*, and *leuW* as well as additional tRNA genes. For transformation, 0.5 - 1 µg of plasmid DNA was aliquotted into sterile 15 ml round- bottom polypropylene Falcon tubes (Catalogue number: 14-959-12A) on ice. To the plasmid DNA, 50 - 100 µl of the competent cells previously thawed on ice (usually for 10 minutes) were added, mixed gently, and incubated on ice for 30 minutes. The mixture was heat-pulsed at 42^0C for 20 seconds for BL21 Codon Plus cells or 45 seconds for XL1-Blue cells and immediately returned on ice for 2 minutes. Five hundred millilitres of Super Optimal broth with Catabolite repression (SOC) media (0.5% w/v yeast extract, 2% w/v tryptone, 1 mM NaCl, 2.5 mM KCl, 10 mM MgCl2, 10 mM MgSO4, 20 mM glucose) was added to the mixture and incubated at 37˚C shaking at 220 rpm for 1 hour. With NEB 5-alpha competent *E coli* (High efficiency), transformation was similar to BL21 and XL1 blue cells except that they were heat sock for 30 seconds and incubated on ice for 5 minutes instead of 2 minutes prior to addition of SOC media. Following incubation, 50 - 100 µl of the cell suspension was spread onto LB agar plates

containing the appropriate antibiotics and incubated at 37˚C overnight. Successfully transformed cells will grow as single colonies on the plates. The plates were sealed with Parafilm and stored at 4^0C until needed.

2.2.3. Plasmid DNA preparation

Following transformation, bacterial cells that have taken up the plasmid were enhanced to propagate by the antibiotic selection. Isolation of plasmid DNA was carried out using mini prep plasmid isolation kit Qiagen, UK.

2.2.4. Plasmid DNA and nucleic quantification by nanodrop

Concentrations of isolated plasmid DNA and nucleic acids were determined by measuring absorbance at 260 nm wavelength using NanoDrop Microvolume Spectrophotometer 3300 (NanoDrop). At this wavelength, an absorbance of 1 is equivalent to 50 µg DNA per ml. Highly concentrated samples were diluted 1:100 µl before quantification. Sample purity was determined by measuring absorbance at 280 nm and a ratio of A260/A280 of 1.8 - 2.0 indicates a pure sample.

2.2.5. Protein expression and purification

The generated plasmids were chemically transformed into competent *Escherichia coli* BL21-CodonPlus (DE3)-RIPL cells (Stratagene cat No- 230280) and grown on Luria Broth (LB) agar at 37˚C overnight. A single colony was used to setup in 50 ml of overnight primary culture and 1-2% of the primary culture was inoculated in 500 ml secondary culture with 50 µg/ml of ampicillin and chloramphenicol as antibiotic. After the cells reached the mid-log phase of growth with optical density (OD_{600}) between 0.6 and 0.8, 100 µM IPTG (Isopropyl ß-D-1-thiogalactopyranoside) was used to induce the production of *Pf*CLK1 at 22^0C and *Pf*CLK3 at 37˚C shaking for 4 hours at 220 rpm. Cells were then harvested by centrifugation at 8000 xg for 15 minutes and lysed by sonication in lysis buffer containing 20 mM Tris, 150 mM NaCl and 20 mM Imidazole, pH-8.0. The lysate was purified using nickel- nitrilotriacetic acid (Ni-NTA) affinity chromatography and eluted in elution buffer containing 20 mM Tris, 150 mM NaCl and 350 mM Imidazole pH-7.4. The protein was dialyzed overnight

in dialysis buffer containing 20 mM Tris and 150 mM NaCl pH-7.4 at 4^0C and finally stored at -80^0C in 10% glycerol. All the mutant forms of plasmids used in this project were generated by site directed mutagenesis PCR from these parent plasmids.

2.2.6. *In-vitro* kinase activity assay

Kinase assays for *Pf*CLKs were carried in kinase buffer containing (20 mM Hepes, pH 7.4, 10 mM $MgCl_2$, 1 mM DTT, 50 µM adenosine triphosphate (ATP), 0.1 MBq γ-32P-ATP) using 0.5 µg purified recombinant protein kinases. As exogenous substrate, kinases were incubated with 2 µg histone type IIA; 2 µg myelin basic protein (MBP); and 2 µg α-Casein for 30 minutes at 37˚C. Kinase reactions were stopped by adding equal volume of 2X Laemmli sample buffer (12.5 mM Tris-base, pH 6.8, 4% SDS w/v, 20% glycerol, 50 mM DTT and 0.01% bromophenol blue) to give a final 1X concentration. Samples were incubated for 5 minutes at 60^0C and centrifuged for 1 minute at 1200 rpm. 25 µl of each sample was separated on 12% SDS-PAGE ran at 180 V for at least 60 minutes. Gels were stained with Coomassie and dried by means of vacuum gel drying. Dried gels were exposed to X-ray film overnight at -20^0C and autoradiography collected the phosphorylation signal.

2.2.7. Time Resolved Florescence Energy Transfer (TR- FRET)

Biochemical kinase assays were carried out using time-resolved florescence energy transfer (TR-FRET) to determine kinase activity, $ATPK_m$ and IC_{50} (concentration of inhibitor to reduce kinase activity by half) values for the respective enzymes. TR- FRET reactions were performed using the appropriate amount of kinase (5 nM for *Pf*CLK1 and 50 nM for *Pf*CLK3 wild type and mutant, G449P) in a kinase buffer (containing 50 mM HEPES, 10 mM $MgCl_2$, 2 mM DTT, 0.01% Tween 20, and 1 mM EGTA), U*Light*-labeled peptide substrate (MBP peptide (sequence: CFFKNIVTPRTPPPSQGK) and CREPtide (Sequence: CKRREILSRRPSYRK)) and the corresponding europium-labeled anti-phospho antibody in two steps. First, in a 10 µL reaction volume, 5 µl of twice the required enzyme concentration and 5 µl of twice the required substrate concentration mix containing cold ATP were incubated in a black 384 plate well

plate at 37˚C for 1 hour. Following incubation, 30 mM EDTA in 1X Lance detection buffer containing 3 nM Europium-labeled anti-phospho specific antibody is added to the plate to stop the reaction and enhance detection. This mixture was incubated at RT for 1 hour and then the signal read using the ClarioStar. Kinase substrate phosphorylation results in the Europium-labeled anti-phospho specific antibody recognizing the phosphorylated site on the substrate. The Europium donor fluorophore is excited at 320 or 340 nm and energy is transferred to the U*Light* acceptor dye on the substrate, which finally results in the emission of light at 665 nm. The level of U*Light* peptide phosphorylation correlates with the intensity of the emission. To test for inhibition by small molecules such as TCMDC-135051, JZ208105-178D1 and HGC-0017530023-NX-1 serial dilution of the inhibitor (made at four times the required concentration) was made and added to the protein mixture before adding the substrate mix at four times the required concentration. For normalization, a no kinase and a no inhibitor reaction wells were included and all experiments conducted in triplicates.

2.3 *Plasmodium falciparum* culture

P. falciparum parasite culture was done in RPMI media supplemented with 100 µM hypoxanthine, 25 mM Hepes, L- glutamine and 12.5 µg/ml gentamicin as antibiotic and 0.5% (w/v) Albumax I. For continuous culture, the parasites were kept at 4% haematocrit in human erythrocytes from donors and between 0.5 - 3% parasitaemia incubated at 37˚C in an incubator maintained at 5% carbon dioxide (CO_2), 5% oxygen (O_2) and 90% nitrogen (N_2) in a 37˚C incubator. Cultures were only manipulated in laminar flow cabinets using standard aseptic techniques. Gloves and personal protective equipment were used at all times and all materials used were sterile. Incomplete RPMI medium was used for all washes.

2.3.1 Geimsa staining and slide microscopy

To monitor parasites for continuous growth by microscopy, thin blood smears were prepared. To prepare a thin smear, about 5 µl of blood was taken from the culture plate and a thin smear is made on a frosted slide using a cover slide. The smear was air-dried quickly with the aid of a hair-drier and fixed with absolute methanol in a Coplin jar by dipping the slide for about 20 seconds. The air- dried

slide was stained with 10% Giemsa stain in buffered water pH 7.0-7.2 (1:10, v/v) for 15 minutes. Slides were washed under a running tap water, air-dried, and then observed with 100X eyepiece objective lens using a light microscope.

2.3.2 Culture synchronisation

Parasites were synchronised using one of two techniques or both: sorbitol – it is versatile and simple to perform and concentrate the young stages of the parasite whereas Percoll helps concentrate the older parasite stages mainly the mature schizonts (Roncalés et al., 2015). For tighter synchronisation, two-step synchronisations were employed.

Sorbitol synchronisation is based on the differential permeability of parasitized erythrocyte membranes. Mature forms of the malaria parasites induce structural modifications to erythrocytes resulting in them being permeable to sorbitol to which they are naturally impermeable. With this property, erythrocytes containing the mature forms of the parasites are selectively killed due to the osmotic shock, and the uninfected and ring stage parasitized erythrocytes remain unaffected (Roncalés et al., 2015).

For sorbitol synchronisation, cultures were spun down and the supernatant discarded. To the pellet, 9 volumes of pre-warmed 5% sorbitol (w/v) solution was added and mixed vigorously by vortexing for 30 seconds. Parasite-sorbitol mixtures were then incubated at 37˚C for 10 minutes shaking at 240 rpm. The mixture was centrifuged at 250 xg for 5 minutes at 37˚C and a red coloured supernatant was observed, indicating lysis of RBCs containing mature parasite forms. This was discarded and the remaining pellet washed twice with 10 ml of wash media. After washing, smears were prepared to assess ring enrichment and confirm the absence of mature parasite forms. Parasitaemia was confirmed at this stage before proceeding with any further experiments.

The 70% Percoll, the wash media and the complete media were warmed to 37˚C before starting. Cultures were centrifuged at 250 xg for 5 minutes at 37˚C and supernatant discarded saving the red cell pellets. For easy recovery of mature forms, as much of the supernatant as possible was removed to help get a thin upper layer of schizonts in the tubes after centrifugation for collection. To 15 ml tubes, 4 ml of 70% Percoll (v/v) was added. To the top of the Percoll, 0.5 - 1 ml of the pelleted infected erythrocytes were gently added by carefully pouring

down the side of the tube with a pipette aid to avoid mixing the Percoll and the RBC. The Percoll-RBC tube was then centrifuged at 1200 xg for 10 minutes at 37˚C without brakes. The top layer containing schizonts and late trophozoites parasitized erythrocytes were removed using sterile plastic Pasteur pipette and transferred to a fresh 15 ml tube. This was washed twice with wash media, a slide prepared and assessed before adding an appropriate volume of blood for continuous culture in 10 ml growth media.

2.3.3 Determining 50% effective concentration (EC_{50}) of inhibitor compounds

Drugs were dissolved either in water or dimethyl sulfoxide (DMSO) as stock solutions and diluted to intermediate and working solutions in complete growth media. Starting concentrations in nanomolar and the dilution factors of individual drugs are as shown in the tables below. The dilutions, at twice the required final concentrations were made in 96 deep-well plates and stored in aliquots of 50 µl at -20^{0}C in black assay plates. EC_{50s} were determined using cultures between 0.5- and 1% parasitaemia of young rings at 4% haematocrit maintained at 5% carbon dioxide (CO_2), 5% oxygen (O_2) and 90% nitrogen (N_2) in a 37˚C incubator. Standard antimalarial drugs used were Artemisinin and Chloroquine (MFQ). To set up the drug plates, parasites were prepared at 8% haematocrit (2X required) at the required parasitaemia and equal volume (50 µl) and added to the previously diluted drug plates and mixed by pipetting up and down several times. This gives a final culture volume of 100 µl at the required drug concentration and haematocrit. To the 'no drug' control, growth media was added, and the respective stock drug concentrations were added to the kill well (contains high concentration of chloroquine to kill all parasites) to confirm killing for each plate. The outer wells of the plates without cultures were filled with media to reduce evaporation from the experimental wells and the plates incubated. After about 48 hours (±2 hours), the plates were monitored for growth by making a thin smear from the control wells to confirm developmental stage. Plates were only harvested for reading if the parasites grew to the next generation of rings otherwise, they are allowed to grow until they re-invade. The plates were collected and frozen at least overnight to enhance lysis of the red blood cells for staining of parasite DNA.

For quantification, previously frozen plates were thawed at room temperature for at least 1 hour and 100 µl of lysis buffer (20 mM Tris-HCl; 5 mM EDTA; 0.004% saponin and triton X-100) in PBS containing Sybr Green I (1 µl in 5 ml) was added to each well and mixed by pipetting up and down several times. The plates were then incubated at RT for 1 hour shaking in the dark. Using a Fluroskan plate reader at excitation of 485 nm and emission of 538 nm, plate absorbances were acquired and percentage growth calculated using the formula below. Analysis and graphs were generated using Graph Pad Prism 7 and the EC_{50} values were determined using the non-linear regression log (inhibitor) versus response (three parameter) curve.

2.3.4 Drug treatment for parasite killing rate fast assay

The conditions for the parasite reduction rate assay were chosen to mimic those used for standard EC_{50} determination (2% haematocrit, 0.5% parasitaemia with ≥80% ring stages). Asynchronous cultures were incubated at 37˚C for the required time. A culture volume of 50 µl per well with parasites at 4% haematocrit and 0.5% parasitaemia was dispensed into flat- bottom, 96 well plates containing 50 µl of previously diluted drugs prepared to give a final volume of 100 µl per well. Four drug concentrations were tested; 1, 5, 10 and 100X the respective EC_{50} values earlier determined. Treated samples were exposed to drugs for 24, 48, and 72 hours at 37˚C using standard incubation conditions. Drugs were replenished every 24 hours by replacing the old drug with fresh media containing drug at the required concentration. After each time point, drug pressure was removed by washing twice with complete media. For removal, 80 µl of media containing drug was removed and 100 µl media added to the remaining culture. The plates were then centrifuged at 1200 rpm for 10 minutes and 100 µl media removed again; the same is repeated to ensure complete removal of the drugs. The washed parasitized cells were then re-suspended to 100 µl of growth media. Plates were then incubated for 48 hours at 37˚C to allow new infections to develop as a measure of the presence of viable parasites. Control wells containing no drug were setup and treated identical to the experimental wells. The outer wells of the plate were filled with incomplete media to avoid evaporation from the experimental wells.

2.3.5 Parasite stage susceptibility assay

Standard asexual blood stage susceptibility results were collected by exposing synchronous 3D7 parasite cultures to 10 different concentrations plus no-compound controls for 72 hr. To determine the specific asexual blood stage at which the compounds are active, schizonts were synchronized with 5% sorbitol. These parasites were then plated in five 96-well plates and exposed to compounds as early rings (0-10 hr), late rings (10-20 hr), early trophozoites (20 - 30 hr), late trophozoites (30 -40 hr) or schizonts (40 -50 hr). Incubation times were adjusted to the 40 hr asexual blood stage cycle of the 3D7 parasite line. Synchronicity of the cultures was confirmed by imaging parasites per time point in control conditions. Compounds were removed through three rounds of washing including two plate changes in 37°C prewarmed culture media after each exposure. For the stage specificity assay, growth inhibition was assessed at the 60 hr time point at which parasites had expanded, reinvaded new RBCs, and developed into the trophozoite stage for quantification. This is very similar to the standard 72 hr assay in which parasites are allowed to reinvade and develop further for another half life cycle. Parasite survival for both the 72 hr and stage-specific 10 hr exposures was assessed by SYBR Green staining. EC_{50} values were derived from growth inhibition data using nonlinear regression (Prism 7, GraphPad). All asexual blood stage assays were repeated on at least three independent occasions with two technical replicates.

2.3.6 Parasite stage inhibition - morphology assay

To evaluate which parasite blood stages are most sensitive to JZ208105-178D1, cultures of synchronised *P. falciparum* 3D7 parasites were set up and parasites treated with JZ208105-178D1 at time point 0, 10, 20, 30, and 40 hours to a final concentration of 1 μM and allowed to grow for 70 hours. For morphological analysis of JZ208105-178D1 treatement, thin blood smears were collected every 10 hours from time point 0, 10, 20, 30, and 40 hours. The slides were stained with 10% Giemsa and parasite development stages determined by light microscopy and images were taken for all the time points at 100X magnification.

2.3.7 Gametocyte toxicity assay

In this study, gametocyte toxicity assay was utilized to evaluate the capacity of CLK inhibitors to inhibit gametocytes at their early stages, therefore preventing the formation of mature gametocytes, which is necessary for parasite transmission. *P.falciparum* wild type parasites were cultured at high parasitemia to promote gametocyte commitment. Upon obtaining stage II gametocytes, 1 ml of culture was aliquoted in triplicates in a 24-well-plate in the presence of respective inhibitor EC50 concentrations. As positive control. DMSO was used as solvent control, as all tested inhibitors were

solved in DMSO. The aliquots were cultivated within the influence of the inhibitors for 48 h. After the 48 h-treatment, the cultures in the wells were further maintained for additional five days to allow healthy gametocytes to mature to stage IV and V in compound-free medium. Medium was replenished daily by replacing 800 µl compound-free medium. At day 7, Giemsa- stained blood smears were prepared and gametocytemia was monitored by counting the numbers of gametocyte stages IV and V in a total amount of 1 000 erythrocytes per inhibitor/well. The gametocytes in each setting were counted in triplicates. Two independent experiments were performed and the mean gametocytemia was calculated for each compound. Data from the experimental cultures was normalized to the DMSO control, which was set to 100 %.

2.4 Data analysis

Statistical analyses were carried out using GraphPad Prism 9 software. For statistical analysis of differences between groups of measures, data were assumed to be normally distributed and were therefore compared using parametric tests. Generally, either two-tailed unpaired student's t test (for two groups) or two-way ANalysis of Variance (ANOVA) (for three or more groups).

Furthermore, one-way ANOVA and two-way ANOVA were used to analyse the

effect of factors on a variable response. One-way ANOVA examined the influence of a single factor, comparing means across multiple groups. Two-way ANOVA assessed the combined effect of two factors and their interaction on the response variable (Armstrong et al., 2002).These analyses allowed for the

identification of significant differences among groups or levels of a factor, as well as the examination of main effects and interaction effects. By using one-way ANOVA and two-way ANOVA, this thesis gained insights into how factors affected the variable response and drew meaningful conclusions from the data analysis.

For experiments with drugs concentrations Concentration–effect curves obtained from functional assays were fitted according to a four-parameter logistic equation in GraphPad Prism 9 to determine EC_{50} for each compound.

The collected data is subjected to curve fitting, which involves fitting a mathematical model to the data points. Common models used for curve fitting include the sigmoidal dose-response models in linear models (such as the linear regression). Once the curve is fitted to the data, the potency of the compound can be calculated. The potency is typically defined as the concentration or dose of the compound required to produce a specific response level (e.g., 50% of the maximum response). This value is often referred to as the EC_{50} (effective concentration 50%) or IC_{50}. Curve fitting and potency calculations are essential components in determining the potency of a compound and evaluating its activity. These techniques provide quantitative measures of the concentration-response relationship and help determine the potency values with statistical confidence.

Chapter 3 Enzymatic parameters of PfCLK1

Introduction

In other eukaryotes, the CLK family regulate mRNA splicing through phosphorylation of Serine/Arginine-rich proteins and have been extensively studied, making them attractive targets for drugs (Dekel et al., 2020). Consistent with its role as a CLK kinase, CLK1 is involved in the phosphorylation of SR proteins, a process required for SR proteins to leave nuclear speckles and move to sites of active RNA polymerase II (Pol II) transcription for pre-mRNA binding and downstream co-transcriptional splicing (Song et al., 2023). The release of SR proteins from CLK1 has been shown to be facilitated by another kinase SRPK1 in what is referred to as a "symbiotic kinase system"(Figure 3.1) (Aubol et al., 2016). In humans, dysregulated or nonfunctional splicing contributes to the development and progression of neurodegenerative disorders, hypercholesterolemia, and various viral infections, for instance CLK1-mediated phosphorylation of SR proteins has been shown as a key mechanism that is implicated in the development of Cancer (L. Wan et al., 2022). Given the demonstrated essentiality of alternative splicing in eukaryotic cell cycle mechanisms, these kinase family was studied in *P.falciparum* to unravel mechanisms of splicing regulation across all stages of the life cycle as part of an effort to the identify new drug targets (Ong et al., 2023).

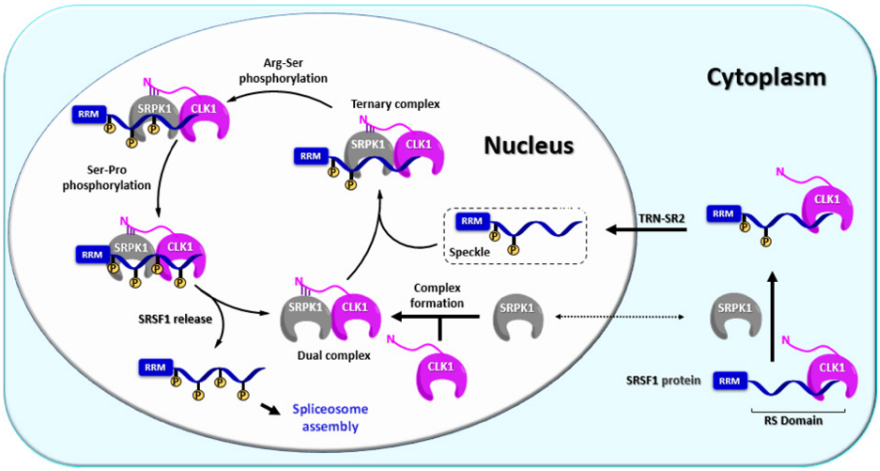

Figure 3.1 Schematic representation of the phosphorylation mechanism involving CLK1. In this process, CLK1 and SRPK1 work co-operatively as a complex. The complex containing CLK1 in active form first recruits hypo-phosphorylated SRSF1 from nuclear speckles which act as a pool of SR proteins in the nucleus, whereby a ternary complex CLK1-SRPK1-SRSF1 is formed. The ternary complex executes full phosphorylation of SRSF1 and subsequently releases it (Aubol et al., 2016).

Previous studies have demonstrated the genetic essentiality of CLKs in *asexual* blood stages and gametocyte development. Using reverse genetics all four P*f*CLKs were confirmed as indispensable for the completion of the asexual replication cycle and were found predominantly present in the nucleus of the parasite during the trophozoite stages switching to cytoplasmatic localization in schizonts and gametocytes (Kern et al., 2014). In addition, *in vitro* studies revealed putative substrates such the Sky1p substrate, splicing factor Npl3p, and the plasmodial SR protein alternative splicing factors P*f*ASF-1, P*f*SRSF12, P*f*SFRS4 and P*f*SF-1 that were phosphorylated by P*f*CLKs for splicing regulation (Agarwal et al., 2011). The combined literatures point to these kinases as attractive targets for antimalarial and transmission blocking drug development. (Rezende Lima et al., 2016).

Based on this premise, a study by our group developed a selective and specific inhibitor that was used to validate P*f*CLK3 as an essential kinase. Two inhibitor compounds that displayed specificity towards the second member kinase P*f*CLK1 have been identified from a library screen and are being developed towards polypharmacology or in combination therapy as part of the efforts to circumvent the emergence of potential parasite resistance to new drugs. The quantitative enzymological studies of P*f*CLK1 used in the P*f*CLK3 validation studies have primarily been limited to soluble, active fragments of the kinase domain. Although much has been learned from these studies, a complete picture of P*f*CLK1 kinase activity is necessarily lacking. And a caveat of using only the kinase domain for kinase-targeted drug discovery is that the more divergence from the natural protein, the more probable it is to likely miss compounds that work under physiological conditions or to identify compounds that lack the physiologically relevant mechanism (Doğan et al., 2021).

This chapter covers the approaches and methods employed to characterise full length P*f*CLK1 (PF3D7_1445400) as a potential start point for pharmacological inhibition. Member kinase P*f*CLK3 and the kinase domain P*f*CLK1 were used as positive controls to establish the biochemical characterisation of the full length P*f*CLK1. Therefore, this chapter aims to:

- Optimise expression of recombinant full length P*f*CLK1 proteins using P*f*CLK3 and kinase domain P*f*CLK1 as expression controls
- Determine full length P*f*CLK1 kinase activity, using the established TR-FRET assay as default plus other kinase assay kits
- Use P*f*CLK3 as control to establish P*f*CLK1 as a reliable and reproducible start points for the downstream characterisation of compounds JZ208105-178D1 and HGC-0017530023-NX-1 in the next chapter.

3.1 Results

3.1.1 Kinase domain *Pf*CLK1 phosphorylates exogenous substrate proteins and U*Light* peptides in biochemical assays.

The kinase gene is recombinantly expressed as protein for use in downstream applications to investigate small molecule-protein interactions. This will help guide in understanding how they control the parasite biology. The full length P*f*CLK3 gene amplified from cDNA and the P*f*CLK1 kinase domain truncated from residues phenylalanine- 552 to leucine-874 at the C-terminal catalytic domain were cloned into a C- terminal His-tagged pLEICES-05 vector. The full length P*f*CLK1 gene sequence was obtained from Plasmodb.com and submitted to GENSCRIPT for cloning into a pET-21a(+) vector with 6 histidine residues at the C-terminal. The resulting plasmids were bacterially expressed for recombinant protein for 4 hours at 37˚C for P*f*CLK3 and 22˚C for both P*f*CLK1 isoforms. Purified using Ni-NTA affinity chromatography, the elutes were assessed by SDS-polyacrylamide gel electrophoresis to determine purity as detailed in chapter 2 (Figure 3.2). The purified fractions were pulled together for each kinase and dialysed. Following dialysis, a single predominant band was observed on SDS-PAGE gel analysis that migrated with an apparent molecular weight of roughly ~100kDa P*f*CLK3 (Figure 3.3 A). The presence high intensity blue bands corresponding at multiple molecular weights below and above ~75kDa for full length and ~37kDa for kinase domain P*f*CLK1 suggests co-contaminants or protein fragmentation (Figure 3.3 B). To confirm the expression of P*f*CLK1 proteins, the dialysate was probed in a western blot with 6x-His tag monoclonal antibody. The bands detected at ~75kDa and ~37kDa for the full length and kinase domain were the same as in the SDS-PAGE analysis (Figure 3.3 C). However, lower bands at ~60 – 65kDa were also detected and might represent fragments of the full length or highly histidine rich bacteria proteins that cross-react with the antibody. For downstream biochemical analysis, the protein concentration used for each kinase was extrapolated from SDS-PAGE quantification with bovine serum albumin (BSA) standards of known concentration (Figure 3.3 A and B).

To determine kinase activity of the full length P*f*CLK1, the purified protein was assayed for substrate phosphorylation in a biochemical assay using the established full length P*f*CLK3 and kinase domain *Pf*CLK1 activity assay described

by Alam et al., 2019. To optimise the assay for full length P*f*CLK1, the different components of the buffer were tested at varying concentrations: concentration of ATP, substrate, protein kinase and the composition of the reaction buffer. This section details the evaluation of each step in the assay optimization strategy and how this information is used to yield reliable and reproducible information that will feed the downstream biochemical characterisation of the inhibitors.

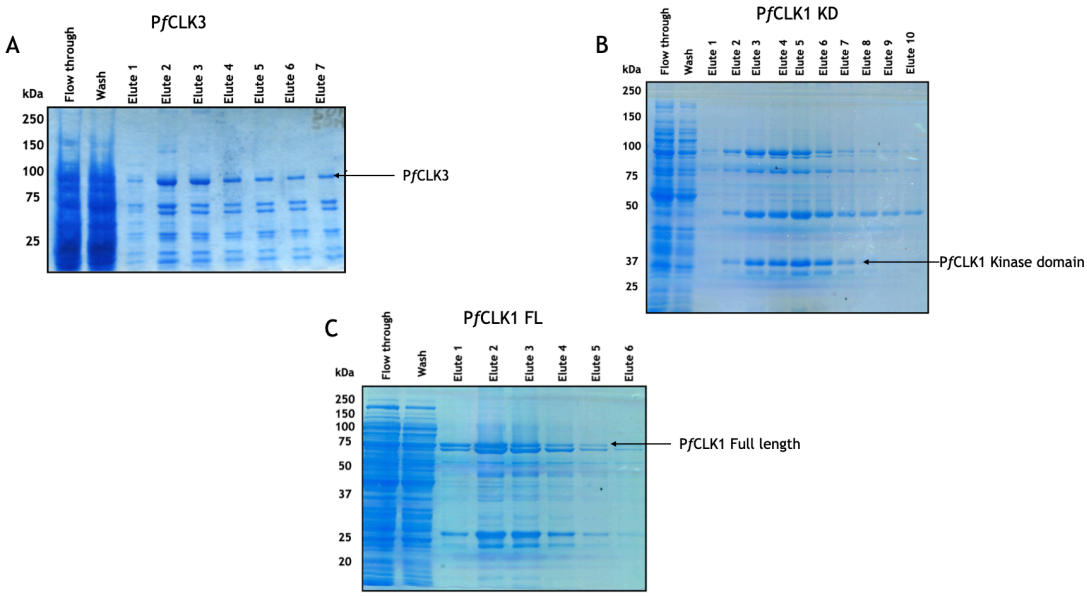

Figure 3.2 P*f*CLK genes are expressed and purified as a soluble protein.
Representative gels of P*f*CLK3 (A), P*f*CLK 1 Kinase domain (B) and P*f*CLK 1 Full length (C) expressed in *E. coli* and purified by immobilised metal affinity chromatography.

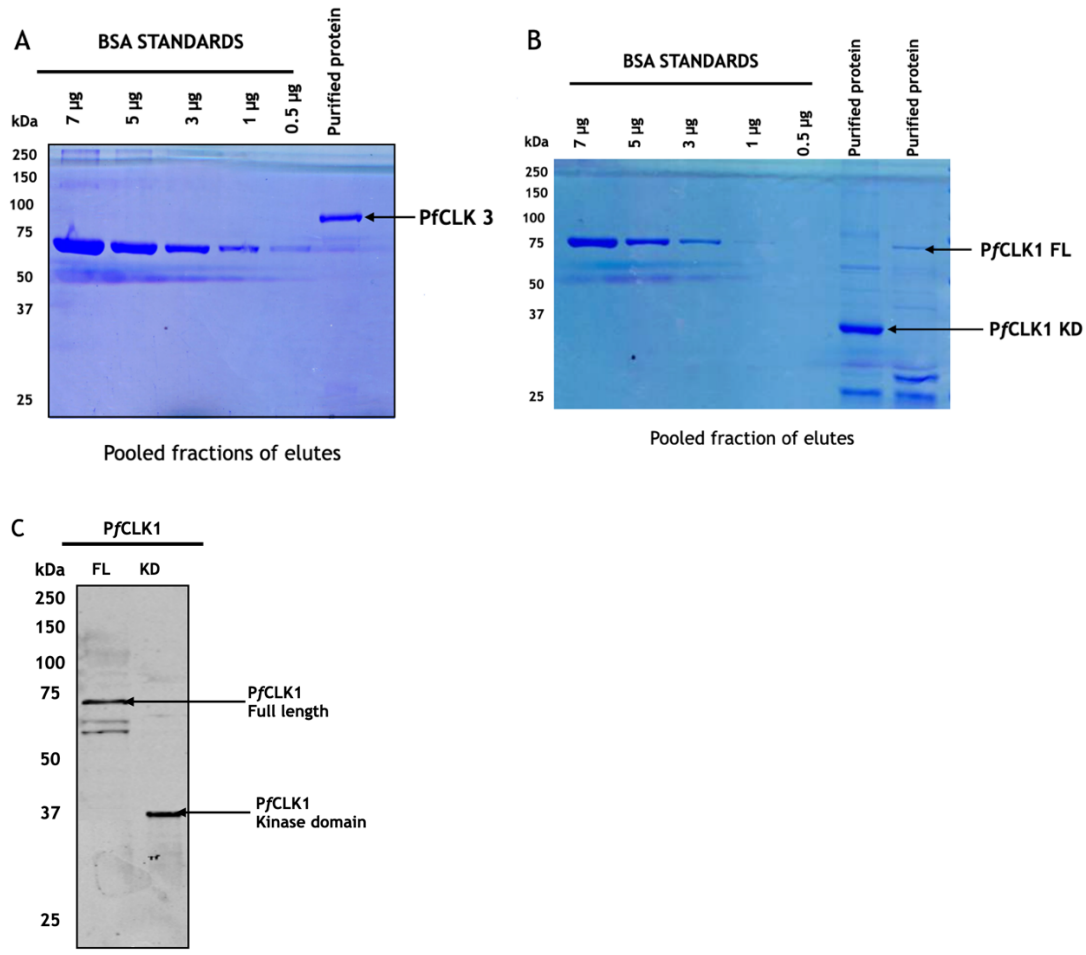

Figure 3.3 BSA quantification and Western blot confirmation of purified P*f*CLK genes. Dialysed protein fractions are quantified for protein concentration A) P*f*CLK3 protein band running at expected molecular weight ~100 kDa. B) Kinase domain P*f*CLK1 in lane 6 at ~37 kDa and full length in lane 7 at ~75 kDa. C) Confirmation of successfully purified P*f*CLK1 proteins using an anti-HIS antibody. Gels are representative of duplicate experiments. Molecular mass markers are indicated in kilodaltons (kDa).

3.1.1. Substrate identification for full length and kinase domain P*f*CLK1

Biochemical assays require the incubation of co-factors such ATP, magnesium, sometimes manganese and a substrate with the kinase to quantify activity(Menegay et al., 2000). The first essential step is finding a suitable substrate to start the assay optimization. Approaches for establishing a functional kinase assay include measuring auto-activation and the use of generic substrates such as Casein, myelin basic protein, and histone. Alam et al. 2019 has previously used radiolabeled [γ-32P] ATP assays with exogenous substrates (histone H1, myelin basic protein (MBP), and Casein and fluorometric assays with generic peptide substrates (CREBtide peptide (sequence: CKRREILSRRPSYRK) and MBP peptide sequence: CFFKNIVTPRTPPPSQGK-amide) labeled with U*Light*™ dye

to establish enzymatic activities in recombinant kinase domain P*f*CLK1 and P*f*CLK3.

Although the full-length *Pf*CLK1 contains all the conserved kinase subdomains and catalytic residues, it is important to confirm that the recombinant P*f*CLK1 protein possesses kinase activity. Standard radiolabeled phosphotransfer was used to measure activity in the full-length *Pf*CLK1 using the above-mentioned exogenous substrates with exception of histone H1 with kinase domain P*f*CLK1 as positive control. Recombinant full-length *Pf*CLK1 displayed no kinase activity against a range of substrates. In contrast, kinase domain P*f*CLK1 showed activity as expected with MBP phosphorylation detected at 18 kDa and Casein at about 30 kDa. Radioactive signal at 37 kDa for kinase domain P*f*CLK1 corresponding with the band at the same molecular weight in the Coomassie-stained gel is suggestive of autophosphorylation (Figure 3.4).

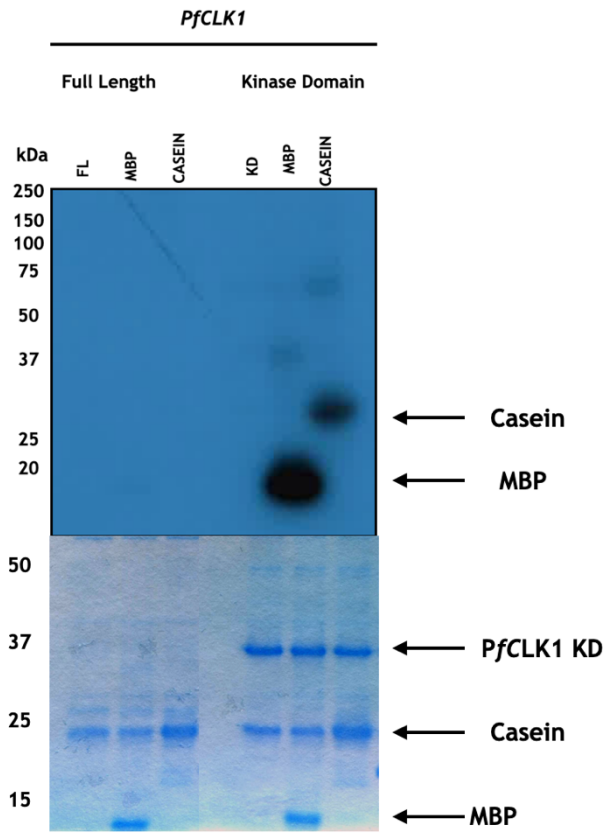

Figure 3.4 Kinase phosphorylation assay of exogenous substrate using γ-32P-ATP assay. *In vitro* kinase assay with [32P]-γ-ATP, recombinant protein kinases. Coomassie-stained SDS-PAGE gels (Bottom panels) indicate equal loading of all proteins in each condition. Autoradiographs (Top panels) indicate the phosphorylation of MBP and Casein by P*f*CLK1 kinase domain (KD) and full length (FL). Blots are representative of duplicate experiments. Molecular mass markers are indicated in kilodaltons (kDa).

Two peptide substrates were tested in the presence of increasing kinase concentrations. Substrate dependent phosphorylation activity was monitored in standard buffer conditions with U*Light* MBP/CREBtide and ATP incubated with increasing concentrations of P*f*CLK3, kinase domain and full-length P*f*CLK1(5 nM, 10 nM and 20 nM). Reactions lacking the U*Light* substrate components were compared as controls to determine signal specificity. An Eu-labelled anti-phosphosubstrate antibody (Eu-Ab) is added to the reaction in a second incubation step to allow binding to the phosphorylated U*Light*-labeled substrate which brings the donor and acceptor molecules into proximity. The reaction was terminated by irradiation at 320 or 340 nm to facilitate energy transfer from the Eu donor to the U*Light* acceptor dye which, in turn, generates light emission at 665 nm (Figure 3.5). The amount of phosphorylated substrate is quantified by the intensity of the light emission proportional to the level of U*Light*-substrate phosphorylation. The U*Light* MBP peptide was found to be strongly phosphorylated by the P*f*CLK3 and the kinase domain P*f*CLK1 as seen in Figure 3.6. Similarly, a concertation dependent increase of TR-FRET signal with the maximum signal at 20nM of kinase domain P*f*CLK1 was observed for U*Light* CREBtide. In the absence of substrate, consistently no dose-dependent TR-FRET signal was detected, the same output was demonstrated by the full-length PfCLK1 for both U*Light* peptides.

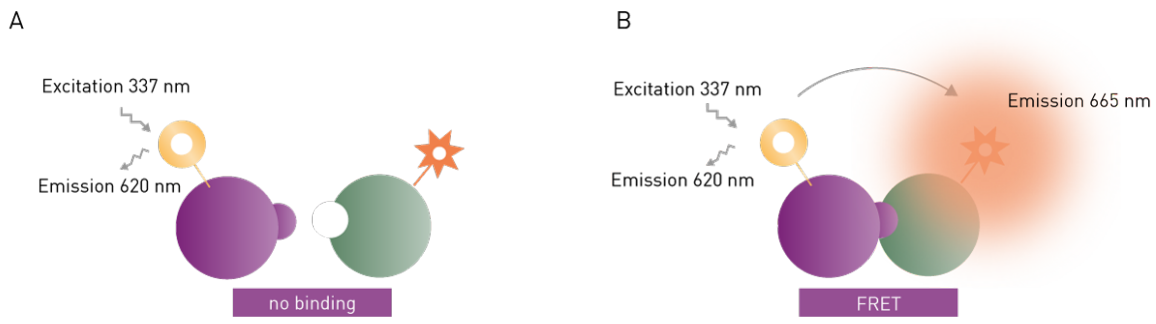

Figure 3.5 Time-resolved fluorescence energy transfer technology for kinase assay.
(A) Where kinase reaction is not irradiated, the donor is excited at 320 nm and emits at 620nm. (B) After kinase reaction is irradiated at 337 nm, the acceptor emits at 665 nm. Source: BMG Labtech.

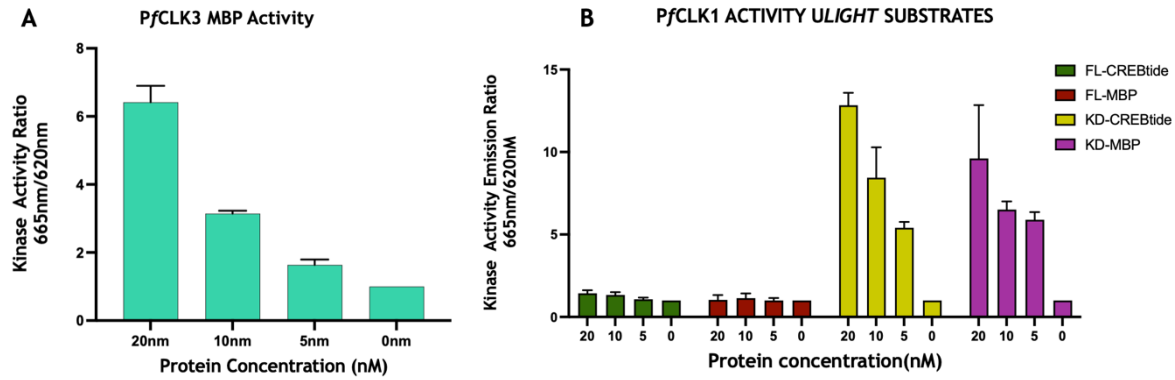

Figure 3.6 Time-resolved fluorescence energy transfer to measure substrate phosphorylation.
Kinase activity is measured by substrate phosphorylation (A) P*f*CLK3 phosphorylates U*Light* MBP (B) Kinase domain P*f*CLK1 phosphotylates U*Light* MBP and CREBtide. Data presented is an average of three independent experiments performed in triplicates and the error bars are ± S.E.M.

3.1.2. Michaelis-Menten Constant (ATP K_m)

The catalytic efficiency (k_{cat}/K_m) of the enzyme molecule determines the concentration of enzyme required in the assay to obtain a good signal(Roth et al., 2021). In a scenario where the enzyme molecules are inactive or have very low catalytic efficiency, higher concentration of enzyme will be required for good signal output which can limit the ability to distinguish strong and weak inhibitory effects in an assay. Additionally, given that the majority of kinase inhibitors function through ATP competitive inhibition, the concentration of ATP within an assay is a crucial factor in determining the efficacy of a given small-molecule kinase inhibitor(Deng et al., 2017). Therefore, it is important to use ATP at a concentration that equals its K_m value for the individual kinase. The K_m value is defined by the ATP concentration that allows half maximal reaction velocity, the assay signal in the presence of increasing ATP concentrations is measured and fitted to the Michaelis–Menten (ATP K_m) equation (Equation 3.1)(Monti et al., 2018). P*f*CLK3 and kinase domain P*f*CLK1 were used to determine the ATP concentrations sufficient for signal output in the TR-FRET assay for further optimization of full length P*f*CLK1 activity and later on for inhibition assay. The data showed that kinase domain P*f*CLK1 ATP K_m was derived as 91.32 µM in the presence of saturating concentrations of CREBtide substrate however for subsequent TR-FRET assays ATP concentration was set at

100 µM. For P*f*CLK3 MBP phosphorylation the ATP K_m was extrapolated as 8.106µM and rounded to 10 µM as the optimum ATP concentration (Figure 3.7).

$$V = \frac{V_{max}[ATP]}{K_M + [ATP]}$$

Equation 3.1 where V = rate of reaction,

V_{max} = maximal reaction rate,

K_m = Michaelis-Menten constant.

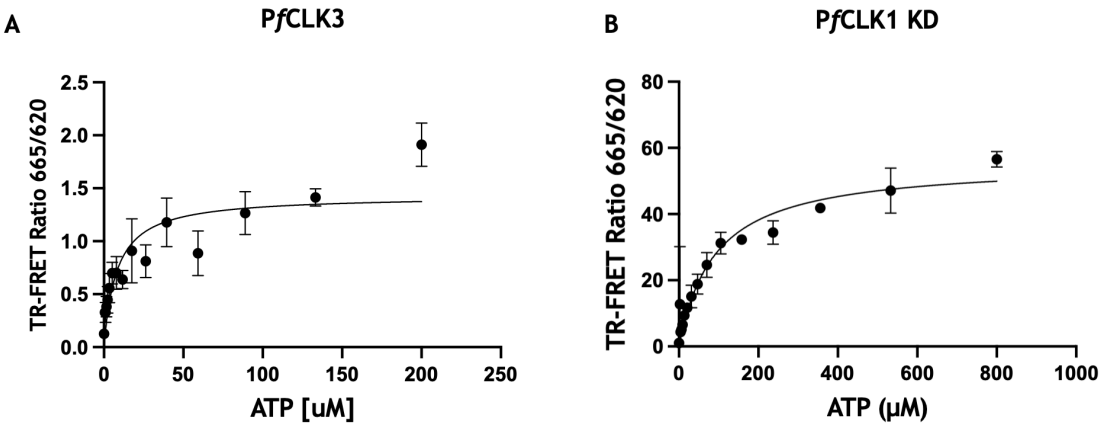

Figure 3.7 Time-resolved fluorescence energy transfer to determine Km for ATP for P*f*CLK3 and P*f*CLK1 Kinase domain (KD).
Michaelis- Menten constant (ATP_{km}) curve determined from ATP at a top concentration serially diluted in the presence of A) *Pf*CLK3 at 50 nM protein concentration with 50 nM U*Light* MBP and B) Kinase domain P*f*CLK1 at 5 nM protein concentration with 25 nM U*Light* CREBtide. Data presented is an average of three independent experiments performed in triplicates and the error bars are ± S.E.M.

3.1.3. Optimization of the Reaction Buffer for full length PfCLK1 activity.

In this optimization step, the composition of the reaction buffer was evaluated. The potential addition of detergents, the ATP concentration, and ion composition are assessed to ensure maximal kinase activity. Since kinases are most dependent on magnesium and manganese(Knape et al., 2017), Magnesium ions Mg^{2+} were added to the kinase buffer in addition to supplementing with calcium chloride $CaCl_2$ and increased ATP concentration at 2x the ATP K_m derived for kinase domain P*f*CLK1. For positive control of signal output, the kinase domain was assayed at these conditions. Figure 3.8 revealed no statically

significant changes in kinase domain activity and full-length P*f*CLK1 inactivity irrespective of increasing magnesium chloride concentration or in the presence of calcium chloride at 200 µM ATP concentration.

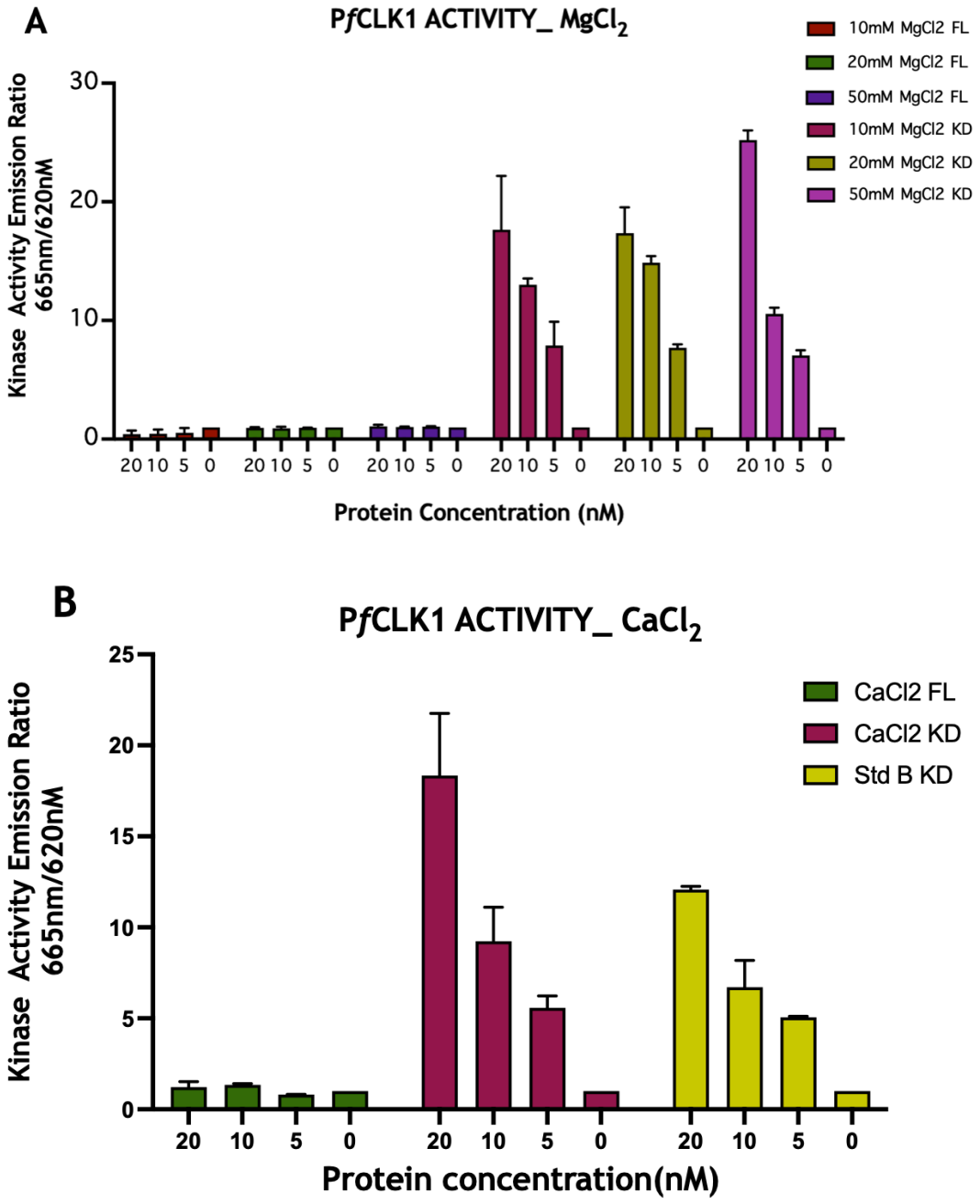

Figure 3.8 Effects of Mg2+ ions and co-factors CaCl2 & 200µM ATPs on P*f*CLK1 kinase activity.
(A) Varying concentrations of $MgCl_2$ and (B) addition of co-factor enzyme $CaCl_2$ concentration in kinase buffer with increased ATP 200 µM effects no changes in activity emission ratio of P*f*CLK1 kinase domain (KD) and full length (FL). Data presented is an average of three independent experiments performed in triplicates and the error bars are ± S.E.M.

3.1.4. Inducing hyper-phosphorylation of full length PfCLK1 N-terminal.

The N-terminal domain in CLK1 has been demonstrated to be required for efficient ASF/SF2 binding(Li et al., 2023). The N-terminal domain resembles an RS domain with multiple arginine-serine dipeptides. According to previous studies SRPK1 hypophosphorylates ASF/SF2 (generating pASF/SF2) which subsequently becomes hyperphosphorylated by CLK1. The CLK family (CLK1-4) possesses lengthy, N-terminal extensions (140-300 residues) that are classified as RS domains owing to the presence of arginine-serine dipeptides. Thus, the CLK1 N-terminus is not only essential for SRSF1 hyper-phosphorylation but is also necessary for high-level phosphorylation (Gehring & Roignant, 2021). This phenomenon was exploited to induce hyperphosphorylation at the N-terminal domain in the full-length P*f*CLK1 as measure of activity in γ-32P ATP assay using human SR1(*h*SR1) and SF2 (*h*SF2) proteins as experimental substrates with MBP, Casein with kinase domain P*f*CLK1 and the human CLK1 protein (*h*CLK1) as a positive control.

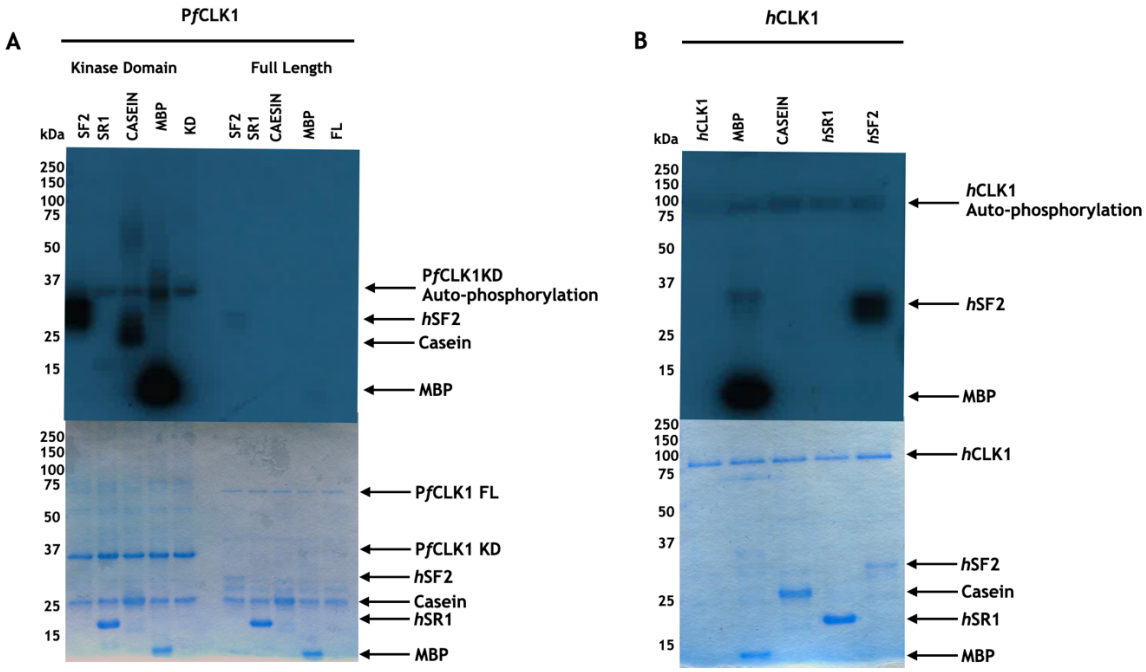

Figure 3.9 CLK1 N-Terminus interacts with the SF2 protein.
In vitro kinase assay with [32P]-γ-ATP, recombinant protein kinases. Coomassie-stained SDS-PAGE gels (Bottom panels) indicate equal loading of all proteins in each condition. Autoradiographs (Top panels) indicate the phosphorylation of MBP, Casein, human SF2 and SR1 proteins by A) P*f*CLK1 kinase domain, full length and B) human CLK1. Autophosphorylation of P*f*CLK1 KD and *h*CLK1 is also detected. Blots are representative of duplicate experiments. Molecular mass markers are indicated in kilodaltons (kDa).

The audiogram showed that kinase domain P*f*CLK1 phosphorylated MBP at 18kDa, Casein at ~30kDa and *h*SF2 at ~33kDa (Figure 3.9a). *h*CLK1 on the other hand only phosphorylated MBP and *h*SF2 (Figure 3.9b). Both kinases displayed a significant level of auto- phosphorylation by the presence of bands close to ~37kDa for kinase domain P*f*CLK1 and at ~100kDa for *h*CLK1. Full-length P*f*CLK1 appeared to phosphorylate *h*SF2 by the presence of a faint band running at ~33kDa. No radioactive signals were detected for *h*SR1 substrate across all kinase protein lanes. The phosphorylation data suggests *h*SF2 as a common substrate phosphorylated by homologues of this kinase family

3.2. Discussion

The eukaryotic CLK1 exhibits a domain structure in which the highly conserved catalytic domain is positioned at the C terminus and a putative regulatory domain comprising of 160 amino acids at the N terminus. Also present at the N-terminal is the conserved "EHLAMMERILG" signature motif which has been suggested to dictate CLK substrate specificity and a bipartite nuclear localization signal (Saldivia et al., 2020). Phosphorylation has been shown to be involved in the regulation of the activity and the intracellular localization of the enzyme (Aubol et al., 2014). Interestingly, CLK kinases have unusual dual specificity with propensity to autophosphorylate on serine, threonine, and tyrosine residues. However, further evidence indicated CLK1 activity to be dependent on serine/threonine or of tyrosine residue phosphorylation but not both (Lindberg & Meijer, 2021). Some studies have however proposed CLK1 tyrosine phosphorylation as an important determinant of enzyme activity on the basis that majority of CLK1 activity can be immunoprecipitated with phosphotyrosine antibodies (Dekel et al., 2020).

Traditionally, proteins, such as MBP, histones, or Casein, have been used as exogenous substrates *in vitro* to evaluate substrate specificity (Onyeogaziri & Papaneophytou, 2019). Phosphoamino acid analysis have shown CLK1 phosphorylation on serine residues predominantly for MBP, arginine rich Histone and Casein proteins with high specificity recorded on Ser109 site in MBP. Threonine and tyrosine residue phosphorylation were also observed in Casein although at lower levels (Haubrich & Swinney, 2016). Further experiments to map the phosphorylation consensus site in human CLK1 (*h*CLK1) revealed the significant role of a consensus site such as R-X-X-(S/T)-X-X-R flanked by +3 and −3 basic residues in determining substrate specificity (Keshwani et al., 2015). Indeed, biochemical evidence from this study indicated that Crebtide (REILSRRPSYRK), MBP 104-118 (GKGRGLS-LSRFSWGA) and other peptides with these relatively positioned positive and negatively charged basic residues were efficiently phosphorylated by CLK1. These results so far have been demonstrated for *h*CLK1 and it is has been evidenced in the literature that CLK1 homologues isolated from a number of organisms including: Arabidopsis, Drosophila, mouse and human share a highly conserved domain structure (Song et al., 2023). This

raises the possibility that the presence of these consensus sites in the *Plasmodium* homologue may have distinct biochemical roles *in vitro*.

To investigate if the P*f*CLK1 full length will display levels of activity as seen in the kinase domain, the kinetic parameters for kinase activities were determined using recombinant proteins of the full length and kinase domain P*f*CLK1. Two assay approaches were used for measuring kinase activity, fluorescent (TR-FRET) and radiolabeled ([γ-32P] ATP) assays.

The *in vitro* [γ-32P] ATP kinase assay is the gold standard for assessing kinase activity. This methodology involves immunoprecipitating the kinase of interest from homogenized tissue(Deng et al., 2017). The activity of the kinase is then assessed *in vitro* against a kinase-specific or kinase family-specific substrate. Gamma (γ)-32P ATP is subsequently used to measure the incorporation of phosphate into the substrate via liquid scintillation counting, thus enabling a quantitative assessment of activity (McGlory et al., 2014). TR-FRET is an advanced principle based on the practical combination of the low background aspect in time-resolved fluorometry (TRF) with Förster resonance energy transfer (FRET) involving two fluorophores, a donor and an acceptor (Ergin et al., 2016). Excitation of the first antibody conjugated to the fluorescent nanoparticles (donor) by an energy source produces an energy transfer to the second antibody that is coupled with fluorescent molecules (acceptor). If both antibodies within a given proximity to each other recognize the target and display suitable dipole orientation. The acceptor in turn emits light at its characteristic wavelength and a signal can be detected using a time-resolved fluorescence reader to obtain specific and quantitative results (Xu et al., 2024). The initial results revealed that both [γ-32P] ATP radioactivity for exogenous MBP phosphorylation were observed for kinase domain P*f*CLK1. In TR-FRET assay, the same concentration dependent TR-FRET emission for U*Light* MBP phosphorylation observed in P*f*CLK3 was observed for the kinase domain P*f*CLK1 mediated phosphorylation of both U*Light* MBP and U*Light* CREBtide substrates.

The principle of a kinetic assay is that, if the substrate concentration is sufficiently high in comparison to enzyme, then the reaction rate will be proportional to the enzyme concentration. The relationship between reaction rate and substrate concentration depends on the enzyme affinity for its

substrate (Robinson, 2015). This is usually an inverse measure of affinity expressed as the Michaelis constant K_m of the enzyme. For practical purposes, K_m is the concentration of substrate which permits the enzyme to achieve half V_{max}. The rate of reaction when the enzyme is saturated with substrate is the maximum rate of reaction, V_{max}(Monti et al., 2018). A concern with activity-based screens is that most inhibitors compete with ATP for binding, for which reason the results depend on the ATP concentration (Rudolf et al., 2014). Because the potency of ATP-competitive compounds is affected by the affinity of the kinase for ATP and the concentration, the ATP K_m was measured for the active constructs P*f*CLK3 and kinase domain P*f*CLK1. This ensures comparability of compound potency between the kinases and K_m values determined at the standard assay conditions were as follows; P*f*CLK3 [K_m = 8.106 µM, V_{max} = 1.430] and P*f*CLK1 [K_m = 91.32 µM, V_{max} = 55.63].

The concentrations of detergents, buffers, carrier proteins, reducing agents, and divalent metal ions can affect the specific signal and the apparent activity of kinases in TR-FRET assays(Ergin et al., 2016). The LANCE™ Ultra kinase kit manufacturer, Revvity have recommended optimising TR-FRET assay for specific kinases by screening requirements for bivalent cations (like M^{2+} and Mg^{2+}) in the basic kinase buffer or by adding any essential kinase supplements (e.g., $MnCl_2$, $CaCl_2$, calmodulin, cGMP, lipids etc.) that may influence stability and for the activity of the enzyme.

As metalloenzymes eukaryotic protein kinases utilise divalent metal ions for nucleotide co-binding and to aid in catalysis for the regulation of eukaryotic signal transduction(Knape et al., 2017). Surface plasmon resonance (SPR) analysis of the catalytic (C) subunit of cAMP-dependent protein kinase (PKA) interaction with a substrate in the presence of Mg^{2+} and ATP have established that besides being highly physiologically relevant, magnesium plays a unique role as a common biologically relevant divalent cation that enables stable substrate binding and orientation as well as the acceleration of product release that allows for efficient turnover catalysis (Knape et al., 2017). In addition, a two-

metal mechanism was shown in other kinases like the cyclin-dependent protein kinase 2 (CDK2) where the transient binding of the second Mg^{2+} ion was required for optimal phosphotransferase activity (Knape et al., 2015). Furthermore, the generic CREBtide peptide substrate used in TR-FRET biochemical kinase assays is synthetically derived from human cAMP Response Element Binding (CREB) protein with phosphorylation site 'Ser133' which can be phosphorylated by a variety of kinases including MSK1, PKA and protein kinase C (PKC) isoforms. Calmodulin kinase II (CAMK) has been shown to shuttle Ca^{2+}/ calmodulin (Ca^{2+}/ CAM) to the nucleus to trigger CREB phosphorylation and gene expression (Mohanan et al., 2022).

To investigate the role of magnesium concentration in phosphotransferase activity of full length P*f*CLK1 and as to whether the presence of calcium may further facilitate CREB peptide phosphorylation to improve signal output in the TR-FRET assay. P*f*CLK1 kinase domain was assayed as a positive control comparing emission signal in our standard to the optimised buffer. Based on this rationale, $MgCl_2$ concentrations in the basic kinase buffer was increased by 2x and 5x the standard concentration of 10 mM for full length and kinase domain P*f*CLK1. The bar graph generated showed there were no statistically significant changes to emission ratio across the varying concentrations of proteins for the kinase domain (Figure 3.8). Similarly, supplementing the full length P*f*CLK1 with more magnesium effected no change in the lack of kinase activity. Given these results, the kinases were supplemented with $CaCl_2$ under standard assay conditions and no changes were observed in the kinase domain or full length activity.

CLK and SRPK kinases can function as a complex to efficiently mediate the processive phosphorylation of essential splicing SR proteins in the nucleus that regulate spliceosome assembly and activation (Zhou & Fu, 2013). Further studies identified a group of conserved residues within the large lobe of SRPK1 are in interaction with the N terminus of *h*CLK1 stabilizing the SRPK1-CLK1 complex (Aubol et al., 2016). Structural studies characterizing the role of *h*CLK1 have demonstrated that the additional N-terminal domain in *h*CLK1 which resembles an RS domain (Aubol et al., 2021) with multiple arginine-serine dipeptides was required for efficient ASF/SF2 binding. SRPK1 has been shown to

hypophosphorylate ASF/SF2 thereby generating pASF/SF2 which subsequently becomes hyperphosphorylated by CLK1 and is released as ppASF/SF2. Studies have provided evidence that the “hyper and hypo” phosphorylation of SR proteins inhibit splicing activity which in turn represses constitutive splicing and switches alternative splice site selection (M. Sun et al., 2022). These studies above suggest ASF/SF2 proteins and SR proteins as putative substrates of full length CLK1.

To investigate if hyperphosphorylation of ASF/SF2 by the N-terminal in the full length P*f*CLK1 can constitute the sufficient activity read out required in a biochemical assay for pharmacological screening, the full length and kinase domain P*f*CLK1 with *h*CLK1 homologue as positive control in [γ-32P] ATP were assayed with *h*SF2 and *h*SR proteins as substrates in addition to MBP and Casein. Autophosphorylation was indicated by the presence of radioactive intensity observed for the respective kinase bands ~100kDa *h*CLK1 and ~37kDa kinase domain P*f*CLK1. This corroborates a highly conserved catalytic domain in the CLK family across different homologues and suggests that similarly to *h*CLK1, kinase domain P*f*CLK1 may be autophosphorylating on tyrosine residues. Contrary to literature, SR protein phosphorylation was not observed for all the kinases and Casein was only phosphorylated by kinase domain P*f*CLK1. However, comparable to MBP and Casein phosphorylation, *h*SF2 phosphorylation was evidenced across all the CLK forms but at a weak signal for full length P*f*CLK1. The phosphorylation of *h*SF2 protein implies that CLK1 inhibition may disrupt essential splicing process in stages of the parasite life cycle.

While enzyme assay methodologies using recombinant kinases are clearly valuable tools, these methods are incapable of capturing the complex function and regulation of the kinase as seen in native biological systems (Haubrich & C. Swinney, 2016). This is because in the cellular environment the kinase can either act in combination with other enzymes and proteins in a signalling pathway as a single entity or as a part of multimeric complexes. In contrast, a biochemical system is reconstituted so the kinase is isolated and lacking many or all of its native binding partners, this can lead to the significant loss of kinase stability and activity *in vitro* (Roth et al., 2021). However, not all kinases can be used in biochemical assays in their full-length form due to the difficulties in expressing and purifying their native form (Reinhardt & Leonard, 2023).

The absence of enzymatic activity observed for the full length P*f*CLK1, compared the truncated C-terminal kinase domain exhibiting robust activity suggests the presence of regulatory mechanisms within the full length protein. Several possibilities exist, including autoinhibition by the N-terminal or other domains, where they might directly block the active site or induce a conformation that hinders substrate binding or catalysis.(J. Goldberg et al., 1996) Alternatively, the full length protein may require specific post-translational modifications, protein-protein interactions, or cofactors absent in the biochemical assay to achieve proper folding and activity (S. Lee et al., 2017; Nørregaard Jensen, 2004). The larger size and increased structural complexity of the full length P*f*CLK1 could also lead to misfolding or instability in the recombinant expression system, preventing the catalytic domain from adopting active conformation (Jaenicke, 1999). Further investigation into the interactions and structural properties of the full length P*f*CLK1 is necessary to elucidate the precise mechanism of activity regulation. Given the lack of activity for full length P*f*CLK1, the biochemical assays in this chapter were established with the kinase domain P*f*CLK1.

Chapter 4 The pharmacological modulation of P*f*CLK mediated phosphorylation.

Introduction

Drug discovery involves multifaceted processes, from ideation to development and to approval. The entire process involves several different stages of development and series of actions, typically sub-divided into four main stages early drug discovery, pre-clinical phase, clinical phases, and regulatory approval (N. Singh et al., 2023). The early drug discovery phase involves the use of *in silico* platforms, biochemical assays, cell cultures, and various animal models for the identification and optimization of lead compounds that can potentially elicit a desirable effect on a specific disease implicated biological target(N. Singh et al., 2023). This stage flows through sub-processes such as target Identification and validation, high throughput screening (HTS), hit identification, assay development and screening, hit-to-lead (H2L), lead generation and optimization, and *in vivo* and *in vitro* assays for therapeutic efficacy (Biala et al., 2023).

A key factor in drug design is the identification of a druggable target whose biological activity can be modified to elicit a measurable response both *in vitro* and *in vivo* upon binding to a therapeutic molecule, referred to as a "hit" (Henderson et al., 2021). The shift from drug discovery to drug development to enable clinical trials is initiated when the initial experimental compounds are nominated as drug candidates after having been sufficiently optimized for selectivity, potency and safety in preliminary *in vitro* experiments and animal models(D. Sun et al., 2022). To achieve this, an already established druggable target (s) must be modulated by a (or several) therapeutic agent. A wide variety of agents are traditionally classified into two major categories: "small molecules" and the "biologics"(Zhong et al., 2021). The term - small molecules refer to small chemical compounds and some modified short sequence peptides whereas biologics are typically macromolecules such as recombinant proteins, antibodies, siRNAs, long peptides, cells, genes and vaccines(Biala et al., 2023).

The previous chapter details the identification of P*f*CLK1 as a druggable target by published literatures (Kern et al., 2014) and its *in-vitro* characterisation as a potential point for chemical intervention. In the study to validate P*f*CLK3,

recombinantly expressed P*f*CLK1 kinase domain and P*f*CLK3 full length kinases were used in high-throughput screening of nearly 30 000 kinase inhibitor compounds. This screening identified selective compounds for P*f*CLK1 and P*f*CLK3, as well as pan-active inhibitors for both kinases. Interestingly, a highly potent, selective and specific inhibitor, TMCDC-135051(Figure 4.1) was identified to inhibit PfCLK3 (Mahindra et al., 2020).

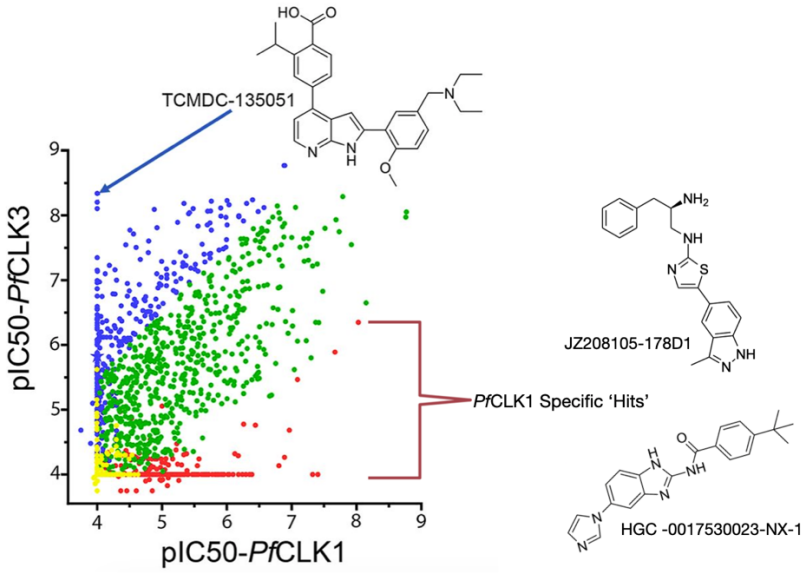

Figure 4.1 High-throughput screen identifies inhibitors of P*f*CLK1 and P*f*CLK3.
Hit compounds were used in concentration response curves. Shown is a comparison of pIC_{50} values for inhibition of P*f*CLK3 versus P*f*CLK1. TCMDC-135051 (structure shown) is highlighted as the most potent and selective P*f*CLK3 hit. JZ208105-178D1 and HGC-0017530023-NX-1(structures shown) are highlighted as specific hits for P*f*CLK1(Alam et al., 2019).

The validation strategy in Alam et al., 2019 involved using a combination of evolved resistance and chemo genetics to generate resistant variants and mutants insensitive to TCMDC-135051 activity. A *Pf*CLK3 '*Pf*CLK1-like mutant'-G449P was generated by point mutations within *Pf*CLK3 using *Pf*CLK1 as a template. Specific active site residue, glycine (G) at position 449 in *Pf*CLK3 was substituted with a proline (P) as seen in *Pf*CLK1 wild type (Figure 4.2). The variant plasmid construct was transfected into 3D7 strains to develop a corresponding mutant parasite line to establish TCMDC-135051- *Pf*CLK3 inhibition as the cause of parasite death in 3D7 wild type viability assays.

TCMDC-135051 has been used as tool molecule to validate P*f*CLK3 as suitable antimalarial drug target with activity across all stages of the asexual blood stages, blocks gametocyte maturation, exflagellation, and mosquito infection,

and actively inhibits liver cells invasion by sporozoites, thus offering opportunity for prophylaxis, cure and transmission blocking of *P. facilarum* parasites (Alam et al., 2019).

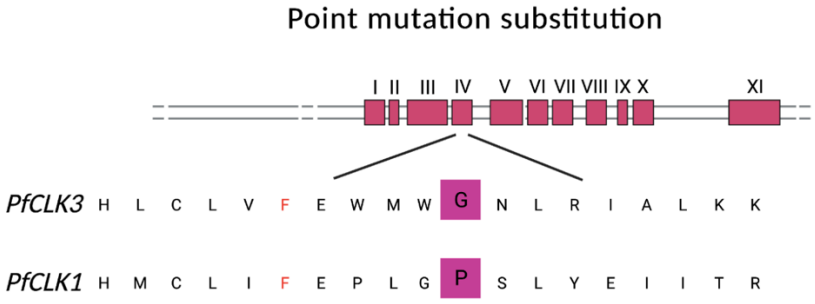

Figure 4.2 Schematic of the point mutation to generate mutant kinase G449P.
Primary amino acid sequence of PfCLK3 showing the 11 kinase subdomains and the sequence of subdomain V of PfCLK1 and PfCLK3. A, Ala; C, Cys; E, Glu; F, Phe; G, Gly; H, His; I, Ile; K, Lys; L, Leu; M, Met; N, Asn; P, Pro; R, Arg; S, Ser; T, Thr; V, Val; W, Trp; Y, Tyr.S (Alam et al., 2019)

In a follow up target-based program on *Pf*CLK3 in development with another promising CLK (*Pf*CLK1), four hits that showed specificity towards *Pf*CLK1 were identified and two compounds JZ208105-178D1 and HGC-0017530023-NX-1 with a reported <30nM recombinant potency were selected to explore the suitability of *Pf*CLK1 as a therapeutic target.

This chapter explores some major steps of early small molecule drug discovery outlined above and whether target modulation will lead to mechanism-based side effects. Here, both compounds JZ208105-178D1 and HGC-0017530023-NX-1 were evaluated for a range of properties that include selectivity, binding mechanism and kinetic analysis, concentration effect curves, and *in vitro* potency. Once these compounds have displayed sufficient significance in these investigations, they were further screened in cell-based assays predictive of parasite infection and disease state to characterize for efficacy and rate of kill in comparison to P*f*CLK3 probe molecule TCMDC-135051, current antimalarials; chloroquine and artemisinin. Therefore, this chapter aims to:

- Determine the specific and selective activity of JZ208105-178D1 and HGC-0017530023-NX-1 towards P*f*CLKs.
- Evaluate JZ208105-178D1 and HGC-0017530023-NX-1 mode of inhibition,
- Investigate P*f*CLK1 dependent inhibition of *P.falciparum* asexual stage.

4.1. Results

Inhibition of kinase-substrate phosphorylation

4.1.1. JZ208105-178D1 and HGC-0017530023-NX-1 confer nanomolar inhibition of P*f*CLK1

Following the identification of JZ208105-178D1 and HGC-0017530023-NX-1 as potential hits, the compounds were characterised using a traditional *in vitro* fluorometric kinase activity assay to confirm the inhibition of P*f*CLK1 substrate phosphorylation. The TR-FRET experiments were used to provide IC_{50} curves that determine the drug concentration at which the target kinase activity is inhibited by 50%. A low IC_{50} value is indicative that that drug is effective at low concentrations and may therefore show lower systemic toxicity when administered to the patient(Garcia-Molina et al., 2022) .

In this experiment, the reaction mixes of recombinant kinase domain P*f*CLK1 incubated with the substrate peptide CREBtide and ATP at the concentration derived by the ATP K_m, was quantified to determine the IC_{50} values for JZ208105-178D1 and HGC-0017530023-NX-1 using the formula below.

$$Percentage\ Kinase\ Inhibition: 100 - (\frac{(\ Inhibitor\ \ activity - Blank)}{(Maximum\ kinase\ activity - Blank)}) * 100$$

Equation 2 where
Inhibitor activity is the 665/620 emission ratio from protein, substrate with inhibitor

Maximum kinase activity is 665/620 emission ratio from protein, substrate with no inhibitor
Blank is the 665/620 emission ratio from kinase buffer only.

A *In-vitro* concentration effect curve P*f*CLK1 Kinase Domain

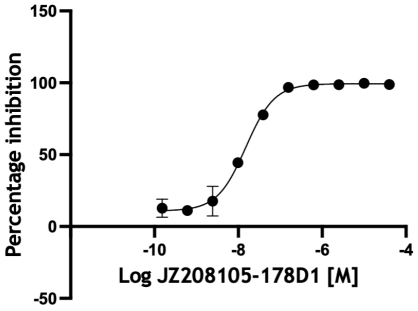

	JZ208105178D1	HGC0017530023NX1
IC_{50}	10 nM	19.5 nM

B *In-vitro* concentration effect curve P*f*CLK1 Kinase Domain

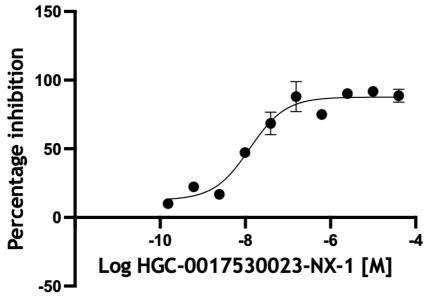

Figure 4.3 Time-resolved fluorescence energy transfer to determine IC50 for JZ208105-178D1 and HGC-0017530023-NX-1.
(A) and (B) Concentration effect curves of kinase domain P*f*CLK1 using the determined ATP K_m (100 µM) and 5 nM recombinant protein kinase in the presence of JZ208105-178D1 and HGC-0017530023-NX-1 inhibitors, serially diluted with a dilution factor of 1 in 3. All experiments were done in triplicates. Data presented is an average of three independent experiments performed in triplicates and the error bars are ± S.E.M.

The concentration effect curves showed compounds JZ208105-178D1 and HGC-0017530023-NX-1 inhibiting kinase domain P*f*CLK1 at low nanomolar concentrations with IC_{50} values of 10 nM for JZ208105-178D1 and 19.5 nM for HGC-0017530023-NX-1 (Figure 4.3). Thus, both JZ208105-178D1 and HGC-0017530023-NX-1 are established as highly potent *Pf*CLK1 inhibitors.

4.1.1. JZ208105-178D1 and HGC-0017530023-NX-1 displayed selectivity for P*f*CLK3.

Given the highly conserved catalytic domain between kinases in the CLK family, the activity of JZ208105-178D1 and HGC-0017530023-NX-1 towards member kinase P*f*CLK3 was also investigated in an *in vitro* TR-FRET kinase inhibition assay. P*f*CLK3 inhibition reaction was set up based on previously established parameters;100 µM ATP concentration based on the ATP K_m, protein concentration at 50 nM, U*Light*-labeled MBP substrate and inhibitor molecule (ranging from 1 to 10,000 nM). P*f*CLK3 selective and specific inhibitor was used as a positive control in these experiments. The inhibition data showed that addition of HGC-0017530023-NX-1 inhibited P*f*CLK3 - MBP phosphorylation at greater potency compared to JZ208105-178D1 with IC_{50} values of 143 nM and 424.2 nM, respectively. However, both compounds exhibited an approximate 2.5-fold lower potency compared to TCMDC-135051 IC_{50} value of 60.2 nM (Figure 4.4). This inhibitory effect displayed by P*f*CLK1 inhibitors on P*f*CLK3 is suggestive of a selective mechanism for the highly conserved domain in the CLK family.

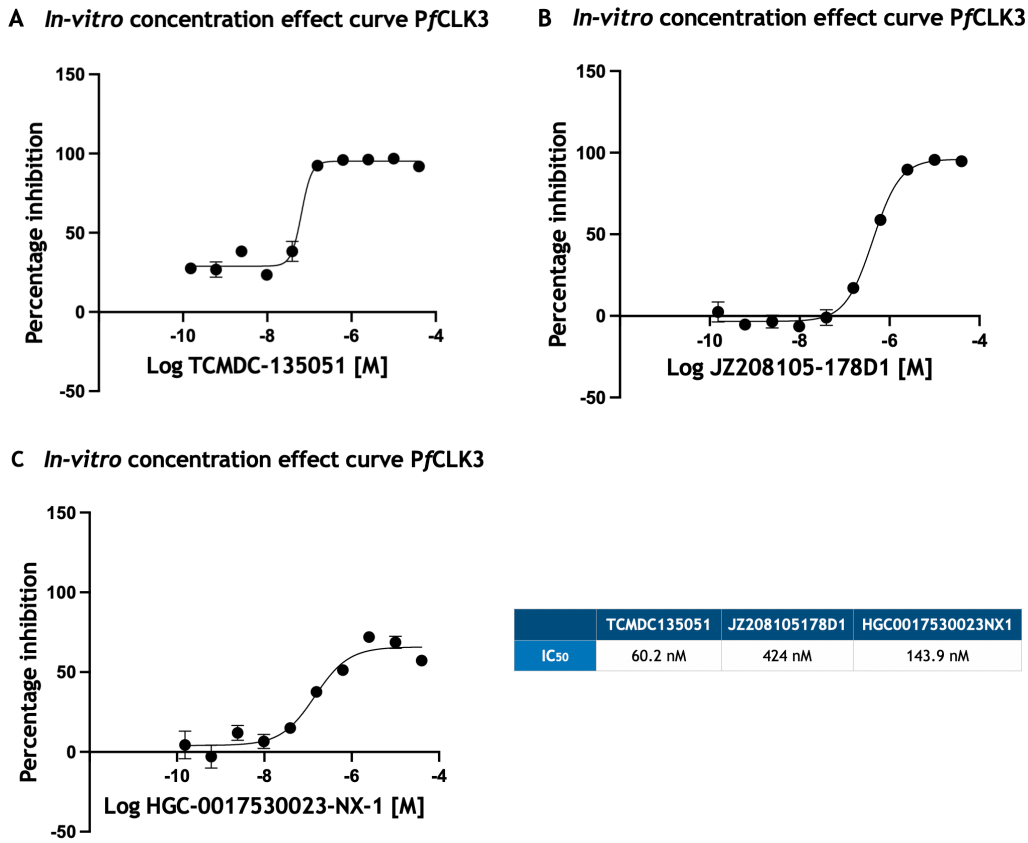

	TCMDC135051	JZ208105178D1	HGC0017530023NX1
IC_{50}	60.2 nM	424 nM	143.9 nM

Figure 4.4 Inhibition of other member kinase P*f*CLK3 with JZ208105-178D1 and HGC-0017530023-NX-1 using TCMDC-135051 as control.
(A) TCMDC-135051 inhibits P*f*CLK3 at IC_{50} 60.2 nM in line with published IC_{50} value 40.86 nM. P*f*CLK1 inhibitors (B) JZ208105-178D1 and (C) HGC-0017530023-NX-inhibit P*f*CLK3-mediated MBP phosphorylation at sub-micromolar and potencies 424 nM and 143.9 nM respectively. Data presented is an average of three independent experiments performed in triplicates and the error bars are ± S.E.M.

4.1.2. Measuring the binding affinity of P*f*CLK1 inhibitors

To investigate the effect of ATP on binding affinity, both compounds were assayed in phosphorylation assays with varying fixed ATP concentrations as opposed to matching ATP concentration to ATP K_m. Initially, a small-scale TR-FRET inhibitor assay set up at the ATP K_m and 50X ATP K_m resulted in the response curve shift to the right. At increased ATP concentrations, there was a 3-fold difference between the IC_{50} values for JZ208105-178D1 at 11.12 nM ATP K_m and 35.5 nM 50X ATP K_m (Figure 4.5 A). For HGC-0017530023-NX-1, increased ATP concentration effected a ~2-fold difference in potency at 19.5 nM ATP K_m and 38.51 nM 50X ATP K_m (Figure 4.5 B). The data suggests an ATP- dependent binding for JZ208105-178D1 and ATP-independent binding for HGC-0017530023-

NX-1. A scaled-up ATP-competitive assay was set up to confirm these preliminary results.

A

***In-vitro* concentration effect curve *Pf*CLK1 Kinase Domain**

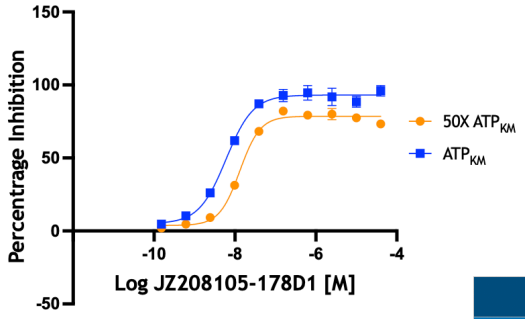

	IC_{50} (ATP KM)	IC_{50} (50X ATP KM)
JZ208105178D1	6.52 nM	13.29 nM
HGC0017530023NX1	12.66 nM	15.34

B

***In-vitro* concentration effect curve *Pf*CLK1 Kinase Domain**

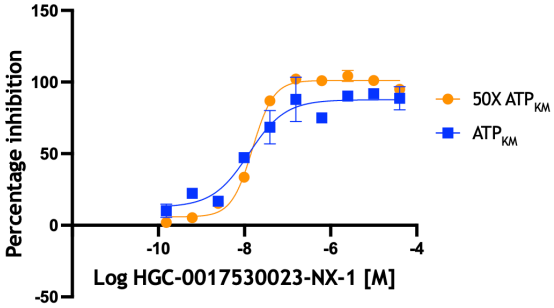

Figure 4.5 Effect of ATP concentration on the potency of JZ208105-178D1 and HGC-0017530023-NX-1 against kinase domain PfCLK1 in TR-FRET kinase assay.

This was done by measuring the different concentrations of the two inhibitors on either side of their IC_{50} values against fixed protein (5 nM) and substrate (25 nM) concentration with a range of ATP concentrations on either side of the ATP K_m value in a TR-FRET inhibition assay. The concentration effect curves showed that increased concentrations of JZ208105-178D1 resulted in higher ATP K_m values and a change in the ATP K_m curves. Furthermore, increased ATP concentrations at 800 µM affected the inhibition potency of JZ208105-178D1, caused a shift in IC_{50} value from 35.62 nM to 472.9 nM at 1 µM ATP. In contrast, for HGC-0017530023-NX-1, an increase in IC_{50} concentrations implicated no significant changes in ATP K_m and vice versa (Figure 4.6)(Table 4.1).

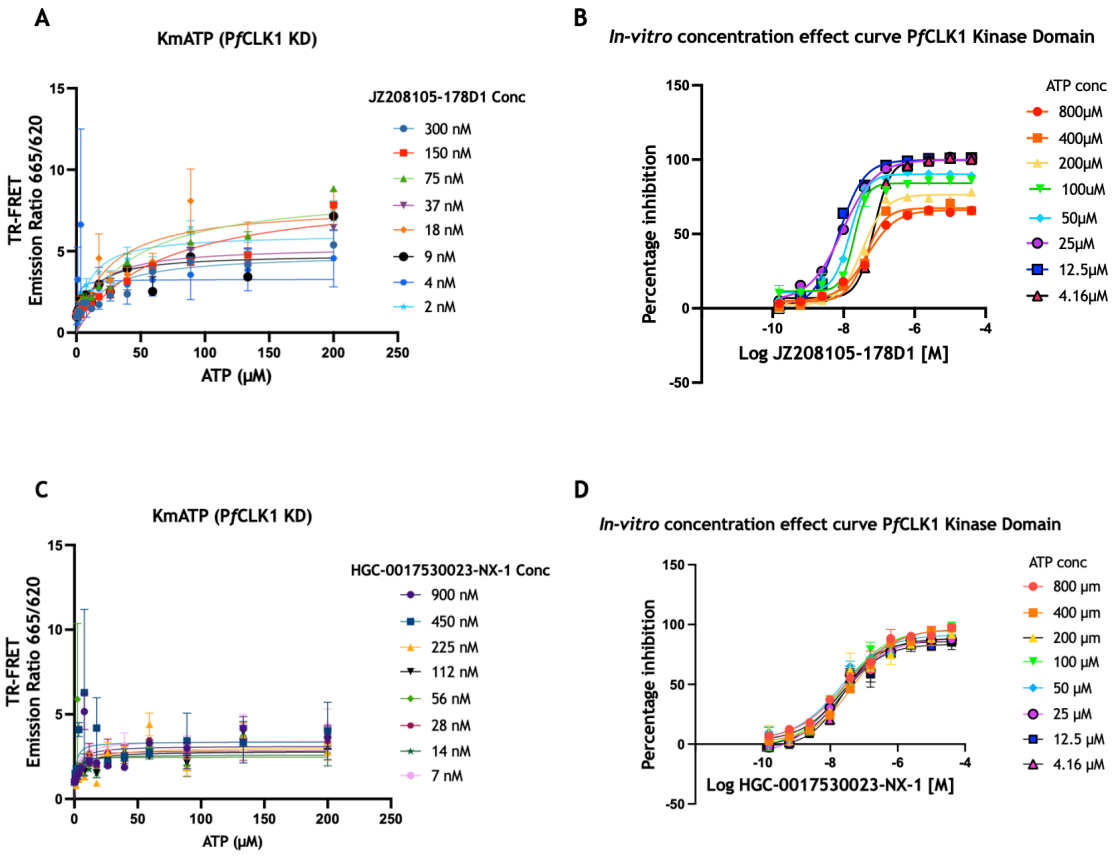

Figure 4.6 ATP Dependence analysis of Kinase domain PfCLK1 inhibition by JZ208105-178D1 and HGC-0017530023-NX-1 using TR-FRET assay.
(A and C) ATP K_m curves represent data fitted to Michaelis-Menten equation using nonlinear regression analysis for data obtained at constant amount of substrate and protein (kinase domain P*f*CLK1) and various concentrations of ATP and inhibitors (JZ208105-178D1 and HGC-0017530023-NX-1respectively). B and D) Kinase domain P*f*CLK1 kinase inhibition assays were performed using TR-FRET assay described in methods section with various concentrations of ATP and inhibitor (JZ208105-178D1 and HGC-0017530023-NX-1respectively). The curves were generated by analysing the values of individual samples and plotted as function of inhibitor concentration; the acquired IC_{50} values are shown in Table 4.1. Data presented here is the average of three independent experiments done in triplicates with mean ±S.E.M.

Table 4.1 ATP Dependence analysis IC_{50} values.

ATP [μM]	JZ208105-178D1 IC_{50} [nM]	HGC-0017530023-NX-1 IC_{50} [nM]
4.65 μM	41.44	23.93
12.5	3.209	22.4
25	3.209	16.84
50	4.7	19.86
100	6.5	23.42
200	19.34	25.68
400	17.43	48.37
800	15.36	27.85

Table 4.2. ATP Dependence analysis ATP Km.

JZ208105-178D1 [nM]	ATP $_{KM}$	HGC-0017530023-NX-1 [nM]	ATP $_{KM}$
2	9.293	7	2.986
4	0.8621	14	1.940
9	23.93	28	1.815
18	13.37	56	0.4543
37	10.13	112	3.064
75	39.73	225	4.482
150	61.54	450	1.058
300	18.77	900	2.274

4.1.1 Parasite inhibition

4.1.3. JZ208105-178D1 and HGC-0017530023-NX-1 disrupt asexual blood stage replication

The potency of the HGC-0017530023-NX-1, JZ208105-178D1 against asexual *P. falciparum* parasites were determined in comparison to TCMDC-135051, artemisinin and chloroquineusing *in vivo* growth inhibition assays. This was carried out using synchronised 3D7 asexual ring stages at about 0.5% parasitaemia. The parasites were cultured for at least 48 hours and the assay was terminated by freezing at -20˚C prior to staining with SYBR green. The fluorescence intensity quantified was used in the formula below to derive the percentage inhibition of parasites. The death curves showed all five inhibitors blocked *P. falciparum* blood stage replication at low nanomolar to micromolar range. JZ208105-178D1 and HGC-0017530023-NX-1 displayed antimalarial activities at EC_{50} values of 1.3μM and 2.3μM respectively (Figure 4.7 B and C.). TCMDC-135051, artemisinin and chloroquine had EC_{50} potencies of 281 nM, 53 nM and 47 nM respectively (Figure 4.7 A, D and E).

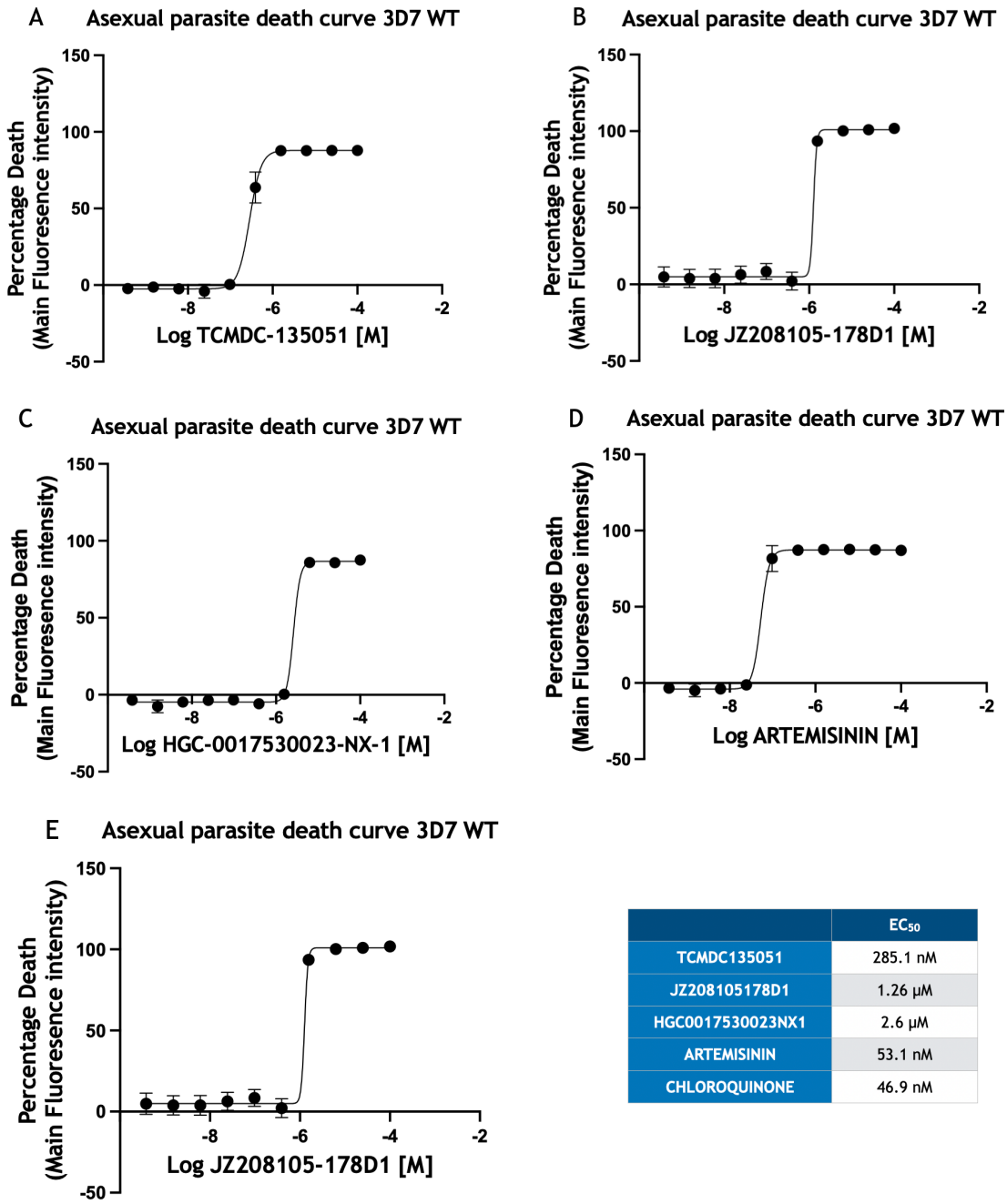

	EC_{50}
TCMDC135051	285.1 nM
JZ208105178D1	1.26 µM
HGC0017530023NX1	2.6 µM
ARTEMISININ	53.1 nM
CHLOROQUINONE	46.9 nM

Figure 4.7 ATP Dependence analysis of Kinase domain P*f*CLK1 inhibition by JZ208105-178D1 and HGC-0017530023-NX-1 using TR-FRET assay.
Dose dependent antimalarial activity against 3D7 wildtype parasites was observed in A) TCMDC-135051 at EC_{50} 285.1nM B) JZ208105-178D1 at EC_{50} 1.26 µM C) HGC-0017530023-NX-1 at EC_{50} 2.6 µM, antimalarial drugs D) Artemisinin at EC_{50} 53.1nM and E) Chloroquine at EC_{50} 46.9 nM. Data is the average of three independent experiments in triplicates ±S.E.M.

4.1.5. **Chemical Validation**

To investigate if P*f*CLK1 specific inhibition might be the cause of parasite death by JZ208105-178D1 and HGC-0017530023-NX-1 in the wild type of viability assay, the P*f*CLK3_G449P mutant was used to test both compounds *in vitro* and *in vivo*. Recombinant G449P inhibition curves showed that sensitivity towards TCMDC-135051 was reduced as expected for negative control (Figure 4.8 C). A similar reduction in potency was observed for HGC-0017530023-NX-1, compared to wild type P*f*CLK1 inhibition in vitro, G449P was inhibited at sub-micro molar concentration of IC_{50} 9.5µM (Figure 4.8 B). In contrast, JZ208105-178D1 remained potent with an IC_{50} value of 68nM (Figure 4.8 A).

A *In-vitro* concentration effect curve P*f*CLK3_G449P

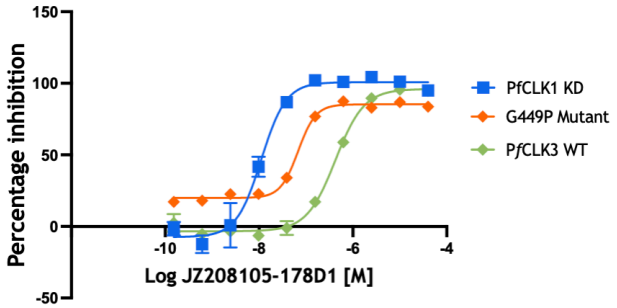

	IC_{50}
P*f*CLK1 KD	10.14 nM
G449P Mutant	67.99 nM
P*f*CLK3 WT	424.4 nM

B

In-vitro concentration effect curve P*f*CLK3_G449P

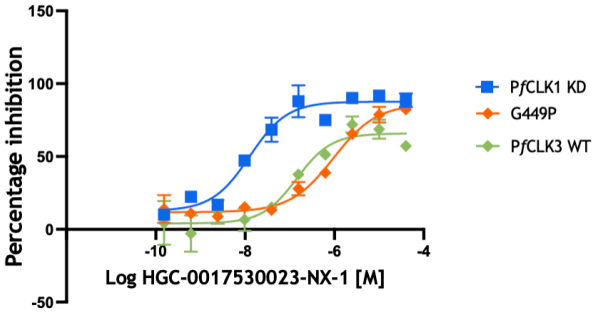

	IC_{50}
P*f*CLK1 KD	14.66 nM
G449P Mutant	952.6 nM
P*f*CLK3 WT	143.9 nM

C

In-vitro concentration effect curve P*f*CLK3_G449P

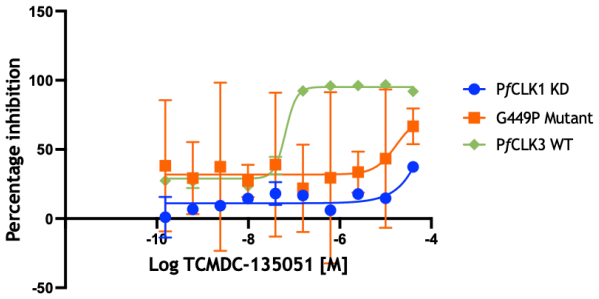

	IC_{50}
P*f*CLK1 KD	In-active
G449P Mutant	16.9 µM
P*f*CLK3 WT	64.69 nM

Figure 4.8 TR-FRET Inhibition assay to determine IC50 for JZ208105-178D1 and HGC-0017530023-NX-1 against G449P Mutant using PfCKL1 wildtype as control.
Inhibition curves of *Pf*CLK1 WT and G449P mutant protein kinases in response to (A) JZ208105-178D1 and (B) HGC-0017530023-NX-1 using (C) TCMDC-135051 as control. Data presented is the average of three independent experiments run in triplicates. Graphs are drawn with Graph Pad Prism and presented as S.E.M.

To investigate if the above *in vitro* results will translate to cellular activity, highly synchronised *P. falciparum* ring stages of the *Pf*CLK3_G449P mutant parasite line were set up in a growth inhibition assay to determine if JZ208105-178D1 and HGC-0017530023-NX-1 are comparable with TCMDC-135051. In addition, antimalarial drugs artemisinin and chloroquine were included as reference. The death curves showed no variation between the EC_{50} potency in P*f*CLK3_G449P mutant and wild type parasite assay for both P*f*CLK1 inhibitors. It was also observed that artemisinin and chloroquine killed P*f*CLK3_G449P mutant just as potently as in 3D7 wildtype. As expected for TCMDC-135051, there was a ~30-fold reduction between its inhibtion effect towards 3D7 wild type and P*f*CLK3_G449P mutant (Figure 4.9). This cellular efficacy demonstrated in this section suggests a link between P*f*CLK1 dependent inhibition and the antimalarial activity of JZ208105-178D1 and HGC-0017530023-NX-1 against asexual blood stages.

A

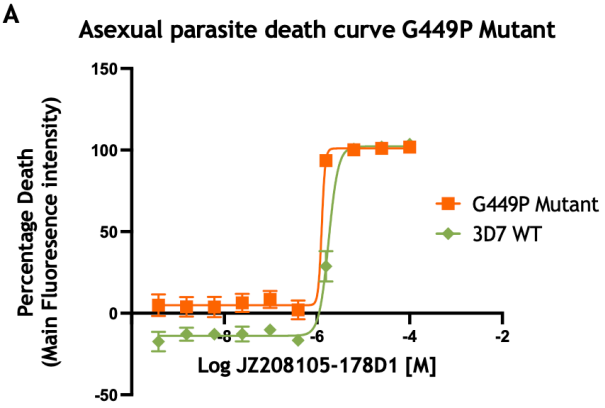

	EC_{50}
G449P Mutant	1.26 µM
3D7 WT	1.78 µM

B

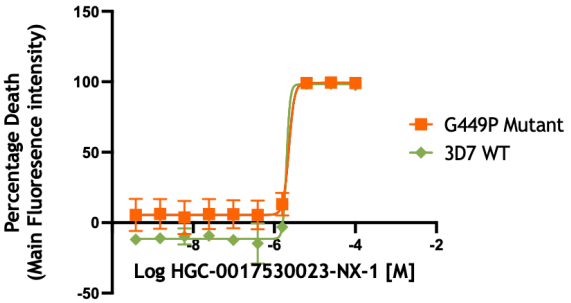

	EC_{50}
G449P Mutant	2.3 µM
3D7 WT	2 µM

C

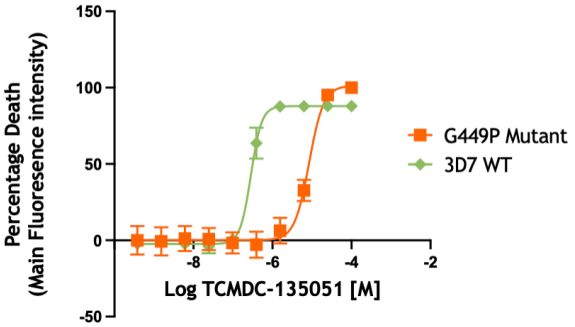

	EC_{50}
G449P Mutant	8.5 µM
3D7 WT	285 nM

D

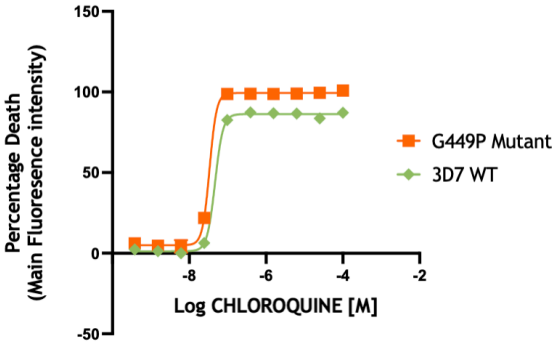

	EC_{50}
G449P Mutant	33.67 nM
3D7 WT	46.87 nM

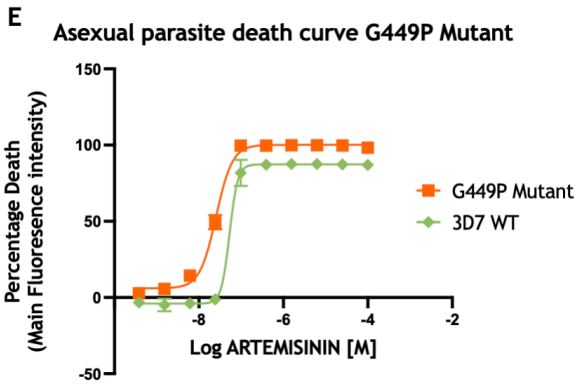

	EC_{50}
G449P Mutant	25.49 nM
3D7 WT	53.08 nM

Figure 4.9 TCMDC-135051 insensitive PfCLK3-G449P mutant parasites in a growth viability assay with JZ208105-178D1 and HGC-0017530023-NX-1 and TCMDC-135051 as a negative control.
A) TCMDC-135051- G449P mutant plasmodial activity is reduced by 28-fold difference compared to 3D7 WT activity B) JZ208105-178D1 and C) HGC-0017530023-NX-1 maintain micromolar potency in G449P mutant same as in 3D7 WT. The antimalarial drugs D) Chloroquine and E) Artemisinin potency suggest CLK independent inhibition. Data is the average of three independent experiments in triplicates ±S.E.M.

4.2 Discussions

In this chapter, tools to inhibit P*f*CLK1 were identified, assessed for their mode of inhibition, and their interaction with the plasmodial protein kinase. In the past 10 years, a variety of *in vitro* assays have been developed and proven to be useful for the prediction of the pharmacokinetic (PK) parameters of an inhibitor (Yadav et al., 2021). The TR-FRET assay established in chapter 3 was used for the *in vitro* measurement of parameters that determine the PK behaviour of JZ208105-178D1 and HGC-0017530023-NX-1. The activity of the P*f*CLK1 kinase domain quantified in the presence of increasing concentrations of both compounds was shown to be modulated at low nanomolar concentrations. This *in-vitro* activity by the P*f*CLK1 inhibitors is comparable to the reported activities of potent inhibitors developed for *h*CLK1 (ElHady et al., 2023).

The extensive research into developing inhibitors for the treatment of various human diseases underlined by CLK1 phosphorylation has yielded in synthesizing and characterising several CLK1 inhibitors(El-Gamil et al., 2023). Reports have revealed that targeting the ATP binding pocket is a common mechanism of action across a diverse range of natural and synthetically derived *h*CLK1 inhibitors(Saldivia et al., 2020). Consequently, these inhibitors were also found to exhibit limited selectivity for *h*CLK1 over other kinases within the CMGC family and related enzymes due to the high structural similarity of their ATP binding sites. The high degree of sequence homology observed between *h*CLK 1 and *h*CLK 2 (54%), *h*CLK 1 and *h*CLK 3 (48.4%), and *h*CLK 1 and *h*CLK 4 (78.4%) complicates the development of selective CLK1 inhibitors. Nevertheless, there are numerous successful examples of Inhibitors that are selective for *h*CLK1 over *h*CLK3 have been reported in literature, they are listed in Table 4.3: compounds 3,36,53 and 63 (ElHady et al., 2023).

To investigate if this common mechanism of action applies to the P*f*CLK1 inhibitors, both compounds were profiled for selective activity in a TR-FRET assay against P*f*CLK3 and compared to TCMDC-135051 - P*f*CLK3 inhibition. Interestingly, the two compounds were found to be selective for P*f*CLK1 over P*f*CLK3, although the degree of selectivity was almost three times reduced in HGC-0017530023-NX-1 compared to in JZ208105-178D1. This would suggest that the P*f*CLK1 inhibitors, in particular JZ208105-178D1 may be exhibiting the same

mode of action as reported for several hCLK1 inhibitors where the ATP binding site is targeted to modulate substrate binding *in vitro*.

To explore the possibility ATP binding mode, the *in vitro* ATP competitiveness of JZ208105-178D1 and HGC-0017530023-NX-1 was evaluated, first in a compact experiment and then in a more robust assay across a range of ATP and inhibitor concentrations. The IC_{50} of an ATP competitive inhibitor will increase in the presence of elevated ATP concentrations and the IC_{50} values remain unchanged with increasing ATP for non-ATP competitive or can be indicative of mixed type of inhibition (Garcia-Molina et al., 2022). In the assay set up, the IC_{50} and ATP K_m values determined for JZ208105-178D1 revealed a direct proportional relationship between high concentrations of ATP and inhibitor indicative of a high affinity for ATP. There were no significant changes in the IC_{50} values determined for HGC-0017530023-NX-1, this is suggestive of a non-competitive allosteric inhibition and deviates from the predictions of the literatures cited in paragraph two. By comparing the results obtained for both compounds, the assay set up is well suited to discriminate between different modes of inhibition.

Table 4.3. Reported IC_{50}s for potent CLK1 inhibitors.

Inhibitor	IC_{50} for Clk1 (nM)	IC_{50} for Clk2 (nM)	IC_{50} for Clk3 (nM)	IC_{50} for Clk4 (nM)
3[111]	20	200	Inactive	15
36[138]	2	23	Inactive	4
42[140]	1.1	2.4	n.d.	n.d.
44[66]	0.67	15	110	n.d.
53[156]	8	20	Inactive	12
59[18]	7	19.1	58	2.3
60[67]	12.7	125	>1 μM	n.d.
61[158]	4	>250	n.d.	n.d.
62[158]	9.7	486	n.d.	6.6
66[159]	2	31	Inactive	8

Abbreviation: n.d., not determined.

Enzyme assays and recombinant proteins have been used thus far in this study to profile the activity and specificity of the P*f*CLK1 inhibitors. While these experiments have been invaluable, there is a limitation to the accurate reflection of normal physiological processes. For example, cellular concentrations of ATP is generally much higher than ATP K_m, which may require a high concentration of drug for efficacy, particularly with ATP-competitive inhibitors, bringing potential toxicity problems (Vasta et al., 2018). Such information is very important in determining whether a candidate inhibitor should be developed further (Berrouet et al., 2020). To determine whether asexual blood stage replication can be interrupted by the experimental compounds, the treatment of 3D7 asexual stages with increasing concentrations of P*f*CLK1 inhibitors over the course of one life cycle was compared to the proven effectiveness of TCMDC-135051, artemisinin and chloroquine. The parasite viability assays showed that anti-plasmodial activity was highest for artemsinin and chloroquine followed by TCMDC-135051 then JZ208105-178D1 and HGC-0017530023-NX-1 (Figure 4.7). Surprisingly, the activity of the P*f*CLK1 inhibitors reduced significantly in live parasites by ~100 to ~200 fold. This could be because of factors like the differences in ATP K_m of the kinases as mentioned above, differences in kinase abundance within the cells or differences in the sensitivity of the cells to targeted pathways (Olivieri et al., 2022).

The discrepancy between molecular and phenotypic screening has been reported as a common feature of molecules tested for potential antimalarial properties and is mainly a result of large variability in their capacity to cross several cellular membranes (Vasta et al., 2018). In a culture system such as a mix of live parasites and red blood cells, the ability of any inhibitor to penetrate the erythrocytic plasma membrane represents the first barrier to overcome. Another limiting step is a small molecule that needs to cross the parasite membrane, in addition, hurdles such as plasma/serum proteins that bind and sequester the inhibitor out of its site of action can also explain why potent molecules against purified enzyme turn out to be poor inhibitors when tested in cell culture conditions(Forte et al., 2021). Given that the study published by Kern and co-workers has clearly shown that the pharmacological inhibition of P*f*CLK1 might lead to parasite growth limitation is indicative that potent inhibitors reaching

intracellular P*f*CLK1 will translate systematically into a decrease of intraerythrocytic parasitaemia.

To correlate the exposure of an inhibitor at the site of action to a pharmacological and phenotypic readout, it is important to validate the target as proof of target engagement (Hanson et al., 2019). This can also provide information about the required drug dose to fully occupy a target without inducing undesired off target activity (Aykul & Martinez-Hackert, 2016). An "indirect" approach was utilised to establish the P*f*CLK1 inhibition pathway as the cause of parasite death in the viability assay. This involved using the P*f*CLK3_G449P mutant to determine P*f*CLK1 specific inhibition *in vitro* and selective activity *in vivo* based on the rationale that the P*f*CLK1 template present in the mutant should confer similar sensitivity as the wild type of kinase to inhibitors. Results from the concentration effect curves are highly suggestive that the mutations around the gatekeeper region in the subdomain IV negatively affect HGC-0017530023-NX-1 mode of action. The gate keeper residue is important for inhibitor binding to kinases and mutations can to lower ATP affinity and attenuate catalytic activity (Schröder et al., 2020). There are three types of inhibitors known to bind the gatekeeper namely, type I½ inhibitors, ATP-competitive (Type I) inhibitors and non-covalent inhibitors (Martinez et al., 2020a). Type I and type I½ inhibitors occupy part of the adenine binding pocket and form hydrogen bonds with the hinge region connecting the small and large lobes of the enzyme (Martinez et al., 2020). The results here suggest a different binding mechanism to what was demonstrated in the ATP competitive assay and that HGC-0017530023-NX-1 might exhibit a type I or type I½ binding. The high potency displayed for JZ208105-178D1 - P*f*CLK3_G449P mutant inhibition may be the closest prediction of P*f*CLK1 full length *in vitro* inhibition given that the full length P*f*CLK3_G449P mutant was tested in this assay.

Lastly, the findings that P*f*CLK3_G449P mutant asexual blood stage parasite replication is disrupted at the exact same potency of JZ208105-178D1 and HGC-0017530023-NX-1 3D7 wild type inhibition supports a model in which the mechanism of action to reduce parasitaemia and induce consequent parasite death is facilitated by the inhibition of P*f*CLK1 phosphorylation pathways. Thereby chemically validating P*f*CLK1 as a potential therapeutic target.

Chapter 5 Stage specific susceptibility

Several studies have shown that *Plasmodium* kinases are expressed at different life-cycle stages (Arendse et al., 2021) and it is important to understand at what stage our kinase of interest is expressed and its vulnerability to inhibition at each stage. The expression of the P*f*CLK kinases is well established by co-localisation studies that have revealed a distinct punctate P*f*CLK1 expression within the nuclei of trophozoites and schizonts, the nucleus and cytoplasm of gametocytes. P*f*CLK3 was found mainly present in the nucleus of trophozoites, while primarily located in the cytoplasm of schizonts and gametocyte (Agarwal et al., 2011; Kern et al., 2014). Ideally a good target kinase is essential across multiple life-cycle stages because targeting an essential kinase to the liver, asexual blood, and the gametocyte or mosquito stages of the life cycle can potentially deliver an antimalarial with prophylactic, curative, and transmission-blocking activity (Arendse et al., 2021).

The asexual blood stages in human red blood cells (RBCs) is the symptomatic phase of malaria disease (Venugopal et al., 2020). The stage-specific action of antimalarials has been investigated as far back as the early 1980s (Siqueira-Neto et al., 2023) and is the basis for malaria chronotherapy, the science of timing drug application to achieve optimal chemotherapeutic intervention (Tse et al., 2019). For instance, the former frontline antimalarials, chloroquine and sulfadoxine-pyrimethamine mainly affect trophozoite stages by the inhibiting the hemoglobin catabolism pathway which provides nutrients for the parasite and the folate biosynthesis pathway that delivers the building blocks for DNA synthesis, respectively (Roux et al., 2021). More recent candidate antimalarials such as phosphatidylinositol 4-kinase (PI4K) inhibitor KAI407 have been shown to specifically inhibit schizont development but mostly targeting trophozoites and schizonts sequestration in the microvasculature (Murithi et al., 2020). The compounds that target ring stage parasites in circulation throughout the blood stream, are desirable to prevent further vasculature blockage and artemisinins were the first clinical antimalarials with ring-stage activity (Blasco et al., 2017). Artemisinin-based combination therapies have proven effective in reducing malaria death and burden. However, parasites resistant to artemisinins and their partner drugs have emerged and now undermining malaria control (Suresh & Haldar, 2018).

Malaria transmission is mediated by mature sexual forms referred to as gametocytes (Paonessa et al., 2022). These stages facilitate human-to-vector transmission by staying in circulation within the vertebrate host and are taken up during a bloodmeal to continue sexual development in the mosquito vector. The gametocyte phase represents a bottleneck of the lifecycle that exploited for preventative malaria therapies (Dash et al., 2022).

Concurrently, knowing which of these hits are fast-acting compounds is of great interest. In an ideal scenario inhibiting a kinase either leads to a fast rate of kill of the blood stages or if at a moderate/slow rate of kill, will occur on multiple life-cycle stages (Walz et al., 2023). Firstly, a fast action will ensure rapid relief of symptoms for the patient. Secondly, by rapidly reducing the parasitaemia, this could minimize the occurrence of mutations leading to new drug resistance mechanisms (Siddiqui et al., 2021). The rate of kill can be measured using the standard parasite reduction ratio (PRR) assay as described in Walz et al., (2023). However, this protocol can take three weeks to completed, other studies have designed alternative assays to circumvent the time constraint. For example, Linares et al., (2015) developed and validated a rapid *in vitro* fast viability assay to assess anti-malarial killing profiles 48hours after drug treatment. This protocol was adapted and modified to SYBR-green staining in this study to identify the rapid parasiticidal activity of antimalarial drug compounds.

Target identification forms a major bottleneck for the further optimisation of potential inhibitors into leads with increased target binding, selectivity, and whole-cell activity. The Malaria Drug Accelerator (MalDA) consortium aims to identify new antimalarial leads through *in vitro* phenotypic screens, in line with this mandate (T. Yang et al., 2021), the stage-specific susceptibility of asexual *P. falciparum* blood stages and gametocytes to the P*f*CLK1 specific inhibitors were analysed. This chapter discusses in detail the stage specific potencies of the P*f*CLK inhibitors. It also shows the morphological effects of JZ208105-178D1 treatment on specific asexual stages and gametocytes. Lastly, the killing rate for JZ208105-178D1 was determined as a measure of drug effect. Therefore, this chapter aims to:

- Determine the peak activity for JZ208105-178D1 and HGC-0017530023-NX-1 in intraerythrocytic cycle.
- Determine the killing rate of JZ208105-178D1,
- Assess the gametocidal activity of the most potent P*f*CLK1 inhibitor
- Evaluate the potential to fulfil MMV's target candidate profile.

5.1 Results

5.1.1 Specific half maximal lethal doses illustrate peak activity of CLK inhibitors on the most susceptible parasite blood stages.

A medium-throughput *in vitro* assay was designed to quantitatively analyse the susceptibility of distinct stages of intra-erythrocytic development to JZ208105-178D1 and HGC-0017530023-NX-1 activity. TCMDC-135051 was included as a compound with a known target to serve as a reference. Highly synchronized 3D7 parasites were exposed to a range of compound concentrations at consecutive 10 h treatment periods during the early ring, late ring, early trophozoite, late trophozoite, and schizont stages (Figure 5.1). Parasites were cultured in 96-well plates and allowed to further develop for 72 hours, in the absence of drugs extending through to the invasion of new RBCs and development until the trophozoite stage. Parasites were incubated with lysis buffer containing SYBR and quantified by fluorescence intensity. The EC_{50} concentrations derived by non-linear regression analyses of the dose-response data, based on the 10 h exposures at specific asexual blood stages are referred to as the EC_{50}^{10h}. The EC_{50} value calculated from the standard 72 h exposure assay is the EC_{50}^{72h}.

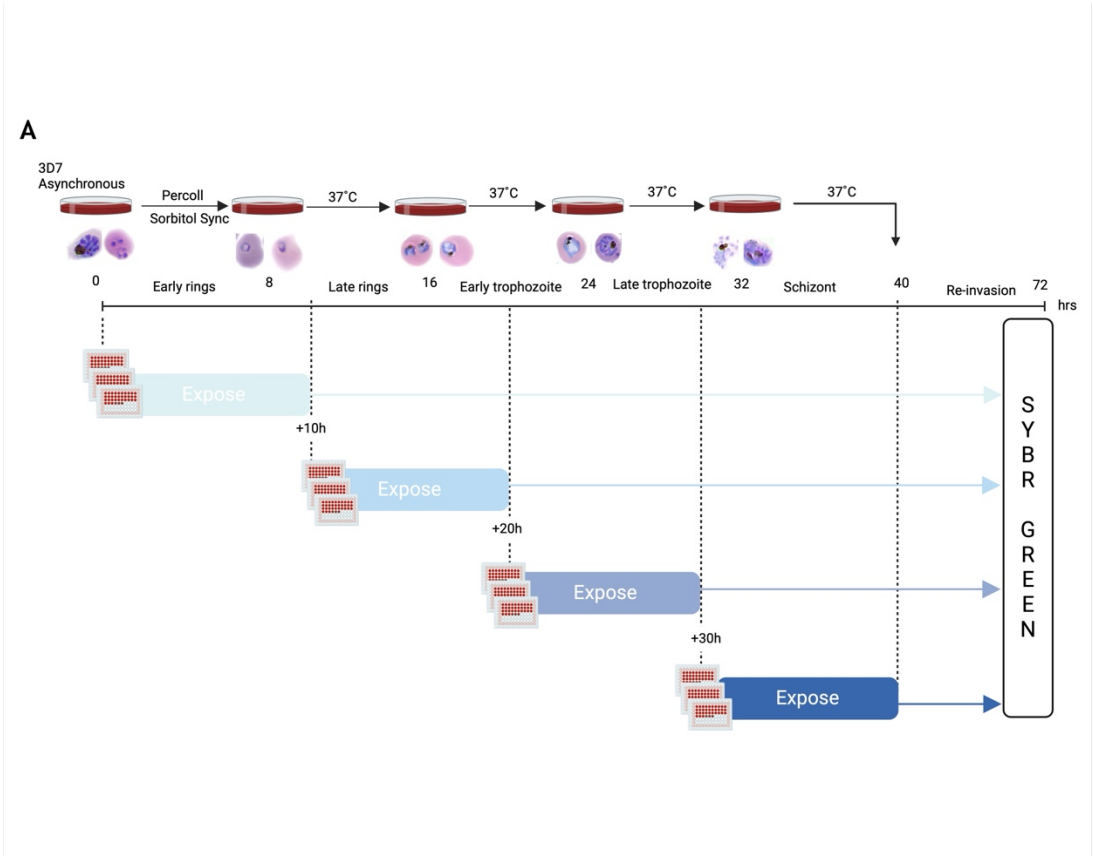

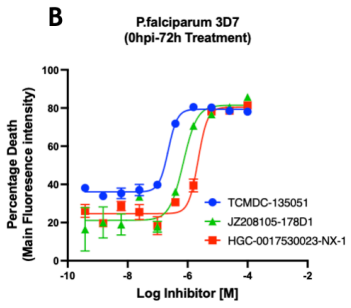

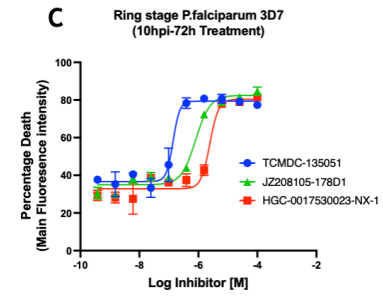

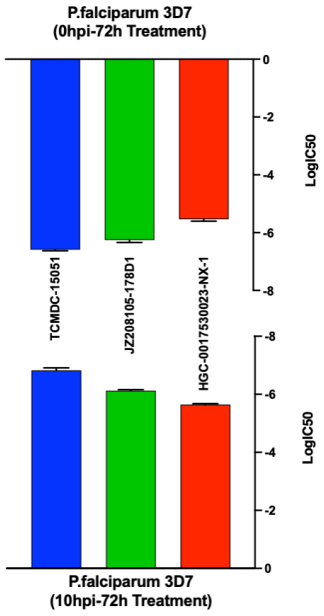

0H	EC_{50}	Km	Vmax
TCMDC135051	225nM	2.5	33
JZ208105178D1	715.nM	3.1	21
HGC0017530023NX1	2.2μM	3.2	19

10H	EC_{50}	Km	Vmax
TCMDC135051	138nM	2.5	34
JZ208105178D1	807.nM	3	28
HGC0017530023NX1	2.4μM	3	23

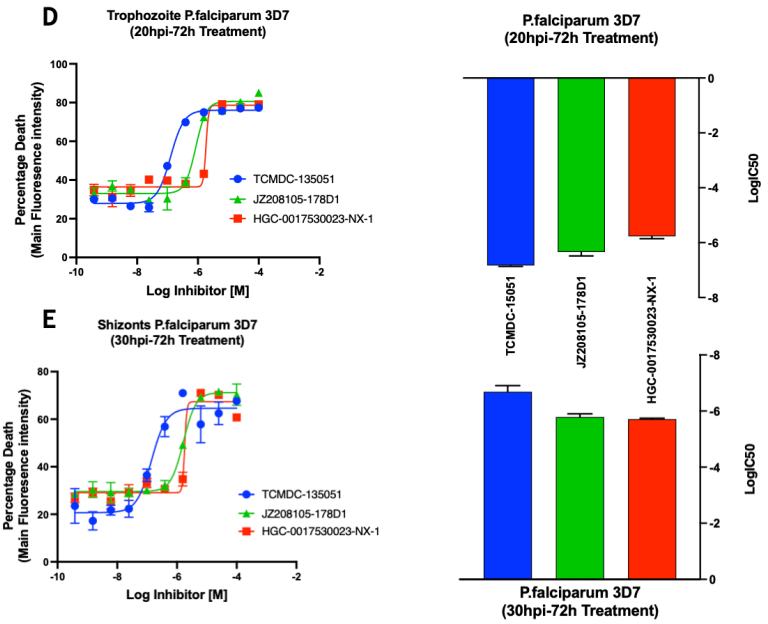

20H	EC_{50}	Km	Vmax
TCMDC135051	126nM	2.6	29
JZ208105178D1	847.nM	3	26
HGC0017530023NX1	1.84µM	3	25

30H	EC_{50}	Km	Vmax
TCMDC135051	140nM	2.6	23
JZ208105178D1	1.6µM	3.1	22
HGC0017530023NX1	1.8µM	3.2	21

Figure 5.1 Experimental design for asexual blood stage specificity profiling of antimalarials and activity profiles of JZ208105-178D1, HGC-0017530023-NX-1 and TCMDC-135051.
(A) Synchronized parasites were exposed for 10 h at the stages indicated. Survival at 72 h post-invasion was assessed by fluorescence quantification. (B - E) Unique stage specificity profiles of JZ208105-178D1, HGC-0017530023-NX-1, and TCMDC-135051. Bar plots indicate the IC_{50}^{10h} when parasites were exposed only during the early ring, late ring, early trophozoite, late trophozoite, or schizont stage. Data is the average of three independent experiments in triplicates ±S.E.M.

Light microscopy confirmed a correspondence between different periods of exposure and developmental stages showing that schizont sequestration occurred within the 32 to 40 h time point indicating that all asexual blood stages were profiled (Figure 5.1a). Although TCMDC-135051 showed little variation in EC_{50}^{10h} values throughout the ring to schizont stages and was consequently confirmed with peak activity at all asexual stages. On the other hand, JZ208105-178D1 measured a 2-fold reduction in potency at the schizont stage at EC_{50}^{10h} 1.6µM compared to the early stages incubated for longer time. The least potent specificity profile was observed in HGC-0017530023-NX-1 with little to no variation in the EC_{50}^{10h} and EC_{50}^{72h} values at ~2µM (Figure 5.1).

5.1.2 **Morphology analysis of JZ208105-178D1 schizonticidal activity.**

JZ208105-178D1 has now emerged as the more potent P*f*CLK1 inhibitor in this study. The trophozoite to schizont stage parasites appeared most resilient to inhibition and to evaluate the effect of P*f*CLK1 inhibition on schizont morphology. Synchronised cultures of *P. falciparum* 3D7 parasites were set up and treated with 1 µM of JZ208105-178D1 at 0, 0-10, 10-20, 20-30 and 30-40 hpi. Thin blood smears were collected at every time point and giemsa stained for light microscopy analysis. As shown in Figure 5.2, untreated parasites developed normally within the expected timeline. However, treating ring-stage parasites at 0 h had maximum impact, with parasite growth arrested and not progressing further than early trophozoites that looked condensed and pigmented. The treatment lasting 10 h appeared to stunt parasite progression past late trophozoite stage with the appearance of pycnotic nuclei and condensation of nuclear material. Although drug treated trophozoites at 30 h developed to schizont stage, however growth was stunted and resulted ultimately in parasite death. Treatment at 40 h appeared to only delay schizont segmentation but did not induce parasite death which is evidenced by the lack of nuclear condensation and pigmentation (Figure 5.2).

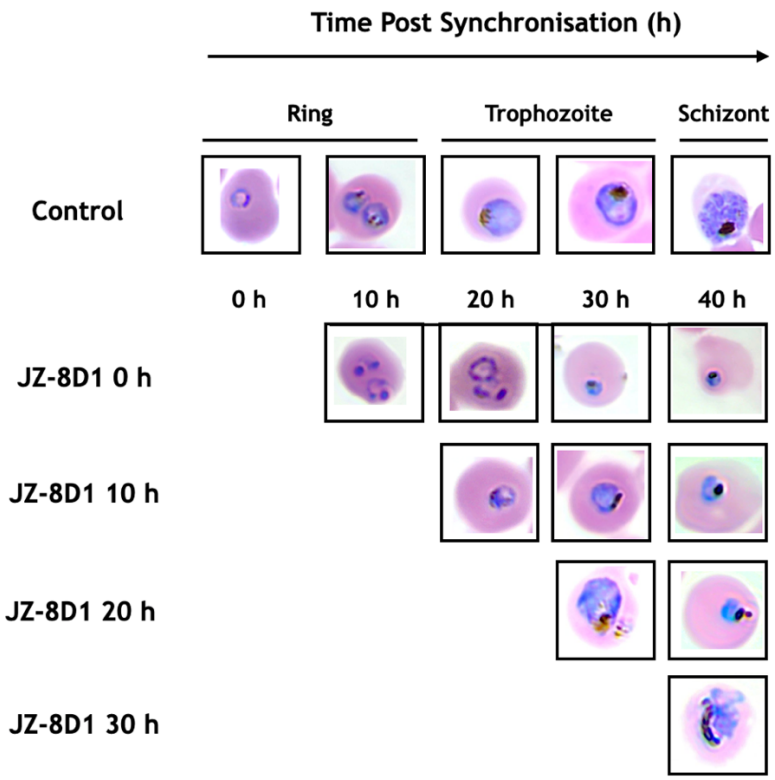

Figure 5.2 JZ208105-178D1 inhibits asexual parasite growth and development at all stages. Synchronised *P. falciparum* parasites were challenged with continuous drug exposure from time point zero hours to 40 hours with drug added every 10 hours. Samples were collected from 0, 10, 20, 30, 40 and thin smear blood films were prepared, giemsa stained, and images of parasites captured using *evos* microscope with magnification of 100X. As shown, irrespective of the time the drug was added, parasite growth is stalled once the inhibitor was added resulting to parasite growth stagnation and eventual death. The untreated control, however, grew to trophozoites and segregated schizont within 40 hours as expected. This demonstrates that JZ208105-178D1 is potent against multiple stages of the parasite life cycle.

Overall, the morphological analysis showed that JZ208105-178D1 displayed activity across all developmental stages, however, the presence of nuclear activity in treated schizonts implies the occurrence of SYBR green binding to the nuclei and the subsequent fluorescence quantification that may have been observed as increased EC_{50}^{10h} values against schizonts for the stage susceptibility potency assay in the previous section.

5.1.3 **Parasite** viability fast assay

To accurately determine pharmacodynamic (PD) parameters such as the rapid onset of drug action and the rate of parasite clearance required to rapidly reduce clinical symptoms for a new candidate drug, it is important to discriminate between viable and nonviable parasites (Walz et al., 2023). Relying on proxies to measure viability can result in the misclassification of viable parasites as nonviable (or vice versa) after treatment and cause inaccuracies in parasite death estimation consequently leading to the over- or underestimation of drug activity. However total parasitemia measurements *in vivo* may be complicated by the failure to detect metabolically inactive viable parasites (e.g., dormant parasites) whilst metabolically active dying or dead parasites are detectable (Radohery et al., 2022). Other instances such as delayed parasite death observed with antibiotics for malaria treatment or drug affected metabolic pathway measurement with no alteration to parasites viability could also lead to erroneous measurement assumptions. These different situations are proof that metabolic activity and viability can be uncoupled naturally or in response to drug treatment, therefore relying on the first to measure the latter can be a possible source of artefacts (Thriemer et al., 2014).

As described above, fluorescence-based assays do not permit to discriminate between cytotoxic (actively killed parasites at high efficacy) and cytostatic (incomplete parasite clearance causing resistance selection) anti-infective activities and clinical efficacy (Genetu Bayih et al., 2017). The reduction of circulating parasitized erythrocytes generally follows a log-linear curve that can function as a predictive therapeutic index, the parasite reduction ratio [PRR]. The killing rate of antimalarial drugs *in vivo* can be estimated by PRR which is the ratio of parasitemia at the time of drug treatment to the ratio of parasitemia post 48 hours of drug treatment, corresponding to one asexual life cycle (Walz et al., 2023). Based on the killing rate, PRR values can vary greatly for example, fast-killing drugs like artemisinin can reduce parasitemia by 99.99% during one life cycle and exert a PRR of 10^3 -10^4 whereas slow-killing drugs such as clindamycin effect low *in vivo* PRR in the order of magnitude of only 10. Hence, beyond the killing rate, drug inhibitory effect can also be affected by the type of growth inhibition involved (Radohery et al., 2022).

Here the direct measurement of intraerytrocytic *P. falciparum* viability in response to drug treatment over two time points, 24 and 48 hours, was used to profile the killing rate of JZ208105-178D1. Because drugs vary in potency and to compare their effects, treatments were performed at concentrations based on the drug-specific 50% effective concentration (EC_{50}), which is the concentration required to inhibit the growth of a parasite population by 50% (Thriemer et al., 2014). To determine parasite viability and compare difference in drug treatments and time points, parasitaemia of infected erythrocytes following treatment were calculated as a percentage of untreated control erythrocytes expressed as a percentage using the formula below:

$$Parasite\ viability = \frac{New\ infections\ in\ treated\ wells}{New\ infections\ in\ control} * 100$$

Equation 3 where

new infections in treated wells is the fluorescence quantified for treated parasites.

new infections in control is the fluorescence quantified for untreated parasites.

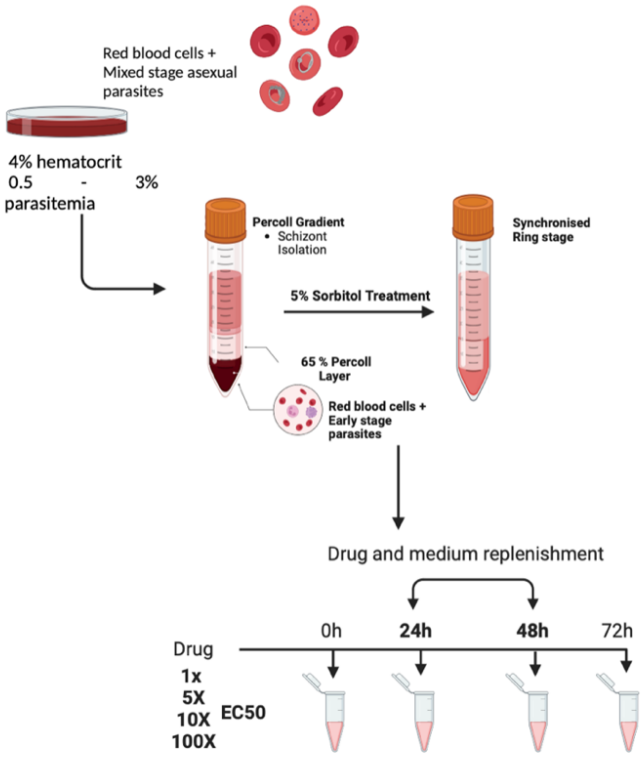

Figure 5.3 Experimental setup for in vitro parasite viability fast assay.
Intraerythrocytic *P. falciparum* cultured at 0.5% parasitemia and 2% hematocrit were treated with drugs at 1x, 5x,10× and 100x the predetermined IC_{50}. The medium is exchanged, and the drug replenished every 24 h. Culture aliquots are taken out at defined time points, washed. Drug-free parasites cultured with fresh erythrocytes under limiting serial dilution conditions are subsequently monitored for 50 h to allow the viable parasites resume growth to a measurable culture. Finally, the number of viable parasites present after washing can be extrapolated from the number of dilutions still yielding parasite-positive wells.

The assay was validated against two antimalarial agents with well-characterized rapid parasite killing profiles: chloroquine and artemisinin. Ring stage parasites were synchronised and serially diluted when cultured in the presence of JZ208105-178D1, TCMDC-135051, artemisinin and chloroquine for 50 hours to allow reinfection of newly formed rings. Results in Figure 5.4 showed that the assay was able to distinguish killing rate within 48 h after drug treatment. Treatment with artemisinin, JZ208105-178D1 and TCMDC-135051 at their EC_{50} led to a rapid decrease in viable parasites within 48 h. Consequently, 24 h and 48 h were identified as the most relevant time points that could provide the information required to identify the rapid killing compounds.

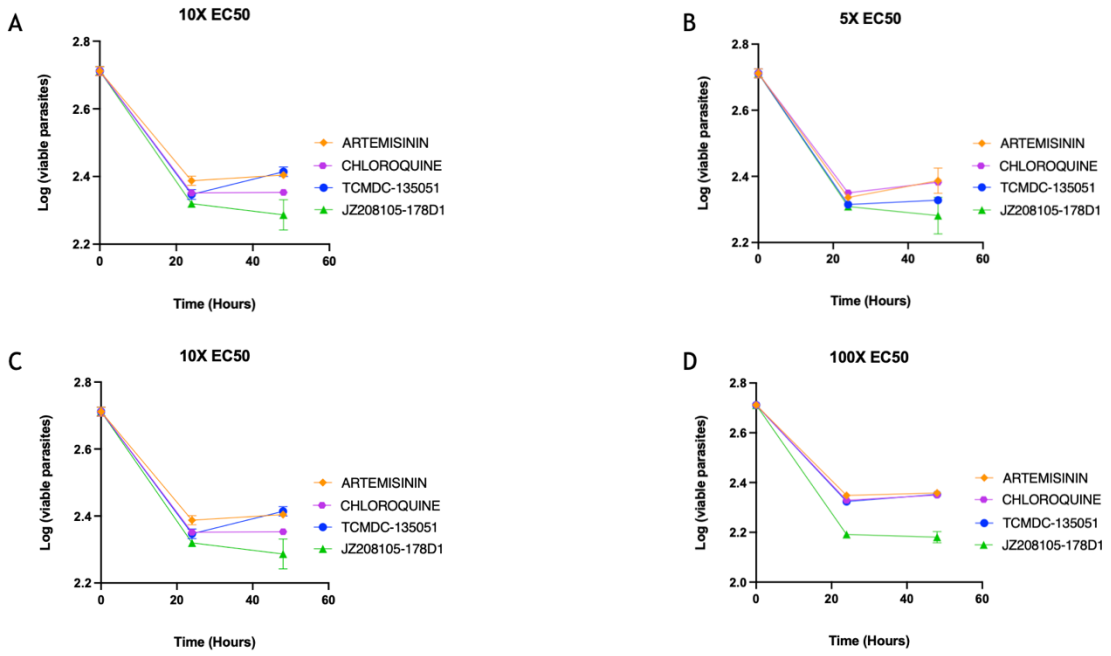

Figure 5.4 Two-time point viability analysis using an abbreviated killing rate procedure. Killing profiles for artemisinin (art), chloroquine(chq), TCMDC-135051, and JZ208105-178D1 at 1X, 5X, 10X, and 100X the EC_{50} concentrations over the course of 50 h following incubation with parasites. Data is the average of three independent experiments in triplicates ±S.E.M.

5.1.4 Inhibitors JZ208105-178D1 and HGC-0017530023-NX-1 exhibit potential transmission blocking efficacy.

To investiagte for the gametocytocidal effect of the P*f*CLK1 inhibitor JZ208105-178D1 compred to TCMDC-135051, gametocyte toxicity assays were carried out. Asexual parasites were tightly synchronised and then artificially induced to stress with high parasitemia and partly spent media to trigger gametocytogenesis induction. Following induction, sexually committed parasites that re-invade new erythrocytes were supplemented with *N*-acetylglucosamine to prevent subsequent invasion events and to clear the cultures of residual asexual parasites. The remaining healthy stage II gametocytes were treated daily with 0.5x, 1x, 2x, 4x and 8x EC_{50} drug concentration of TCMDC-135051 and JZ208105-178D1 over the cause of 12 days to cover the developmental process to stage V gametocytes.

The viable gametocytes were counted from microscopic observation of thin-smear Giemsa-stained slides to determine the gametocytemia.The results

showed a concentration dependent decline in stage V gametocytemia with induced morphological alterations. At sub micromolar concentrations, both inhibitors are shown to reduce the number of mature gametocytes in culture by a half fold difference and the morphology of the gametocytes appeared stunted (Figure 5.5).

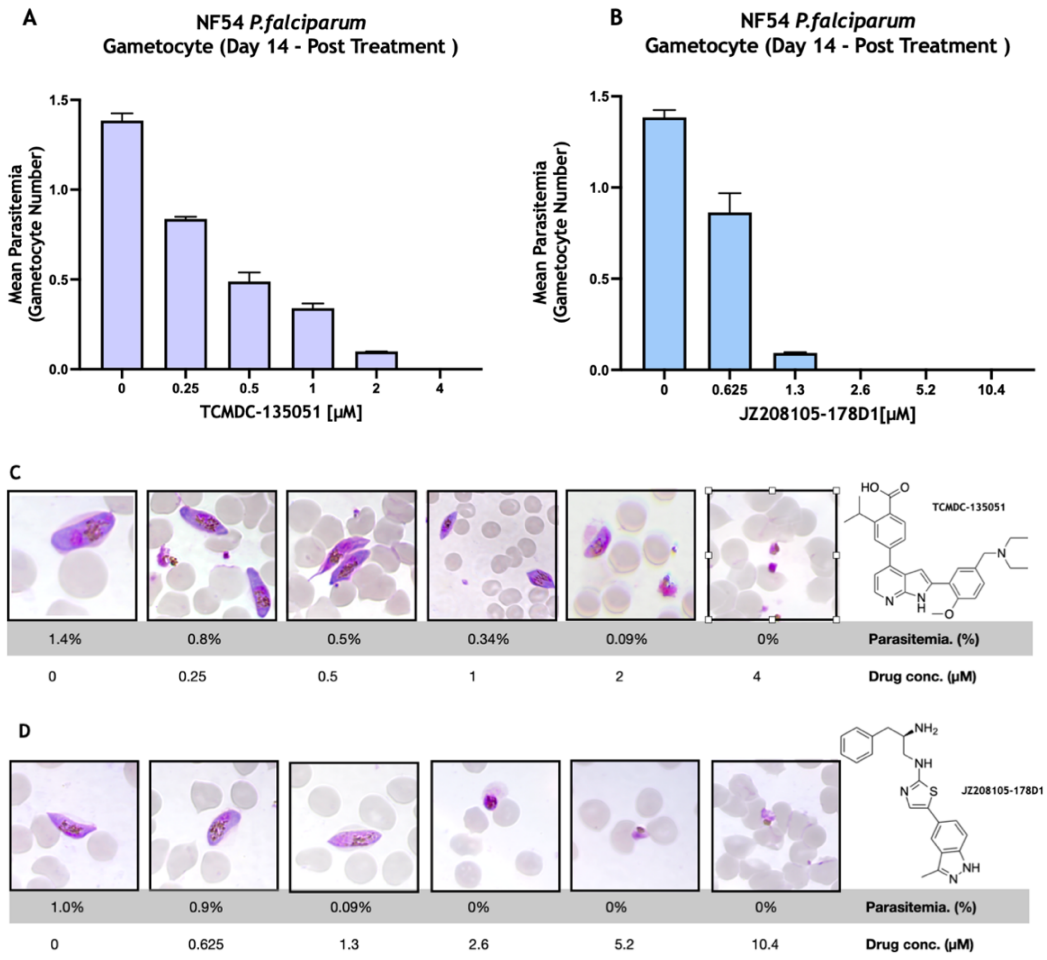

Figure 5.5 NF54 Gametocyte toxicity assay with JZ208105-178D1 and TCMDC-135051. Compounds were added at concentrations 0.5x, 1x, 2x, 4x and 8x EC_{50} to stage II gametocyte cultures for two days. Drug pressure was removed, and cultures were maintained in compound free medium. After 14 days, the numbers of stage IV and V gametocytes were counted in a total of 1000 RBCs and correlated to the gametocyte numbers of untreated control. TCMDC-135051 has established gametocytocidal activity and was utilized as positive control. A) Gametocytemia after drug treatment and B) Morphological differences between treated and untreated gametocytes.

5.2 Discussions

Investigating the timing of peak activity for the P*f*CLK inhibitors required a susceptibility profile to provide more resolution into the different modes of actions. This was achieved by identifying the specific time points across the asexual blood stage development where these compounds have displayed the most activity. As expected, all stages of the parasite were found susceptible to all three P*f*CLK compounds for treatment starting at time 0 h. Activity for TCMDC-135051 peaked at the 20h during trophozoite development (Figure 5.1 D). In contrast activity for JZ208105-178D1 was observed to peak when added to parasites no later than 10 h into the intraerythrocytic cycle where it targets and inhibits early stage trophozoites. Surprisingly, no peak activity was observed for HGC-0017530023-NX-1 at any point of the lifecycle stage, taken together with its high micromolar plasmodial activity, HGC-0017530023-NX-1 has emerged as the least potent P*f*CLK1 inhibitor and will no longer be used for further investigation. Asexual blood stage susceptibility profiling may also help prioritize screening hits. The stage specificity of antimalarial agents is of clinical importance particularly in terms of parasite clearance kinetics and recrudescence rates (McCarthy et al., 2021). Compounds with potent IC_{50}^{10h} values across all stages are of particular interest for further development as such activity profiles might compensate for a faster clearance or other pharmacokinetic-related issues that reduce *in vivo* exposure time.

Notably, the trophozoite stage specificity profiles for TCMDC-135051 is consistent with the timing of its target expression: P*f*CLK3 expression spans the trophozoite to schizont stages (Kern et al., 2014). Furthermore, the asexual blood stage specificity profiles can also inform the selection of partner drugs for combination therapies. Ideally, combinations would target all different asexual blood stages. As an example, schizont-specific compounds could be partnered with compounds that target rings and trophozoites. These profiles can also be used to devise strategies to delay the emergence of resistance (Dechering et al., 2022). For instance, the trophozoite-active compound TCMDC-135051 could be combined with another compound with a broader activity profile including late trophozoite to delay the emergence of TCMDC-135051 resistance.

The management of malaria currently relies heavily on the use of ACTs for the treatment of acute *P. falciparum* malaria. Recent reports of resistance to ACTs, such as dihydroartemisinin and piperaquine, have emphasized the need to discover new antimalarial medicines with novel mechanisms of action(Siddiqui et al., 2021). The push toward an elimination and eradication agenda for malaria has gained momentum in recent years, and these ambitious goals will require a range of antimalarials with activity against different stages of the parasite to effectively eliminate the spread of disease(T. Yang et al., 2021). The MMV has outlined a range of target candidate profiles with lists of requirements that are necessary to address these specific needs (Burrows et al., 2017). The target candidate profiles are listed out in the introduction chapter of this thesis (Figure1.4). The high-throughput screens can identify potent chemical scaffolds but not knowing their target often hampers their further development(Horne et al., 2024).While the *in vivo* assays have shown that JZ208105-178D1 inhibits parasite replication in the red blood cell cultures, it was important to determine whether such inhibitory effects were due to blocking parasite growth or killing them. This was assessed by setting up a morphological profile for drug treated parasites compared to the untreated control during the same time point. The analysis showed that parasite death was induced following growth arrest. Furthermore, analysing the morphology of inhibited schizont stages suggests there may be an inaccurate estimate of drug activity concerning parasite viability. This is a consequence of the limitations using fluorescence-based assay that are incapable of discriminating between viable and nonviable parasites. Parasites committed to death can still display metabolic activities or steady levels of marker expression and be classified as viable in fluorescence assays and vice versa (Kulkeaw, 2021). Another observation was that drug treated schizonts at 30 h appeared stunted, typically at this point in the cycle schizonts undergo segmentation to form daughter merozoites that upon rupturing from the infected cell will egress to invade new erythrocytes and initiate the next cycle (Perrin et al., 2021). The stunted schizonts still possess nuclei that can be potentially bound by SYBR green molecule in a growth inhibition assay stain and be quantified for fluorescence analysis as viable parasites thereby reducing the potency of JZ208105-178D1 as observed in Figure 5.1 C.

Drug removal followed by a regrowth period makes it possible to discriminate cytostatic from cidal compounds at the relevant time points. JZ208105-178D1 was evaluated to determine its speed of action compared to TCMDC-135051, artemisinin and chloroquine using the *in-vitro* parasite viability fast assay. The data reported for the viability assay showed that similarly to artemisinin, TCMDC-135051 and JZ208105-178D1 known to target P*f*CLKs that are expressed during the early stages potently inhibit the growth of these cultures within 24 h of exposure and reducing the parasite survival by ~ 50% at their respective EC_{50}, concentrations. JZ208105-178D1 demonstrates fast acting antimalarial activity at sufficient drug concentration and the results showed that drug removal was not proportional to the loss of potency in treated parasites which suggests that JZ208105-178D1 mode of action may be irreversible.

To verify the gametocytocidal effect of JZ208105-178D1 as the selected potent inhibitor of the experimental series, gametocyte toxicity assays were carried out as previously described in methods chapter 2. TCMDC-135051 has been shown to exert inhibition between infected red blood cell commitment to stage II gametocytes [pEC_{50} = 6.04 $\pm$ 0.11 (EC_{50} = 0.91 μM)] (Alam et al., 2019). The observations were made that comparable to TCMDC-135051, JZ208105-178D1 tested in this assay significantly, gametocyte maturation was compromised by 40-60% compared to un-treated control. High gametocytocidal effect was exhibited for treatment with 1x EC_{50}. Future research would be aimed towards comparing parasiticidal activity with selective toxicity for the parasites against mammalian cells.

This chapter showed JZ208105-178D1 to be active against all blood stages of the *P. falciparum* asexual life cycle with a fast onset of action with potential transmission blocking activity. The JZ208105-178D1 compound offers great promise for further optimization toward the development of a new medicine for the treatment of symptomatic malaria.

Chapter 6 Discussion

The results presented in this thesis provide insight into the effects of the pharmacological modulation of CLK1 phosphorylation events in *Plasmodium falciparum* life cycle stages. In eukaryotes, the CLK family have been considered as potential therapeutic targets that mediate pathological processes through alternative splicing modulation or changes in transcriptional activities (Song et al., 2023). Significant preclinical and clinical data on the development of selective small inhibitors for CLKs have revealed that CLKs exert important functions through splicing or non-splicing processes(Muraki et al., 2004; Tam et al., 2020). Like all CLKs, CLK1 is a critical player in SR protein phosphorylation which is essential in recruiting the splicing apparatus and the splice site pairing, two major steps in the mechanism of alternative splicing (Aubol et al., 2016). An alteration in the concentration of SR proteins has been hypothesised as crucial to the control of alternative splicing and the dysregulation of alternative splicing is frequently found underlying human diseases, including neurodegenerative diseases, autoimmue, cancer tumors (More & Kumar, 2020) . The need for new drug targets and antimalarials with novel mode of action to circumvent the recurrent emergence of resistance in mosquitoes and parasites to insecticides and antimalarials led to mapping of the *P.falciparum* kinome (Solyakov et al., 2011; Ward et al., 2004). Several protein kinases were discovered to mediate essential developmental processes for the parasite life cycle stages. The CLK family in *Plasmodium* were implied in splicing processes required for the parasite survival (Solyakov et al., 2011). The aim was to characterise the role of the CLK1 isoform in *P.falciaprum* using small molecule inhibitors as biological tools and to develop the inhibitors as a potential new class of antimalarials.

6.1 The pharmacological modification of P*f*CLK mediated phosphorylation

In principle it is advantageous to bridge the gap between *in vitro* phosphorylation and physiological phosphorylation events, however the true physiological conditions in the microcellular environment are not always known. For example, fully regulated full-length kinases are often impossible to express, in such cases for practical reasons the non-regulated kinase domains are used in screening (Glickman, 2012). The biochemical characteristics of P*f*CLK1 are poorly studied, and its structure has not yet been elucidated. No group has been able to express significant amounts of recombinant full-length P*f*CLK1 protein for biochemical analysis. Previous studies of P*f*CLK1 kinase activity have used co-immunoprecipitation assays on lysates of asexual 3D7 parasite cultures using mouse polyclonal antibodies against P*f*CLK1 and the resulting precipitated proteins were separated by SDS–PAGE to select protein bands for mass spectrometric analysis to subsequently use the detected peptides for MASCOT searches and identify full-length proteins(Agarwal et al., 2011). Endogenous precipitated proteins revealed phosphorylation activity when exogenous substrates such as histone H1, MBP, or α/ß Casein were added in the presence of ATP. The results have shown the only substrate that has been significantly phosphorylated in more than one study is splicing factor Npl3p (Agarwal et al., 2011; Kern et al., 2014).

To study the molecular mechanism by which P*f*CLK1 influences its targets, the full-length and enzymatically active kinase domain proteins were expressed and purified using a tandem affinity purification protocol and assayed both for *in vitro* phosphorylation of MBP, Casein, CREBtide and *h*SF2 proteins. It was discovered that the kinase domain proteins do indeed have robust kinase activity, and suggests that the N-terminal domain might exert significant negative regulation on activity in the catalytic domain. Furthermore, the presence of the only band observed for full length P*f*CLK1 [γ-32P] ATP assay in chapter 3 (Figure 3.2) suggests that in line with literature reviews on human CLK1 (Aubol et al., 2014) the full length P*f*CLK1 might be hyper phosphorylating the splicing factor *h*SF2 at the N-terminal. *In silico* analysis of *P.falciparum* CLK substrate amino acid sequences identified a putative plasmodial ortholog of the alternative splicing factor ASF-1 (PF11_0205) with homology to yeast Npl3p and

to the human CLK kinase substrate, ASF/SF2 (Kern et al., 2014). The presence of high intensity bands observed for *h*SF2 phosphorylation by the kinase domain in chapter 3 agrees with the possibility that P*f*CLK1 specific inhibition in parasite assay might induce aberrant splicing events.

The recent pharmacological validation of P*f*CLK1 essentiality in *P. falciparum* has raised interest in designing potent inhibitors of this kinase with antimalarial properties (Kern et al., 2014). In chapter 4, the compound screening of hit molecules JZ208105-178D1 and HGC-0017530023-NX-1 against the recombinant kinase domain of P*f*CLK1 gene in the TR-FRET assay showed that both compounds highly inhibit kinase activity at low nano molar potencies comparable to established CLK1 inhibitors for other diseases. For example, Saldivia et al., 2020 demonstrated that for treating sleeping sickness, compound AB1 killed *Trypanosoma brucei* by CLK1 inhibition at IC_{50} value of 10 nM. Human CLK1 inhibitor, CLK1-IN-1 used to exert anticancer effect, is another potent and selective inhibitor, with an IC_{50} of 2 nM (Q.-Z. Sun et al., 2017). This data in line with other studies cited above establishes the P*f*CLK1 specific molecules as potent inhibitors.

Studies have also shown that a major drawback of most CLK1 inhibitors is their insufficient selectivity, particularly that Dyrk kinases, haspin and other CLK isoforms are frequently identified as off-targets (ElHady et al., 2023). Only a few inhibitors have been shown to be selective for CLK1 over CLK3. Kinases most closely related in primary sequence are likely to share inhibitor sensitivity, and these are the most important targets to test (Vieth et al., 2004). P*f*CLK1 and P*f*CLK3 share 31% identity (Alam et al., 2019) in primary amino acid sequence which can potentially be exploited in the context of polypharmacology (action of drugs against multiple targets) with a highly selective inhibitor. To explore the selective mechanism of inhibition of the two different series of small molecules, the ATP concentration for each assay was adjusted to the K_m for each kinase.

The ATP K_m derived for both kinases in chapter 3 were used for direct measurements of kinase inhibition in enzymatic assays that revealed low nano molar potencies. The results suggest that both HGC-0017530023-NX-1 and JZ208105-178D1 have distinct inhibition profiles selective for P*f*CLK1 and almost 10 to 40-fold selectivity against the P*f*CLK3 isoform respectively. A similar mode

of action is demonstrated by human CLK1 inhibitors , two molecules of the dichloroindolyl enaminonitrile series, the pure E-isomer KH-CB20 (CLK1 IC_{50} = 16.5 nM; CLK3 IC_{50} = 488 nM) and the E/Z-mixture KH-CB19 (CLK1 IC_{50} =19.7 nM; CLK3 IC_{50} = 530 nM) (Fedorov et al., 2011). Selectivity over P*f*CLK3 was observed to be higher with JZ208105-178D1 than HGC-0017530023-NX-1.

Understanding the different sources of pharmacological variation can impact kinase-inhibitor selectivity, even if it is not possible to predict the magnitude of these effects (Stephenson & Higgins, 2023). Highly related kinases such as members within the same kinase family often share many sources of variation for instance, a common phosphatase, comparable levels of specific activity relative to substrate availability, and downstream effectors with similar kinetics and thresholds of activation (Knight & Shokat, 2005). The presence of these shared signalling components can reduce the number of potential deviation sources for the *in vivo* activity of different small-molecule inhibitors of these targets (Knight & Shokat, 2005). This argues, counterintuitively, that closely related isoforms should be easier for selective inhibition in a cellular environment at a given fixed level of biochemical selectivity of a small-molecule inhibitor. Therefore, biochemical affinities are measured *in vitro* for the prediction of concentration ranges for kinase inhibitor activity in cells(Knight & Shokat, 2005).

As well as biochemical assays to measure phosphorylation, ATP competitive assays can be used to derive the Kinetic constant (Ki) and the concentration of inhibitor that causes half maximal inhibition (Aykul & Martinez-Hackert, 2016). It serves as a type of equilibrium constant (K_d) that represents the binding affinity between an inhibitor and target kinase. As smaller Ki means greater binding affinity and less inhibitor is needed to inhibit the kinase activity (Sager et al., 2014). Characterising HGC-0017530023-NX-1, it was discovered to demonstrate a response suggestive of non- ATP competitive mode of inhibition as a function of constant inhibitor potency insensitive to significant changes in ATP concentration. Non-ATP competitive inhibitors display improved selectivity and potency towards their target due to binding outside the ATP site that blocks kinase activity (Arter et al., 2022). In contrast, the IC_{50} values for JZ208105-178D1 varied by ~2-fold increases with the concentration of ATP in the assay and

the affinity of the kinase for ATP (expressed as ATP K_m). The mechanism of inhibition is non-competitive inhibition if the relationship between Ki and IC_{50} values determined when the concentration of substrate is equal to the Km, therefore Ki = IC_{50}; in competitive and uncompetitive inhibition, Ki = $IC_{50}/2$; whilst mixed inhibition Ki values range from IC_{50} to $IC_{50}/2$ (Garcia-Molina et al., 2022).

In cells, the ATP is generally much higher than ATP K_m and under such conditions, differences in ATP K_m between the enzymes can over saturate the intrinsic biochemical affinity for determining the inhibitor selectivity (Olivieri et al., 2022). Inhibition effect of both inhibitors in comparison to the *in vitro* enzymatic assays showed high nanomolar to low micromolar concentrations that are a very high deviation from the biochemical predictions as discussed above.

The lowest IC_{50} value that can be measured *in vitro* is determined by the concentration of kinase used in the assay (Roth et al., 2021). In an assumed normal reversible binding mechanism, an IC_{50} value cannot be lower than one-half the concentration of kinase, because it is impossible to inactivate more than one kinase per molecule of drug. By extension, it can be argued that the cellular potency of an inhibitor is dependent on the intracellular target kinase concentration (Vasta et al., 2018). A very abundant kinase will sequester a small molecule inhibitor out of solution such that the concentration of the kinase places a lower limit on the cellular IC_{50} for the inhibitor (Knight & Shokat, 2005). In most experimental settings, there is the reasoning that the potency of a kinase inhibitor in cells should be independent of the concentration of its target, where the concentration of kinase is distinguished from the amount of kinase activity is incorrect (Knight & Shokat, 2005). The reason being that kinase inhibitors are abundantly supplied to exchange matter with the cell, and the presence of a high affinity receptor within the cell will increase the steady-state intracellular drug concentration (Grossman & Adler, 2021). For example, for most experiments in the parasite culture assay in chapters 4 and 5, kinase inhibitors were added to the media and then gain entry to the cell by passive diffusion. Standard conditions for the growth of parasite culture cells -10^7 cells growing in a 15 cm dish bathed in 30 ml of media correspond to a volume of cell

culture media 10,000-fold greater than the volume of cells. In this scenario, no change in the concentration of inhibitor within the cell can significantly alter the concentration of inhibitor in the media. For a potent inhibitor of an abundant kinase, *Ki* greater than kinase, the binding affinity between the inhibitor and the kinase will increase the total intracellular concentration of inhibitor because the driving force for diffusion across the membrane is primarily the concentration gradient of unbound inhibitor (Hanson et al., 2019). Therefore, the cellular effectiveness of kinase inhibitors is entirely dependent on the fact that evolution has tuned the kinases biochemical activities to phosphorylate not much more than a significant fraction of their substrates, during the time course of an ordinary stimulus (Knight & Shokat, 2005).

The classic approach to confirm the phenotypic relevance for the target kinase of a small molecule is to create a mutant allele of the kinase that has altered sensitivity to the inhibitor (Garske et al., 2011). For example, a forward chemo genetic approach, was used to generate parasites with resistance to TCMDC-135051 by constant drug exposure and pressure on the parasites increased at sub-lethal concentrations over a 2-month period. A variant showed mutation at proline residue 259 on the *Pf*CLK3 gene, which increased kinase activity by ~3.5 fold and reduced the potency of TCMDC-135051 (Alam et al., 2019). A related approach is to use a kinase allele that is sensitive to a small molecule inhibitor that does not inhibit any wild-type kinase as was observed for TCMDC-135051 with P*f*CLK1 wild type. For protein kinases, mutation of the gatekeeper residue to alanine or glycine can generate such analog-sensitive alleles (Bishop et al., 2000; Lopez et al., 2014), in the case of P*f*CLK3, specific site glycine residues were mutated to bulkier amino acids, corresponding proline residue on P*f*CLK1 wild type to generate the P*f*CLK3_G449P mutant. P*f*CLK3 was identified as the target for TCMDC-135051 through the G449P mutant that is insensitive to TCMDC-135051(Alam et al., 2019). In chapter 4, the converse was applied for P*f*CLK1 inhibitors, JZ208105-178D1 than HGC-0017530023-NX-1, the P*f*CLK3 mutant G449P recombinant system displayed ~6.4-fold reduced sensitivity same as wild type P*f*CLK1 to JZ208105-178D1. In contrast, G449P sensitivity to HGC-0017530023-NX-1 was similar to that of TCMDC-135051, greatly reduced by ~60 fold compared to wild type P*f*CLK1. This data argues with the non-competitive ATP mode of inhibition implied earlier in the ATP competitive assay and rather

suggest a different mode of inhibition for HGC-0017530023-NX-1. This can be further investigated by computer modelling simulation of the binding mode for HGC-0017530023-NX-1 in complex with G449P mutant and wild type P*f*CLK1.

By replacing the endogenous copy of the kinase with the analog-sensitive allele, the effects of inhibiting that kinase in a model system can be studied with a highly specific inhibitor. A key feature of this approach is that it is possible to directly confirm that the phenotype is due to inhibition of the kinase by performing a control experiment in which cells expressing the wild-type kinase are treated with the same inhibitor (Bishop et al., 1998). Interestingly, in chapter 4, a strong correlation was observed between the inhibition of P*f*CLK3_G449P mutant and 3D7 wild type parasite across experimental and clinical compounds. These results are implicative of P*f*CLK1 specific inhibition in *P. falciparum* and supports the chemical validation of P*f*CLK1 as the as the molecular target for both JZ208105-178D1 and HGC-0017530023-NX-1. Interestingly, the data also showed a non-CLK dependent inhibition pathway for artemisinin and chloroquine which highly implies mechanism of resistance could also be different and would suggest no potential cross resistance between the P*f*CLK1 inhibitors and these two first line antimalarials. This speaks to the potential of new antimalarial agents judged by several requirements: novel modes of action with no cross-resistance to the current antimalarial agent, single-dose cures, effective against both the asexual blood stages and the gametocytes responsible for transmission (Tse et al., 2019).

Target candidate profiles provide guidance regarding the assessment of drug efficacy, pharmacokinetics, and toxicity before a compound is progressed toward clinical trials (Burrows et al., 2017). Ideal requirements of novel antimalarials include potent and rapid clearance of blood stage parasites, suitability as a component of a combination therapy, pharmacokinetics that provide therapeutic blood concentrations for an extended period after a single oral dose, a low toxicity profile, absence of detrimental drug-drug interactions with relapse prevention or transmission blocking molecules, and minimal risk of developing resistance (Burrows et al., 2017). In addition, activity against other stages of the parasite life cycle would be an attractive feature to provide the opportunity for prophylactic or transmission-blocking activity(Phillips et al., 2017).

In chapter 5, morphological and pharmacological analyses on drug-treated asexual stages showed that the JZ208105-178D1 arrested parasite growth during the trophozoites-to-schizont transition and furthermore, acted on blood and sexual stage replication in similar concentrations. These data indicate that P*f*CLK1 has an important role during schizogony and might be further crucial during parasite transmission from the human to the mosquito. Taken together, these results suggest that P*f*CLK1 inhibitor suppresses parasite growth and induce death at a fast kill rate through the inhibition of P*f*CLK1 mediated phosphorylation processes required for parasite survival.

According to the malaria eradication agenda, the discovery of new chemical entities that can destroy the parasite at the liver stage, the asexual blood stage, the gametocyte stage, and the insect ookinete stage of the parasite life cycle i.e., exhibiting multistage activity are in high demand, preferably with novel and multiple modes of action(Poonam et al., 2018). Gametocytes are the sole parasite stages that are capable of infecting mosquitoes once they are taken up by the insect vector during a blood meal. Hence, the parasite can continue its life cycle inside the vector, resulting in transmitting the parasite to more human hosts when biting them during a subsequent blood meal (Tadesse et al., 2019). Having established the death of asexual parasites by CLK1 inhibition and the proposed role of CLK in asexual stage replication it was exciting to investigate the implication of this discovery in transmission stages. Hence, killing of the transmissible sexual stages will lead to a block of the transmission of the parasites from one human host to the other via mosquitoes, thereby lowering the infection rate of individuals in close communities (Messina et al., 2018; Paonessa et al., 2022). Morphological analyses of on drug-treated gametocytes showed that JZ208105-178D1 and TCMDC-135051 started to arrest stages IV-V gametocyte replication and significantly reduce parasitaemia at ≥1 µM drug concentrations. There is the possibility of cytotoxicity, however, comparative analysis of the parasite kinome by Adderley & Doerig, 2022 revealed that only a small number of *P. falciparum* kinases namely P*f*CLK3, P*f*SRPK1, P*f*MAPK1, P*f*CKα and P*f*GSK3 associated strong bootstrap support > 80 to the human homologs in a phylogenetic tree. This combined with sequence alignment show *h*CLK1 is not the closely related human homologue to P*f*CLK1 therefore, there are high

divergence limits for selectivity between human and *Plasmodium* CLK inhibition. Toxicity assays in mammalian cells are required for confirmation.

Taking into account the strong blood schizonticidal action, and a potentially transmission blocking mechanism of action for JZ208105-178D1 demonstrated in this study, it would make an ideal candidate for TCP 1, 4 and 5 that can be used in combination therapy with TCMDC-135051 which has the same TCP profile and together classify under TPP2 to provide curative TCP 1, prophylaxis TCP 4 and clear gametocytaemia TCP 5 effects in high-transmission areas or during epidemics (Burrows et al., 2017).

While the stage specificity assays in chapters 4 and 5 identify vulnerable stages to a drug and inform on drug combinations, increasing overall efficacy, translation to an *in vivo* environment presents a key challenge: even if a synchronized parasite population is initially introduced into a host, a single infection will harbour individual parasites that become heterogenous through their development processes within the RBCs (Hodel et al., 2016). This inherent heterogeneity *in vivo* means that drug effects are evaluated against a mixed population, making it difficult to isolate the impact on specific parasite stages and complicating the interpretation of drug efficacy (Hodel et al., 2016). Future experiments should incorporate pharmacokinetic/pharmacodynamic models informed by data from asynchronous cultures to properly account parasite heterogeneity in malaria infections and assess the drug actions.

6.2 Conclusion and future work

6.2.1 Conclusion

The compound JZ208105-178D1 has demonstrated an affinity for the conserved kinase domain in P*f*CLKs, exhibiting nanomolar inhibitory activity against both the primary target P*f*CLK1 and member kinase P*f*CLK3 *in vitro*. The compound also exhibited micromolar antiparasitic activity against asexual blood stages, particularly in trophozoite to schizont progression at a fast-killing rate that suggests a potential mode of action that disrupts essential parasite processes during the early developmental stage. But beyond its blood-stage efficacy, the compound demonstrated a disruptive effect on mature gametocyte development, thus indicating a potential role in transmission blocking. This dual activity profile is highly desirable as it offers the prospect of not only treating infected individuals but also preventing disease transmission.

The potent and selective inhibition of P*f*CLK1 kinase, coupled with robust antiparasitic activity and gametocytocidal effects, positions this compound as a promising candidate for preclinical development. To fully realize the therapeutic potential of this molecule, additional studies are required to elucidate its mechanism of action and provide valuable insights into P*f*CLK1 role in parasite biology, pharmacokinetic and pharmacodynamic properties, and *in vivo* efficacy in relevant animal models. Moreover, exploring structure-activity relationships (SAR) within the compound series could lead to the discovery of even more potent and selective inhibitors.

In conclusion, this research underscores the potential of targeting P*f*CLK1 for the development of novel antimalarial therapies. The findings presented in this thesis provide a foundation for future investigations into the development of effective treatments that can ultimately lead to malaria elimination. In the next section, some experiments are proposed to better characterise our target kinase.

6.2.2 Future work

6.2.2.1 Selectivity profile

To define, measure and engineer inhibitor selectivity is crucial both in the development of new drugs and in the application of the inhibitors as tools for chemical biology research (Schenone et al., 2013). Recently, it has become standard protocol to measure the inhibitory activity of new inhibitors against kinases (Radu & Chernoff, 2017). One approach involves focusing on kinases in the same family and, therefore, with similar ATP binding site sequences (Afanasyeva et al., 2020). Another approach is to measure effects on functionally related kinases, as inhibiting more than one enzyme on the same signalling pathway may make a significant difference to the action of a drug. A third approach is wider kinome profiling to screen against a wide variety of kinases to get an overall view of selectivity (Stroobants et al., 2023).

6.2.2.2 Mammalian toxicity assay

The toxicity evaluation aims to anticipate harmful effects that an organism may suffer following exposure to a given compound (Espíndola et al., 2022). As opposed to animal models, for ethical reasons a variety of *in vitro* assays are available to assess toxicity of a compound, these include the trypan blue test, the tetrazolium salt assays (MTT, MTS, XTT, or WST), neutral red (NR) and the lactate dehydrogenase (LDH) test that can be used to determine if an inhibitor is selectively toxic to the parasite (Ali et al., 2020; de Souza et al., 2019; Lazaro & Gay, 1998).

6.2.2.3 Genetic validation

For direct validation the two main complementary approaches can be categorised as “chemical” and “genetic”, where small molecule inhibitors or genetic methods are used to modulate the functional activity of a target (T. Yang et al., 2021). Chemical validation provides chemical evidence for druggability of the target and favourable selective toxicity against the parasite versus the host (cell, tissue or whole animal) while genetic validation provides genetic evidence of essentiality of function within the parasite (Forte et al., 2021). Chemical validation has been covered to some extent in this thesis. For genetic validation there are tools available to achieve either target knockdown (e.g. using reversible inhibitors or RNA interference) or target knockout (e.g. using irreversible inhibitors or gene deletion). However, target knockout or knockdown is not without its limitations, emphasising the need for a chemo-genetic approach where both chemical and genetic evidence increase the confidence that a putative target is both essential and druggable(G. Wyatt et al., 2011).

6.2.2.4 Transmission blocking assays

The search for compounds with transmission-blocking activity prioritizes drugs able to prevent infections by blocking parasite transmission from infected individuals to mosquito vectors, since they are more amenable to medium- or high-throughput screening. However, there are no standardized *in vitro* assays reported for evaluating drug activity against the *P. falciparum* sporogonic cycle, and the only assays available for investigating compound activity against these stages have been developed for the rodent malaria parasite *P. berghei* . A number of assays including but not limited to Dual Gamete Formation Assay (DGFA) (Ruecker et al., 2014), Standard Membrane Feeding Assay, and Ookinete Development Assay (ODA) (Delves et al., 2012) are used to assess the influence of potential drugs on gametocyte development. The DGFA is used to evaluate the ability of compounds to inhibit the production of gametes (Delves et al., 2018). The SMFA is employed to assess the transmission-blocking potential of drug candidates. In its indirect form, the SMFA informs on the effect of small molecules on *Plasmodium* gametocytogenesis (B. Henry et al., 2023), whereas in

its direct version, it informs on the impact on gamete development into the oocyst (D'Alessandro et al., 2013). The ODA performed in *P. berghei* mouse models enables the assessment of the effects of potential drugs on early sporogonic stages (gametes, zygotes, and ookinetes) of parasites in the mosquito midgut (Appetecchia et al., 2024; Delves et al., 2018).

References

A. Haubrich, B., & C. Swinney, D. (2016). Enzyme Activity Assays for Protein Kinases: Strategies to Identify Active Substrates. *Current Drug Discovery Technologies*, *13*(1), 2–15. https://doi.org/10.2174/1570163813666160115125930

Adams, J. H., & Mueller, I. (2017). The Biology of *Plasmodium vivax*. *Cold Spring Harbor Perspectives in Medicine*, *7*(9), a025585. https://doi.org/10.1101/cshperspect.a025585

Adderley, J., & Doerig, C. (2022). Comparative analysis of the kinomes of Plasmodium falciparum, Plasmodium vivax and their host Homo sapiens. *BMC Genomics*, *23*(1), 237. https://doi.org/10.1186/s12864-022-08457-0

Afanasyeva, A., Nagao, C., & Mizuguchi, K. (2020). Developing a Kinase-Specific Target Selection Method Using a Structure-Based Machine Learning Approach . *Advances and Applications in Bioinformatics and Chemistry*, *Volume 13*, 27–40. https://doi.org/10.2147/AABC.S278900

Agarwal, S., Kern, S., Halbert, J., Przyborski, J. M., Baumeister, S., Dandekar, T., Doerig, C., & Pradel, G. (2011). Two nucleus-localized CDK-like kinases with crucial roles for malaria parasite erythrocytic replication are involved in phosphorylation of splicing factor. *Journal of Cellular Biochemistry*, *112*(5), 1295–1310. https://doi.org/10.1002/jcb.23034

Agyemang-Badu, S. Y., Awuah, E., Oduro-Kwarteng, S., Dzamesi, J. Y. W., Dom, N. C., & Kanno, G. G. (2023). Environmental Management and Sanitation as a Malaria Vector Control Strategy: A Qualitative Cross-Sectional Study Among Stakeholders, Sunyani Municipality, Ghana. *Environmental Health Insights*, *17*, 117863022211468. https://doi.org/10.1177/11786302221146890

Alam, M. M., Sanchez-Azqueta, A., Janha, O., Flannery, E. L., Mahindra, A., Mapesa, K., Char, A. B., Sriranganadane, D., Brancucci, N. M. B., Antonova-Koch, Y., Crouch, K., Simwela, N. V., Millar, S. B., Akinwale, J., Mitcheson, D., Solyakov, L., Dudek, K., Jones, C., Zapatero, C., … Tobin, A. B. (2019). Validation of the protein kinase *Pf* CLK3 as a multistage cross-species malarial drug target. *Science*, *365*(6456). https://doi.org/10.1126/science.aau1682

Alam, M. M., Solyakov, L., Bottrill, A. R., Flueck, C., Siddiqui, F. A., Singh, S., Mistry, S., Viskaduraki, M., Lee, K., Hopp, C. S., Chitnis, C. E., Doerig, C., Moon, R. W., Green, J. L., Holder, A. A., Baker, D. A., & Tobin, A. B. (2015). Phosphoproteomics reveals malaria parasite Protein Kinase G as a signalling hub regulating egress and invasion. *Nature Communications*, *6*(1), 7285. https://doi.org/10.1038/ncomms8285

Ali, A. H., Agustar, H. K., Hassan, N. I., Latip, J., Embi, N., & Sidek, H. M. (2020). Data on antiplasmodial and stage-specific inhibitory effects of Aromatic (Ar)-

Turmerone against Plasmodium falciparum 3D7. *Data in Brief*, *33*, 106592. https://doi.org/10.1016/j.dib.2020.106592

Almeida, M. E. M. de, Vasconcelos, M. G. S. de, Tarragô, A. M., & Mariúba, L. A. M. (2021). Circumsporozoite Surface Protein-based malaria vaccines: a review. *Revista Do Instituto de Medicina Tropical de São Paulo*, *63*. https://doi.org/10.1590/s1678-9946202163011

Anstey, N. M., Grigg, M. J., Rajahram, G. S., Cooper, D. J., William, T., Kho, S., & Barber, B. E. (2021). *Knowlesi malaria: Human risk factors, clinical spectrum, and pathophysiology* (pp. 1–43). https://doi.org/10.1016/bs.apar.2021.08.001

Appetecchia, F., Fabbrizi, E., Fiorentino, F., Consalvi, S., Biava, M., Poce, G., & Rotili, D. (2024). Transmission-Blocking Strategies for Malaria Eradication: Recent Advances in Small-Molecule Drug Development. *Pharmaceuticals*, *17*(7), 962. https://doi.org/10.3390/ph17070962

Ardito, F., Giuliani, M., Perrone, D., Troiano, G., & Muzio, L. Lo. (2017). The crucial role of protein phosphorylation in cell signaling and its use as targeted therapy (Review). *International Journal of Molecular Medicine*, *40*(2), 271–280. https://doi.org/10.3892/ijmm.2017.3036

Arendse, L. B., Wyllie, S., Chibale, K., & Gilbert, I. H. (2021). *Plasmodium* Kinases as Potential Drug Targets for Malaria: Challenges and Opportunities. *ACS Infectious Diseases*, *7*(3), 518–534. https://doi.org/10.1021/acsinfecdis.0c00724

Armstrong, R. A., Eperjesi, F., & Gilmartin, B. (2002). The application of analysis of variance (<scp>ANOVA</scp>) to different experimental designs in optometry. *Ophthalmic and Physiological Optics*, *22*(3), 248–256. https://doi.org/10.1046/j.1475-1313.2002.00020.x

Arter, C., Trask, L., Ward, S., Yeoh, S., & Bayliss, R. (2022). Structural features of the protein kinase domain and targeted binding by small-molecule inhibitors. *Journal of Biological Chemistry*, *298*(8), 102247. https://doi.org/10.1016/j.jbc.2022.102247

Aubol, B. E., Fattet, L., & Adams, J. A. (2021). A conserved sequence motif bridges two protein kinases for enhanced phosphorylation and nuclear function of a splicing factor. *The FEBS Journal*, *288*(2), 566–581. https://doi.org/10.1111/febs.15351

Aubol, B. E., Plocinik, R. M., Keshwani, M. M., McGlone, M. L., Hagopian, J. C., Ghosh, G., Fu, X.-D., & Adams, J. A. (2014). N-terminus of the protein kinase CLK1 induces SR protein hyperphosphorylation. *Biochemical Journal*, *462*(1), 143–152. https://doi.org/10.1042/BJ20140494

Aubol, B. E., Wu, G., Keshwani, M. M., Movassat, M., Fattet, L., Hertel, K. J., Fu, X.-D., & Adams, J. A. (2016). Release of SR Proteins from CLK1 by SRPK1: A Symbiotic Kinase System for Phosphorylation Control of Pre-mRNA Splicing. *Molecular Cell*, *63*(2), 218–228. https://doi.org/10.1016/j.molcel.2016.05.034

Aykul, S., & Martinez-Hackert, E. (2016). Determination of half-maximal inhibitory concentration using biosensor-based protein interaction analysis. *Analytical Biochemistry*, *508*, 97–103. https://doi.org/10.1016/j.ab.2016.06.025

B. Henry, N., Soulama, I., S. Sermé, S., Bolscher, J. M., T. G. Huijs, T., S. Coulibaly, A., Sombié, S., Ouédraogo, N., Diarra, A., Zongo, S., Guelbéogo, W. M., Nébié, I., Sirima, S. B., Tiono, A. B., Pietro, A., Collins, K. A., Dechering, K. J., & Bousema, T. (2023). Assessment of the transmission blocking activity of antimalarial compounds by membrane feeding assays using natural Plasmodium falciparum gametocyte isolates from West-Africa. *PLOS ONE*, *18*(7), e0284751. https://doi.org/10.1371/journal.pone.0284751

Baird, J. K., Nelwan, E. J., & Taylor, W. R. (2019). Approach to the Patient With Malaria. In *Travel Medicine* (pp. 179–186). Elsevier. https://doi.org/10.1016/B978-0-323-54696-6.00017-3

Baralle, F. E., & Giudice, J. (2017). Alternative splicing as a regulator of development and tissue identity. *Nature Reviews Molecular Cell Biology*, *18*(7), 437–451. https://doi.org/10.1038/nrm.2017.27

Barnwell, J. W., Nichols, M. E., & Rubinstein, P. (1989). In vitro evaluation of the role of the Duffy blood group in erythrocyte invasion by Plasmodium vivax. *The Journal of Experimental Medicine*, *169*(5), 1795–1802. https://doi.org/10.1084/jem.169.5.1795

Bassat, Q., Velarde, M., Mueller, I., Lin, J., Leslie, T., Wongsrichanalai, C., & Baird, J. K. (2016). Key Knowledge Gaps for *Plasmodium vivax* Control and Elimination. *The American Journal of Tropical Medicine and Hygiene*, *95*(6 Suppl), 62–71. https://doi.org/10.4269/ajtmh.16-0180

Beck, H., Härter, M., Haß, B., Schmeck, C., & Baerfacker, L. (2022). Small molecules and their impact in drug discovery: A perspective on the occasion of the 125th anniversary of the Bayer Chemical Research Laboratory. *Drug Discovery Today*, *27*(6), 1560–1574. https://doi.org/10.1016/j.drudis.2022.02.015

Beeson, J. G., Drew, D. R., Boyle, M. J., Feng, G., Fowkes, F. J. I., & Richards, J. S. (2016). Merozoite surface proteins in red blood cell invasion, immunity and vaccines against malaria. *FEMS Microbiology Reviews*, *40*(3), 343–372. https://doi.org/10.1093/femsre/fuw001

Bennink, S., Kiesow, M. J., & Pradel, G. (2016). The development of malaria parasites in the mosquito midgut. *Cellular Microbiology*, *18*(7), 905–918. https://doi.org/10.1111/cmi.12604

Berrouet, C., Dorilas, N., Rejniak, K. A., & Tuncer, N. (2020). Comparison of Drug Inhibitory Effects ($$\hbox {IC}_{50}$$) in Monolayer and Spheroid Cultures. *Bulletin of Mathematical Biology*, *82*(6), 68. https://doi.org/10.1007/s11538-020-00746-7

Bhatt, S., Weiss, D. J., Cameron, E., Bisanzio, D., Mappin, B., Dalrymple, U., Battle, K. E., Moyes, C. L., Henry, A., Eckhoff, P. A., Wenger, E. A., Briët, O., Penny, M. A., Smith, T. A., Bennett, A., Yukich, J., Eisele, T. P., Griffin, J. T., Fergus, C. A., … Gething, P. W. (2015). The effect of malaria control on Plasmodium falciparum in Africa between 2000 and 2015. *Nature*, *526*(7572), 207–211. https://doi.org/10.1038/nature15535

Biala, G., Kedzierska, E., Kruk-Slomka, M., Orzelska-Gorka, J., Hmaidan, S., Skrok, A., Kaminski, J., Havrankova, E., Nadaska, D., & Malik, I. (2023). Research in the Field of Drug Design and Development. *Pharmaceuticals*, *16*(9), 1283. https://doi.org/10.3390/ph16091283

Bishop, A. C., Shah, K., Liu, Y., Witucki, L., Kung, C., & Shokat, K. M. (1998). Design of allele-specific inhibitors to probe protein kinase signaling. *Current Biology*, *8*(5), 257–266. https://doi.org/10.1016/S0960-9822(98)70198-8

Bishop, A. C., Ubersax, J. A., Petsch, D. T., Matheos, D. P., Gray, N. S., Blethrow, J., Shimizu, E., Tsien, J. Z., Schultz, P. G., Rose, M. D., Wood, J. L., Morgan, D. O., & Shokat, K. M. (2000). A chemical switch for inhibitor-sensitive alleles of any protein kinase. *Nature*, *407*(6802), 395–401. https://doi.org/10.1038/35030148

Biswas, B., Huang, Y.-H., Craik, D. J., & Wang, C. K. (2024). The prospect of substrate-based kinase inhibitors to improve target selectivity and overcome drug resistance. *Chemical Science*. https://doi.org/10.1039/D4SC01088D

Black, C. S., Whelan, T. A., Garside, E. L., MacMillan, A. M., Fast, N. M., & Rader, S. D. (2023). Spliceosome assembly and regulation: insights from analysis of highly reduced spliceosomes. *RNA*, *29*(5), 531–550. https://doi.org/10.1261/rna.079273.122

Blasco, B., Leroy, D., & Fidock, D. A. (2017). Antimalarial drug resistance: linking Plasmodium falciparum parasite biology to the clinic. *Nature Medicine*, *23*(8), 917–928. https://doi.org/10.1038/nm.4381

Borba, J. V. V. B., Silva, A. de C. e, do Nascimento, M. N., Ferreira, L. T., Rimoldi, A., Starling, L., Ramos, P. I. P., Costa, F. T. M., & Andrade, C. H. (2022). Update and elucidation of Plasmodium kinomes: Prioritization of kinases as potential drug targets for malaria. *Computational and Structural Biotechnology Journal*, *20*, 3708–3717. https://doi.org/10.1016/j.csbj.2022.07.003

Bouafou, L., Makanga, B. K., Rahola, N., Boddé, M., Ngangué, M. F., Daron, J., Berger, A., Mouillaud, T., Makunin, A., Korlević, P., Nwezeobi, J., Kengne, P., Paupy, C., Lawniczak, M. K. N., & Ayala, D. (2024). Host preference patterns in domestic and wild settings: Insights into *Anopheles* feeding behavior. *Evolutionary Applications*, *17*(6). https://doi.org/10.1111/eva.13693

Boualam, M. A., Pradines, B., Drancourt, M., & Barbieri, R. (2021). Malaria in Europe: A Historical Perspective. *Frontiers in Medicine*, *8*. https://doi.org/10.3389/fmed.2021.691095

Bouyssou, I., El Hoss, S., Doderer-Lang, C., Schoenhals, M., Rasoloharimanana, L. T., Vigan-Womas, I., Ratsimbasoa, A., Abate, A., Golassa, L., Mabilotte, S., Kessler, P., Guillotte-Blisnick, M., Martinez, F. J., Chitnis, C. E., Strouboulis, J., & Ménard, D. (2023). Unveiling P. vivax invasion pathways in Duffy-negative individuals. *Cell Host & Microbe*, *31*(12), 2080-2092.e5. https://doi.org/10.1016/j.chom.2023.11.007

Breen, M. E., & Soellner, M. B. (2015). Small Molecule Substrate Phosphorylation Site Inhibitors of Protein Kinases: Approaches and Challenges. *ACS Chemical Biology*, *10*(1), 175–189. https://doi.org/10.1021/cb5008376

Bullock, A. N., Das, S., Debreczeni, J. É., Rellos, P., Fedorov, O., Niesen, F. H., Guo, K., Papagrigoriou, E., Amos, A. L., Cho, S., Turk, B. E., Ghosh, G., & Knapp, S. (2009). Kinase Domain Insertions Define Distinct Roles of CLK Kinases in SR Protein Phosphorylation. *Structure*, *17*(3), 352–362. https://doi.org/10.1016/j.str.2008.12.023

Burrows, J. N., Duparc, S., Gutteridge, W. E., Hooft van Huijsduijnen, R., Kaszubska, W., Macintyre, F., Mazzuri, S., Möhrle, J. J., & Wells, T. N. C. (2017). New developments in anti-malarial target candidate and product profiles. *Malaria Journal*, *16*(1), 26. https://doi.org/10.1186/s12936-016-1675-x

Casanova, J.-L., & Abel, L. (2013). The Genetic Theory of Infectious Diseases: A Brief History and Selected Illustrations. *Annual Review of Genomics and Human Genetics*, *14*(1), 215–243. https://doi.org/10.1146/annurev-genom-091212-153448

Chin, W., Contacos, P. G., Coatney, G. R., & Kimball, H. R. (1965). A Naturally Acquired Quotidian-Type Malaria in Man Transferable to Monkeys. *Science*, *149*(3686), 865–865. https://doi.org/10.1126/science.149.3686.865

Cook, F. A., & Cook, S. J. (2021). Inhibition of RAF dimers: it takes two to tango. *Biochemical Society Transactions*, *49*(1), 237–251. https://doi.org/10.1042/BST20200485

Cox, F. E. (2010). History of the discovery of the malaria parasites and their vectors. *Parasites & Vectors*, *3*(1), 5. https://doi.org/10.1186/1756-3305-3-5

Cozzarolo, C.-S., Glaizot, O., Christe, P., & Pigeault, R. (2020). Enhanced Attraction of Arthropod Vectors to Infected Vertebrates: A Review of Empirical Evidence. *Frontiers in Ecology and Evolution*, *8*. https://doi.org/10.3389/fevo.2020.568140

Currà, C., Kehrer, J., Lemgruber, L., Silva, P. A. G. C., Bertuccini, L., Superti, F., Pace, T., Ponzi, M., Frischknecht, F., Siden-Kiamos, I., & Mair, G. R. (2019). Malaria transmission through the mosquito requires the function of the OMD protein. *PLOS ONE*, *14*(9), e0222226. https://doi.org/10.1371/journal.pone.0222226

Dagen, M. (2020). History of malaria and its treatment. In *Antimalarial Agents* (pp. 1–48). Elsevier. https://doi.org/10.1016/B978-0-08-101210-9.00001-9

D'Alessandro, S., Silvestrini, F., Dechering, K., Corbett, Y., Parapini, S., Timmerman, M., Galastri, L., Basilico, N., Sauerwein, R., Alano, P., & Taramelli, D. (2013). A Plasmodium falciparum screening assay for anti-gametocyte drugs based on parasite lactate dehydrogenase detection. *Journal of Antimicrobial Chemotherapy*, *68*(9), 2048–2058. https://doi.org/10.1093/jac/dkt165

Das, R., Choithramani, A., & Shard, A. (2022). A molecular perspective for the use of type IV tyrosine kinase inhibitors as anticancer therapeutics. *Drug Discovery Today*, *27*(3), 808–821. https://doi.org/10.1016/j.drudis.2021.12.009

Dash, M., Sachdeva, S., Bansal, A., & Sinha, A. (2022). Gametogenesis in Plasmodium: Delving Deeper to Connect the Dots. *Frontiers in Cellular and Infection Microbiology*, *12*. https://doi.org/10.3389/fcimb.2022.877907

Davies, H., Belda, H., Broncel, M., Ye, X., Bisson, C., Introini, V., Dorin-Semblat, D., Semblat, J.-P., Tibúrcio, M., Gamain, B., Kaforou, M., & Treeck, M. (2020). An exported kinase family mediates species-specific erythrocyte remodelling and virulence in human malaria. *Nature Microbiology*, *5*(6), 848–863. https://doi.org/10.1038/s41564-020-0702-4

Day, K. P., Hayward, R. E., Smith, D., & Culvenor, J. G. (1998). CD36-dependent adhesion and knob expression of the transmission stages of Plasmodium falciparum is stage-specific. *Molecular and Biochemical Parasitology*, *93*(2), 167–177. https://doi.org/10.1016/S0166-6851(98)00040-1

de Oliveira, L. S., Alborghetti, M. R., Carneiro, R. G., Bastos, I. M. D., Amino, R., Grellier, P., & Charneau, S. (2021). Calcium in the Backstage of Malaria Parasite Biology. *Frontiers in Cellular and Infection Microbiology*, *11*. https://doi.org/10.3389/fcimb.2021.708834

de Souza, G. E., Bueno, R. V., de Souza, J. O., Zanini, C. L., Cruz, F. C., Oliva, G., Guido, R. V. C., & Aguiar, A. C. C. (2019). Antiplasmodial profile of selected compounds from Malaria Box: in vitro evaluation, speed of action and drug combination studies. *Malaria Journal*, *18*(1), 447. https://doi.org/10.1186/s12936-019-3069-3

Dechering, K. J., Timmerman, M., Rensen, K., Koolen, K. M. J., Honarnejad, S., Vos, M. W., Huijs, T., Henderson, R. W. M., Chenu, E., Laleu, B., Montefiore, B. C., Segall, M. D., Mills, J. E. J., Guantai, E. M., Duffy, J., & Duffey, M. (2022). Replenishing the malaria drug discovery pipeline: Screening and hit evaluation of the MMV Hit Generation Library 1 (HGL1) against asexual blood stage Plasmodium falciparum, using a nano luciferase reporter read-out. *SLAS Discovery*, *27*(6), 337–348. https://doi.org/10.1016/j.slasd.2022.07.002

Dekel, N., Eisenberg-Domovich, Y., Karlas, A., Meyer, T. F., Bracher, F., Lebendiker, M., Danieli, T., & Livnah, O. (2020). Expression, purification and crystallization

of CLK1 kinase – A potential target for antiviral therapy. *Protein Expression and Purification*, *176*, 105742. https://doi.org/10.1016/j.pep.2020.105742

Delves, M. J., Miguel-Blanco, C., Matthews, H., Molina, I., Ruecker, A., Yahiya, S., Straschil, U., Abraham, M., León, M. L., Fischer, O. J., Rueda-Zubiaurre, A., Brandt, J. R., Cortés, Á., Barnard, A., Fuchter, M. J., Calderón, F., Winzeler, E. A., Sinden, R. E., Herreros, E., … Baum, J. (2018). A high throughput screen for next-generation leads targeting malaria parasite transmission. *Nature Communications*, *9*(1), 3805. https://doi.org/10.1038/s41467-018-05777-2

Delves, M. J., Ramakrishnan, C., Blagborough, A. M., Leroy, D., Wells, T. N. C., & Sinden, R. E. (2012). A high-throughput assay for the identification of malarial transmission-blocking drugs and vaccines. *International Journal for Parasitology*, *42*(11), 999–1006. https://doi.org/10.1016/j.ijpara.2012.08.009

Deng, Z., Mao, J., Wang, Y., Zou, H., & Ye, M. (2017). Enzyme Kinetics for Complex System Enables Accurate Determination of Specificity Constants of Numerous Substrates in a Mixture by Proteomics Platform. *Molecular & Cellular Proteomics*, *16*(1), 135–145. https://doi.org/10.1074/mcp.M116.062869

Dev, V., & Manguin, S. (2016). Biology, distribution and control of Anopheles (Cellia) minimus in the context of malaria transmission in northeastern India. *Parasites & Vectors*, *9*(1), 585. https://doi.org/10.1186/s13071-016-1878-6

Didychuk, A. L., Butcher, S. E., & Brow, D. A. (2018). The life of U6 small nuclear RNA, from cradle to grave. *RNA*, *24*(4), 437–460. https://doi.org/10.1261/rna.065136.117

Doğan, T., Akhan Güzelcan, E., Baumann, M., Koyas, A., Atas, H., Baxendale, I. R., Martin, M., & Cetin-Atalay, R. (2021). Protein domain-based prediction of drug/compound–target interactions and experimental validation on LIM kinases. *PLOS Computational Biology*, *17*(11), e1009171. https://doi.org/10.1371/journal.pcbi.1009171

Dorin-Semblat, D., Sicard, A., Doerig, C., Ranford-Cartwright, L., & Doerig, C. (2008). Disruption of the Pf *PK7* Gene Impairs Schizogony and Sporogony in the Human Malaria Parasite *Plasmodium falciparum*. *Eukaryotic Cell*, *7*(2), 279–285. https://doi.org/10.1128/EC.00245-07

Duffy, P. E. (2021). Transmission-Blocking Vaccines: Harnessing Herd Immunity for Malaria Elimination. *Expert Review of Vaccines*, *20*(2), 185–198. https://doi.org/10.1080/14760584.2021.1878028

Duffy, P. E., & Patrick Gorres, J. (2020). Malaria vaccines since 2000: progress, priorities, products. *Npj Vaccines*, *5*(1), 48. https://doi.org/10.1038/s41541-020-0196-3

El-Gamil, D. S., ElHady, A. K., Chen, P.-J., Hwang, T.-L., Abadi, A. H., Abdel-Halim, M., & Engel, M. (2023). Discovery of novel 5-methoxybenzothiophene hydrazides as metabolically stable Clk1 inhibitors with high potency and unprecedented

Clk1 isoenzyme selectivity. *European Journal of Medicinal Chemistry*, *247*, 115019. https://doi.org/10.1016/j.ejmech.2022.115019

ElHady, A. K., El-Gamil, D. S., Abadi, A. H., Abdel-Halim, M., & Engel, M. (2023). An overview of cdc2-like kinase 1 (Clk1) inhibitors and their therapeutic indications. *Medicinal Research Reviews*, *43*(2), 343–398. https://doi.org/10.1002/med.21928

El-Moamly, A. A., & El-Sweify, M. A. (2023). Malaria vaccines: the 60-year journey of hope and final success—lessons learned and future prospects. *Tropical Medicine and Health*, *51*(1), 29. https://doi.org/10.1186/s41182-023-00516-w

Ergin, E., Dogan, A., Parmaksiz, M., Elçin, A., & Elçin, Y. (2016). Time-Resolved Fluorescence Resonance Energy Transfer [TR-FRET] Assays for Biochemical Processes. *Current Pharmaceutical Biotechnology*, *17*(14), 1222–1230. https://doi.org/10.2174/1389201017666160809164527

Espíndola, M. R., Varotti, F. de P., Aguiar, A. C. C., Andrade, S. N., & Rocha, E. M. M. da. (2022). In vitro assessment for cytotoxicity screening of new antimalarial candidates. *Brazilian Journal of Pharmaceutical Sciences*, *58*. https://doi.org/10.1590/s2175-97902022e18308

FB Cogswell. (1992). The Hypnozoite and Relapse in Primate Malaria. *American Society of Microbiology*, *5*(1), 26–35.

Fedorov, O., Huber, K., Eisenreich, A., Filippakopoulos, P., King, O., Bullock, A. N., Szklarczyk, D., Jensen, L. J., Fabbro, D., Trappe, J., Rauch, U., Bracher, F., & Knapp, S. (2011). Specific CLK Inhibitors from a Novel Chemotype for Regulation of Alternative Splicing. *Chemistry & Biology*, *18*(1), 67–76. https://doi.org/10.1016/j.chembiol.2010.11.009

Flannery, E. L., Kangwanrangsan, N., Chuenchob, V., Roobsoong, W., Fishbaugher, M., Zhou, K., Billman, Z. P., Martinson, T., Olsen, T. M., Schäfer, C., Campo, B., Murphy, S. C., Mikolajczak, S. A., Kappe, S. H. I., & Sattabongkot, J. (2022). Plasmodium vivax latent liver infection is characterized by persistent hypnozoites, hypnozoite-derived schizonts, and time-dependent efficacy of primaquine. *Molecular Therapy - Methods & Clinical Development*, *26*, 427–440. https://doi.org/10.1016/j.omtm.2022.07.016

Foguim, F. T., Bogreau, H., Gendrot, M., Mosnier, J., Fonta, I., Benoit, N., Amalvict, R., Madamet, M., Wein, S., Pradines, B., Augis, V., Bastien, P., Benoit-Vical, F., Berry, A., Brouqui, P., Chauvin, P., Cividin, M., Courtier, F., Delaunay, P., … Wolff, A. (2020). Prevalence of mutations in the Plasmodium falciparum chloroquine resistance transporter, PfCRT, and association with ex vivo susceptibility to common anti-malarial drugs against African Plasmodium falciparum isolates. *Malaria Journal*, *19*(1), 201. https://doi.org/10.1186/s12936-020-03281-x

Forte, B., Ottilie, S., Plater, A., Campo, B., Dechering, K. J., Gamo, F. J., Goldberg, D. E., Istvan, E. S., Lee, M., Lukens, A. K., McNamara, C. W., Niles, J. C.,

Okombo, J., Pasaje, C. F. A., Siegel, M. G., Wirth, D., Wyllie, S., Fidock, D. A., Baragaña, B., … Gilbert, I. H. (2021). Prioritization of Molecular Targets for Antimalarial Drug Discovery. *ACS Infectious Diseases*, *7*(10), 2764–2776. https://doi.org/10.1021/acsinfecdis.1c00322

G. Wyatt, P., H. Gilbert, I., D. Read, K., & H. Fairlamb, A. (2011). Target Validation: Linking Target and Chemical Properties to Desired Product Profile. *Current Topics in Medicinal Chemistry*, *11*(10), 1275–1283. https://doi.org/10.2174/156802611795429185

Garcia-Molina, P., Garcia-Molina, F., Teruel-Puche, J. A., Rodriguez-Lopez, J. N., Garcia-Canovas, F., & Muñoz-Muñoz, J. L. (2022). The Relationship between the IC50 Values and the Apparent Inhibition Constant in the Study of Inhibitors of Tyrosinase Diphenolase Activity Helps Confirm the Mechanism of Inhibition. *Molecules*, *27*(10), 3141. https://doi.org/10.3390/molecules27103141

Garske, A. L., Peters, U., Cortesi, A. T., Perez, J. L., & Shokat, K. M. (2011). Chemical genetic strategy for targeting protein kinases based on covalent complementarity. *Proceedings of the National Academy of Sciences of the United States of America*, *108*(37), 15046–15052. https://doi.org/10.1073/pnas.1111239108

Gatton, M. L., Chitnis, N., Churcher, T., Donnelly, M. J., Ghani, A. C., Godfray, H. C. J., Gould, F., Hastings, I., Marshall, J., Ranson, H., Rowland, M., Shaman, J., & Lindsay, S. W. (2013). THE IMPORTANCE OF MOSQUITO BEHAVIOURAL ADAPTATIONS TO MALARIA CONTROL IN AFRICA. *Evolution*, *67*(4), 1218–1230. https://doi.org/10.1111/evo.12063

Gehring, N. H., & Roignant, J.-Y. (2021). Anything but Ordinary – Emerging Splicing Mechanisms in Eukaryotic Gene Regulation. *Trends in Genetics*, *37*(4), 355–372. https://doi.org/10.1016/j.tig.2020.10.008

Genetu Bayih, A., Debnath, A., Mitre, E., Huston, C. D., Laleu, B., Leroy, D., Blasco, B., Campo, B., Wells, T. N. C., Willis, P. A., Sjö, P., Van Voorhis, W. C., & Pillai, D. R. (2017). Susceptibility Testing of Medically Important Parasites. *Clinical Microbiology Reviews*, *30*(3), 647–669. https://doi.org/10.1128/CMR.00111-16

Ghartey-Kwansah, G., Yin, Q., Li, Z., Gumpper, K., Sun, Y., Yang, R., Wang, D., Jones, O., Zhou, X., Wang, L., Bryant, J., Ma, J., Boampong, J. N., & Xu, X. (2020). Calcium-dependent Protein Kinases in Malaria Parasite Development and Infection. *Cell Transplantation*, *29*, 096368971988488. https://doi.org/10.1177/0963689719884888

Gimenez, A. M., Marques, R. F., Regiart, M., & Bargieri, D. Y. (2021). Diagnostic Methods for Non-Falciparum Malaria. *Frontiers in Cellular and Infection Microbiology*, *11*. https://doi.org/10.3389/fcimb.2021.681063

Glickman, J. (2012). *Assay Development for Protein Kinase Enzymes* (S. Markossian, A. Grossman, M. Arkin, & et al., Eds.).

Goldberg, D. E., & Zimmerberg, J. (2020). Hardly Vacuous: The Parasitophorous Vacuolar Membrane of Malaria Parasites. *Trends in Parasitology*, *36*(2), 138–146. https://doi.org/10.1016/j.pt.2019.11.006

Goldberg, J., Nairn, A. C., & Kuriyan, J. (1996). Structural Basis for the Autoinhibition of Calcium/Calmodulin-Dependent Protein Kinase I. *Cell*, *84*(6), 875–887. https://doi.org/10.1016/S0092-8674(00)81066-1

Govindasamy, K., & Bhanot, P. (2020). Overlapping and distinct roles of CDPK family members in the pre-erythrocytic stages of the rodent malaria parasite, Plasmodium berghei. *PLOS Pathogens*, *16*(8), e1008131. https://doi.org/10.1371/journal.ppat.1008131

Grossman, M., & Adler, E. (2021). *Protein Kinase Inhibitors - Selectivity or Toxicity?* https://doi.org/10.5772/intechopen.98640

Guttery, D. S., Poulin, B., Ramaprasad, A., Wall, R. J., Ferguson, D. J. P., Brady, D., Patzewitz, E.-M., Whipple, S., Straschil, U., Wright, M. H., Mohamed, A. M. A. H., Radhakrishnan, A., Arold, S. T., Tate, E. W., Holder, A. A., Wickstead, B., Pain, A., & Tewari, R. (2014). Genome-wide Functional Analysis of Plasmodium Protein Phosphatases Reveals Key Regulators of Parasite Development and Differentiation. *Cell Host & Microbe*, *16*(1), 128–140. https://doi.org/10.1016/j.chom.2014.05.020

Guttery, D. S., Zeeshan, M., Holder, A. A., & Tewari, R. (2024). The molecular mechanisms driving *Plasmodium* cell division. *Biochemical Society Transactions*, *52*(2), 593–602. https://doi.org/10.1042/BST20230403

Hanks, S. K. (2003). Hanks SK. Genomic analysis of the eukaryotic protein kinase superfamily: a perspective. *Genome Biology*, *4*(5), 111. https://doi.org/10.1186/gb-2003-4-5-111

Hanson, S. M., Georghiou, G., Thakur, M. K., Miller, W. T., Rest, J. S., Chodera, J. D., & Seeliger, M. A. (2019). What Makes a Kinase Promiscuous for Inhibitors? *Cell Chemical Biology*, *26*(3), 390-399.e5. https://doi.org/10.1016/j.chembiol.2018.11.005

Harrison, R. E., Brown, M. R., & Strand, M. R. (2021). Whole blood and blood components from vertebrates differentially affect egg formation in three species of anautogenous mosquitoes. *Parasites & Vectors*, *14*(1), 119. https://doi.org/10.1186/s13071-021-04594-9

Health Organization, W. (2023). *World malaria report 2022*. https://www.wipo.int/amc/en/mediation/

Henderson, M. J., Trychta, K. A., Yang, S.-M., Bäck, S., Yasgar, A., Wires, E. S., Danchik, C., Yan, X., Yano, H., Shi, L., Wu, K.-J., Wang, A. Q., Tao, D., Zahoránszky-Kőhalmi, G., Hu, X., Xu, X., Maloney, D., Zakharov, A. V., Rai, G., … Harvey, B. K. (2021). A target-agnostic screen identifies approved drugs to

stabilize the endoplasmic reticulum-resident proteome. *Cell Reports*, *35*(4), 109040. https://doi.org/10.1016/j.celrep.2021.109040

Hodel, E. M., Kay, K., & Hastings, I. M. (2016). Incorporating Stage-Specific Drug Action into Pharmacological Modeling of Antimalarial Drug Treatment. *Antimicrobial Agents and Chemotherapy*, *60*(5), 2747–2756. https://doi.org/10.1128/AAC.01172-15

Horne, R. I., Wilson-Godber, J., González Díaz, A., Brotzakis, Z. F., Seal, S., Gregory, R. C., Possenti, A., Chia, S., & Vendruscolo, M. (2024). Using Generative Modeling to Endow with Potency Initially Inert Compounds with Good Bioavailability and Low Toxicity. *Journal of Chemical Information and Modeling*, *64*(3), 590–596. https://doi.org/10.1021/acs.jcim.3c01777

Howes, R. E., Battle, K. E., Mendis, K. N., Smith, D. L., Cibulskis, R. E., Baird, J. K., & Hay, S. I. (2016). Global Epidemiology of *Plasmodium vivax*. *The American Journal of Tropical Medicine and Hygiene*, *95*(6 Suppl), 15–34. https://doi.org/10.4269/ajtmh.16-0141

Huang, Y.-J., Higgs, S., & Vanlandingham, D. (2017). Biological Control Strategies for Mosquito Vectors of Arboviruses. *Insects*, *8*(1), 21. https://doi.org/10.3390/insects8010021

Hurtig, J. E., Kim, M., Orlando-Coronel, L. J., Ewan, J., Foreman, M., Notice, L.-A., Steiger, M. A., & van Hoof, A. (2020). Origin, conservation, and loss of alternative splicing events that diversify the proteome in Saccharomycotina budding yeasts. *RNA*, *26*(10), 1464–1480. https://doi.org/10.1261/rna.075655.120

Imbahale, S. S., Mweresa, C. K., Takken, W., & Mukabana, W. R. (2011). Development of environmental tools for anopheline larval control. *Parasites & Vectors*, *4*(1), 130. https://doi.org/10.1186/1756-3305-4-130

Ippolito, M. M., Moser, K. A., Kabuya, J.-B. B., Cunningham, C., & Juliano, J. J. (2021). Antimalarial Drug Resistance and Implications for the WHO Global Technical Strategy. *Current Epidemiology Reports*, *8*(2), 46–62. https://doi.org/10.1007/s40471-021-00266-5

Islam, K. (2018). The Bump-and-Hole Tactic: Expanding the Scope of Chemical Genetics. *Cell Chemical Biology*, *25*(10), 1171–1184. https://doi.org/10.1016/j.chembiol.2018.07.001

Jacob, A. G., & Smith, C. W. J. (2017). Intron retention as a component of regulated gene expression programs. *Human Genetics*, *136*(9), 1043–1057. https://doi.org/10.1007/s00439-017-1791-x

Jaenicke, R. (1999). Stability and folding of domain proteins. *Progress in Biophysics and Molecular Biology*, *71*(2), 155–241. https://doi.org/10.1016/S0079-6107(98)00032-7

Jayabalasingham, B., Bano, N., & Coppens, I. (2010). Metamorphosis of the malaria parasite in the liver is associated with organelle clearance. *Cell Research*, *20*(9), 1043–1059. https://doi.org/10.1038/cr.2010.88

Josling, G. A., Williamson, K. C., & Llinás, M. (2018). Regulation of Sexual Commitment and Gametocytogenesis in Malaria Parasites. *Annual Review of Microbiology*, *72*(1), 501–519. https://doi.org/10.1146/annurev-micro-090817-062712

Kanev, G. K., de Graaf, C., de Esch, I. J. P., Leurs, R., Würdinger, T., Westerman, B. A., & Kooistra, A. J. (2019). The Landscape of Atypical and Eukaryotic Protein Kinases. *Trends in Pharmacological Sciences*, *40*(11), 818–832. https://doi.org/10.1016/j.tips.2019.09.002

Kats, L. M., Fernandez, K. M., Glenister, F. K., Herrmann, S., Buckingham, D. W., Siddiqui, G., Sharma, L., Bamert, R., Lucet, I., Guillotte, M., Mercereau-Puijalon, O., & Cooke, B. M. (2014). An exported kinase (FIKK4.2) that mediates virulence-associated changes in Plasmodium falciparum-infected red blood cells. *International Journal for Parasitology*, *44*(5), 319–328. https://doi.org/10.1016/j.ijpara.2014.01.003

Kern, S., Agarwal, S., Huber, K., Gehring, A. P., Ströedke, B., Wirth, C. C., Brügl, T., Abodo, L. O., Dandekar, T., Doerig, C., Fischer, R., Tobin, A. B., Alam, M. M., Bracher, F., & Pradel, G. (2014). Inhibition of the SR Protein-Phosphorylating CLK Kinases of Plasmodium falciparum Impairs Blood Stage Replication and Malaria Transmission. *PLoS ONE*, *9*(9), e105732. https://doi.org/10.1371/journal.pone.0105732

Keshwani, M. M., Aubol, B. E., Fattet, L., Ma, C.-T., Qiu, J., Jennings, P. A., Fu, X.-D., & Adams, J. A. (2015). Conserved proline-directed phosphorylation regulates SR protein conformation and splicing function. *Biochemical Journal*, *466*(2), 311–322. https://doi.org/10.1042/BJ20141373

Keszei, S. J., Váradi, M., & Skoda-Földes, R. (2023). Urea-Functionalized Heterocycles: Structure, Hydrogen Bonding and Applications. *Molecules*, *28*(23), 7757. https://doi.org/10.3390/molecules28237757

Killeen, G. F., Masalu, J. P., Chinula, D., Fotakis, E. A., Kavishe, D. R., Malone, D., & Okumu, F. (2017). Control of Malaria Vector Mosquitoes by Insecticide-Treated Combinations of Window Screens and Eave Baffles. *Emerging Infectious Diseases*, *23*(5), 782–789. https://doi.org/10.3201/eid2305.160662

Klaus, S., Binder, P., Kim, J., Machado, M., Funaya, C., Schaaf, V., Klaschka, D., Kudulyte, A., Cyrklaff, M., Laketa, V., Höfer, T., Guizetti, J., Becker, N. B., Frischknecht, F., Schwarz, U. S., & Ganter, M. (2022). Asynchronous nuclear cycles in multinucleated *Plasmodium falciparum* facilitate rapid proliferation. *Science Advances*, *8*(13). https://doi.org/10.1126/sciadv.abj5362

Knape, M. J., Ahuja, L. G., Bertinetti, D., Burghardt, N. C. G., Zimmermann, B., Taylor, S. S., & Herberg, F. W. (2015). Divalent Metal Ions Mg 2+ and Ca 2+ Have

Distinct Effects on Protein Kinase A Activity and Regulation. *ACS Chemical Biology*, *10*(10), 2303–2315. https://doi.org/10.1021/acschembio.5b00271

Knape, M. J., Ballez, M., Burghardt, N. C., Zimmermann, B., Bertinetti, D., Kornev, A. P., & Herberg, F. W. (2017). Divalent metal ions control activity and inhibition of protein kinases. *Metallomics*, *9*(11), 1576–1584. https://doi.org/10.1039/C7MT00204A

Knapp B., N. U. , H. E. , K. H. A. (1991). Demonstration of alternative splicing of a pre-mRNA expressed in the blood stage form of Plasmodium falciparum. *J Biol Chem.*, 266(11):7148-7154.

Knight, Z. A., & Shokat, K. M. (2005). Features of Selective Kinase Inhibitors. *Chemistry & Biology*, *12*(6), 621–637. https://doi.org/10.1016/j.chembiol.2005.04.011

Kulkeaw, K. (2021). Progress and challenges in the use of fluorescence-based flow cytometric assays for anti-malarial drug susceptibility tests. *Malaria Journal*, *20*(1), 57. https://doi.org/10.1186/s12936-021-03591-8

Kumar, S., Valansi, C., Haile, M. T., Li, X., Flyak, K., Dwivedy, A., Abatiyow, B. A., Leeb, A. S., Kennedy, S. Y., Camargo, N. M., Vaughan, A. M., Brukman, N. G., Podbilewicz, B., & Kappe, S. H. I. (2022). Malaria parasites utilize two essential plasma membrane fusogens for gamete fertilization. *Cellular and Molecular Life Sciences*, *79*(11), 549. https://doi.org/10.1007/s00018-022-04583-w

Kyalo, D., Amratia, P., Mundia, C. W., Mbogo, C. M., Coetzee, M., & Snow, R. W. (2017). A geo-coded inventory of anophelines in the Afrotropical Region south of the Sahara: 1898-2016. *Wellcome Open Research*, *2*, 57. https://doi.org/10.12688/wellcomeopenres.12187.1

Lamarque, M., Besteiro, S., Papoin, J., Roques, M., Vulliez-Le Normand, B., Morlon-Guyot, J., Dubremetz, J.-F., Fauquenoy, S., Tomavo, S., Faber, B. W., Kocken, C. H., Thomas, A. W., Boulanger, M. J., Bentley, G. A., & Lebrun, M. (2011). The RON2-AMA1 Interaction is a Critical Step in Moving Junction-Dependent Invasion by Apicomplexan Parasites. *PLoS Pathogens*, *7*(2), e1001276. https://doi.org/10.1371/journal.ppat.1001276

Laurens, M. B. (2020). RTS,S/AS01 vaccine (MosquirixTM): an overview. *Human Vaccines & Immunotherapeutics*, *16*(3), 480–489. https://doi.org/10.1080/21645515.2019.1669415

Lazaro, J. E., & Gay, F. (1998). Plasmodium falciparum: In Vitro Cytotoxicity Testing Using MTT. *SLAS Discovery*, *3*(1), 49–53. https://doi.org/10.1177/108705719800300107

Lee, P. Y., Yeoh, Y., & Low, T. Y. (2023). A recent update on small-molecule kinase inhibitors for targeted cancer therapy and their therapeutic insights from mass spectrometry-based proteomic analysis. *The FEBS Journal*, *290*(11), 2845–2864. https://doi.org/10.1111/febs.16442

Lee, S., Devamani, T., Song, H. D., Sandhu, M., Larsen, A., Sommese, R., Jain, A., Vaidehi, N., & Sivaramakrishnan, S. (2017). Distinct structural mechanisms determine substrate affinity and kinase activity of protein kinase Cα. *Journal of Biological Chemistry*, *292*(39), 16300–16309. https://doi.org/10.1074/jbc.M117.804781

Li, D., Yu, W., & Lai, M. (2023). Towards understandings of serine/arginine-rich splicing factors. *Acta Pharmaceutica Sinica B*, *13*(8), 3181–3207. https://doi.org/10.1016/j.apsb.2023.05.022

Li, J., Gong, C., Zhou, H., Liu, J., Xia, X., Ha, W., Jiang, Y., Liu, Q., & Xiong, H. (2024). Kinase Inhibitors and Kinase-Targeted Cancer Therapies: Recent Advances and Future Perspectives. *International Journal of Molecular Sciences*, *25*(10), 5489. https://doi.org/10.3390/ijms25105489

Lim, P. S., Sutton, C. R., & Rao, S. (2015). Protein kinase <scp>C</scp> in the immune system: from signalling to chromatin regulation. *Immunology*, *146*(4), 508–522. https://doi.org/10.1111/imm.12510

Linares, M., Viera, S., Crespo, B., Franco, V., Gómez-Lorenzo, M. G., Jiménez-Díaz, M. B., Angulo-Barturen, Í., Sanz, L. M., & Gamo, F.-J. (2015). Identifying rapidly parasiticidal anti-malarial drugs using a simple and reliable in vitro parasite viability fast assay. *Malaria Journal*, *14*(1), 441. https://doi.org/10.1186/s12936-015-0962-2

Lindberg, M. F., & Meijer, L. (2021). Dual-Specificity, Tyrosine Phosphorylation-Regulated Kinases (DYRKs) and cdc2-Like Kinases (CLKs) in Human Disease, an Overview. *International Journal of Molecular Sciences*, *22*(11), 6047. https://doi.org/10.3390/ijms22116047

Lindsay, S. W., Thomas, M. B., & Kleinschmidt, I. (2021). Threats to the effectiveness of insecticide-treated bednets for malaria control: thinking beyond insecticide resistance. *The Lancet Global Health*, *9*(9), e1325–e1331. https://doi.org/10.1016/S2214-109X(21)00216-3

Liu, Z., Miao, J., & Cui, L. (2011). Gametocytogenesis in Malaria Parasite: Commitment, Development and Regulation. *Future Microbiology*, *6*(11), 1351–1369. https://doi.org/10.2217/fmb.11.108

Long, C. A., & Zavala, F. (2016). Malaria vaccines and human immune responses. *Current Opinion in Microbiology*, *32*, 96–102. https://doi.org/10.1016/j.mib.2016.04.006

Long, Y., Sou, W. H., Yung, K. W. Y., Liu, H., Wan, S. W. C., Li, Q., Zeng, C., Law, C. O. K., Chan, G. H. C., Lau, T. C. K., & Ngo, J. C. K. (2019). Distinct mechanisms govern the phosphorylation of different SR protein splicing factors. *Journal of Biological Chemistry*, *294*(4), 1312–1327. https://doi.org/10.1074/jbc.RA118.003392

Lopez, M. S., Kliegman, J. I., & Shokat, K. M. (2014). *The Logic and Design of Analog-Sensitive Kinases and Their Small Molecule Inhibitors* (pp. 189–213). https://doi.org/10.1016/B978-0-12-397918-6.00008-2

Loubens, M., Vincensini, L., Fernandes, P., Briquet, S., Marinach, C., & Silvie, O. (2021). *Plasmodium* sporozoites on the move: Switching from cell traversal to productive invasion of hepatocytes. *Molecular Microbiology*, *115*(5), 870–881. https://doi.org/10.1111/mmi.14645

MacRae, J. I., Dixon, M. W., Dearnley, M. K., Chua, H. H., Chambers, J. M., Kenny, S., Bottova, I., Tilley, L., & McConville, M. J. (2013). Mitochondrial metabolism of sexual and asexual blood stages of the malaria parasite Plasmodium falciparum. *BMC Biology*, *11*(1), 67. https://doi.org/10.1186/1741-7007-11-67

Mahindra, A., Janha, O., Mapesa, K., Sanchez-Azqueta, A., Alam, M. M., Amambua-Ngwa, A., Nwakanma, D. C., Tobin, A. B., & Jamieson, A. G. (2020). Development of Potent *Pf* CLK3 Inhibitors Based on TCMDC-135051 as a New Class of Antimalarials. *Journal of Medicinal Chemistry*, *63*(17), 9300–9315. https://doi.org/10.1021/acs.jmedchem.0c00451

Martín Moyano, P., Němec, V., & Paruch, K. (2020). Cdc-Like Kinases (CLKs): Biology, Chemical Probes, and Therapeutic Potential. *International Journal of Molecular Sciences*, *21*(20), 7549. https://doi.org/10.3390/ijms21207549

Martinez, R., Defnet, A., & Shapiro, P. (2020). Avoiding or Co-Opting ATP Inhibition: Overview of Type III, IV, V, and VI Kinase Inhibitors. In *Next Generation Kinase Inhibitors* (pp. 29–59). Springer International Publishing. https://doi.org/10.1007/978-3-030-48283-1_3

Matthews, K. A., Senagbe, K. M., Nötzel, C., Gonzales, C. A., Tong, X., Rijo-Ferreira, F., Bhanu, N. V., Miguel-Blanco, C., Lafuente-Monasterio, M. J., Garcia, B. A., Kafsack, B. F. C., & Martinez, E. D. (2020). Disruption of the *Plasmodium falciparum* Life Cycle through Transcriptional Reprogramming by Inhibitors of Jumonji Demethylases. *ACS Infectious Diseases*, *6*(5), 1058–1075. https://doi.org/10.1021/acsinfecdis.9b00455

McCarthy, J. S., Yalkinoglu, Ö., Odedra, A., Webster, R., Oeuvray, C., Tappert, A., Bezuidenhout, D., Giddins, M. J., Dhingra, S. K., Fidock, D. A., Marquart, L., Webb, L., Yin, X., Khandelwal, A., & Bagchus, W. M. (2021). Safety, pharmacokinetics, and antimalarial activity of the novel plasmodium eukaryotic translation elongation factor 2 inhibitor M5717: a first-in-human, randomised, placebo-controlled, double-blind, single ascending dose study and volunteer infection study. *The Lancet Infectious Diseases*, *21*(12), 1713–1724. https://doi.org/10.1016/S1473-3099(21)00252-8

McGlory, C., White, A., Treins, C., Drust, B., Close, G. L., MacLaren, D. P. M., Campbell, I. T., Philp, A., Schenk, S., Morton, J. P., & Hamilton, D. L. (2014). Application of the [γ- 32 P] ATP kinase assay to study anabolic signaling in

human skeletal muscle. *Journal of Applied Physiology*, *116*(5), 504–513. https://doi.org/10.1152/japplphysiol.01072.2013

McHugh, E., Bulloch, M. S., Batinovic, S., Patrick, C. J., Sarna, D. K., & Ralph, S. A. (2023). Nonsense-mediated decay machinery in *Plasmodium falciparum* is inefficient and non-essential. *MSphere*, *8*(4). https://doi.org/10.1128/msphere.00233-23

McLean, K. J., & Jacobs-Lorena, M. (2016). Genetic Control Of Malaria Mosquitoes. *Trends in Parasitology*, *32*(3), 174–176. https://doi.org/10.1016/j.pt.2016.01.002

Meibalan, E., & Marti, M. (2017). Biology of Malaria Transmission. *Cold Spring Harbor Perspectives in Medicine*, *7*(3), a025452. https://doi.org/10.1101/cshperspect.a025452

Ménard, R., Tavares, J., Cockburn, I., Markus, M., Zavala, F., & Amino, R. (2013). Looking under the skin: the first steps in malarial infection and immunity. *Nature Reviews Microbiology*, *11*(10), 701–712. https://doi.org/10.1038/nrmicro3111

Mendes, C., Dias, F., Figueiredo, J., Mora, V. G., Cano, J., de Sousa, B., do Rosário, V. E., Benito, A., Berzosa, P., & Arez, A. P. (2011). Duffy Negative Antigen Is No Longer a Barrier to Plasmodium vivax – Molecular Evidences from the African West Coast (Angola and Equatorial Guinea). *PLoS Neglected Tropical Diseases*, *5*(6), e1192. https://doi.org/10.1371/journal.pntd.0001192

Menegay, H. J., Myers, M. P., Moeslein, F. M., & Landreth, G. E. (2000). Biochemical characterization and localization of the dual specificity kinase CLK1. *Journal of Cell Science*, *113*(18), 3241–3253. https://doi.org/10.1242/jcs.113.18.3241

Messina, V., Valtieri, M., Rubio, M., Falchi, M., Mancini, F., Mayor, A., Alano, P., & Silvestrini, F. (2018). Gametocytes of the Malaria Parasite Plasmodium falciparum Interact With and Stimulate Bone Marrow Mesenchymal Cells to Secrete Angiogenetic Factors. *Frontiers in Cellular and Infection Microbiology*, *8*. https://doi.org/10.3389/fcimb.2018.00050

Miller, L. H., Rojas-Jaimes, J., Low, L. M., & Corbellini, G. (2023). What Historical Records Teach Us about the Discovery of Quinine. *The American Journal of Tropical Medicine and Hygiene*, *108*(1), 7–11. https://doi.org/10.4269/ajtmh.22-0404

Miller, R. H., Obuya, C. O., Wanja, E. W., Ogutu, B., Waitumbi, J., Luckhart, S., & Stewart, V. A. (2015). Characterization of Plasmodium ovale curtisi and P. ovale wallikeri in Western Kenya Utilizing a Novel Species-specific Real-time PCR Assay. *PLOS Neglected Tropical Diseases*, *9*(1), e0003469. https://doi.org/10.1371/journal.pntd.0003469

Mlacha, Y. P., Chaki, P. P., Muhili, A., Massue, D. J., Tanner, M., Majambere, S., Killen, G. F., & Govella, N. J. (2020). Reduced human-biting preferences of the

African malaria vectors Anopheles arabiensis and Anopheles gambiae in an urban context: controlled, competitive host-preference experiments in Tanzania. *Malaria Journal*, *19*(1), 418. https://doi.org/10.1186/s12936-020-03495-z

Mohanan, A. G., Gunasekaran, S., Jacob, R. S., & Omkumar, R. V. (2022). Role of Ca2+/Calmodulin-Dependent Protein Kinase Type II in Mediating Function and Dysfunction at Glutamatergic Synapses. *Frontiers in Molecular Neuroscience*, *15*. https://doi.org/10.3389/fnmol.2022.855752

Molina-Franky, J., Patarroyo, M. E., Kalkum, M., & Patarroyo, M. A. (2022). The Cellular and Molecular Interaction Between Erythrocytes and Plasmodium falciparum Merozoites. *Frontiers in Cellular and Infection Microbiology*, *12*. https://doi.org/10.3389/fcimb.2022.816574

Monti, J. L. E., Montes, M. R., & Rossi, R. C. (2018). Steady-state analysis of enzymes with non-Michaelis-Menten kinetics: The transport mechanism of Na+/K+-ATPase. *Journal of Biological Chemistry*, *293*(4), 1373–1385. https://doi.org/10.1074/jbc.M117.799536

More, D. A., & Kumar, A. (2020). SRSF3: Newly discovered functions and roles in human health and diseases. *European Journal of Cell Biology*, *99*(6), 151099. https://doi.org/10.1016/j.ejcb.2020.151099

Mueller, I., Galinski, M. R., Baird, J. K., Carlton, J. M., Kochar, D. K., Alonso, P. L., & del Portillo, H. A. (2009). Key gaps in the knowledge of Plasmodium vivax, a neglected human malaria parasite. *The Lancet Infectious Diseases*, *9*(9), 555–566. https://doi.org/10.1016/S1473-3099(09)70177-X

Muhia, D. K., Swales, C. A., Eckstein-Ludwig, U., Saran, S., Polley, S. D., Kelly, J. M., Schaap, P., Krishna, S., & Baker, D. A. (2003). Multiple Splice Variants Encode a Novel Adenylyl Cyclase of Possible Plastid Origin Expressed in the Sexual Stage of the Malaria Parasite Plasmodium falciparum. *Journal of Biological Chemistry*, *278*(24), 22014–22022. https://doi.org/10.1074/jbc.M301639200

Muraki, M., Ohkawara, B., Hosoya, T., Onogi, H., Koizumi, J., Koizumi, T., Sumi, K., Yomoda, J., Murray, M. V., Kimura, H., Furuichi, K., Shibuya, H., Krainer, A. R., Suzuki, M., & Hagiwara, M. (2004). Manipulation of Alternative Splicing by a Newly Developed Inhibitor of Clks. *Journal of Biological Chemistry*, *279*(23), 24246–24254. https://doi.org/10.1074/jbc.M314298200

Murithi, J. M., Owen, E. S., Istvan, E. S., Lee, M. C. S., Ottilie, S., Chibale, K., Goldberg, D. E., Winzeler, E. A., Llinás, M., Fidock, D. A., & Vanaerschot, M. (2020). Combining Stage Specificity and Metabolomic Profiling to Advance Antimalarial Drug Discovery. *Cell Chemical Biology*, *27*(2), 158-171.e3. https://doi.org/10.1016/j.chembiol.2019.11.009

Nájera, J. A., González-Silva, M., & Alonso, P. L. (2011). Some Lessons for the Future from the Global Malaria Eradication Programme (1955–1969). *PLoS Medicine*, *8*(1), e1000412. https://doi.org/10.1371/journal.pmed.1000412

Nguyen, T. H. D., Galej, W. P., Bai, X., Savva, C. G., Newman, A. J., Scheres, S. H. W., & Nagai, K. (2015). The architecture of the spliceosomal U4/U6.U5 tri-snRNP. *Nature*, *523*(7558), 47–52. https://doi.org/10.1038/nature14548

Niederhauser, C., & Galel, S. A. (2022). Transfusion-Transmitted Malaria and Mitigation Strategies in Nonendemic Regions. *Transfusion Medicine and Hemotherapy*, *49*(4), 205–217. https://doi.org/10.1159/000525414

NISHAL, S., JHAWAT, V., GUPTA, S., & PHAUGAT, P. (2022). Utilization of kinase inhibitors as novel therapeutic drug targets: A review. *Oncology Research*, *30*(5), 221–230. https://doi.org/10.32604/or.2022.027549

Nishi, H., Hashimoto, K., & Panchenko, A. R. (2011). Phosphorylation in Protein-Protein Binding: Effect on Stability and Function. *Structure*, *19*(12), 1807–1815. https://doi.org/10.1016/j.str.2011.09.021

Nørregaard Jensen, O. (2004). Modification-specific proteomics: characterization of post-translational modifications by mass spectrometry. *Current Opinion in Chemical Biology*, *8*(1), 33–41. https://doi.org/10.1016/j.cbpa.2003.12.009

Nunes, M. C., Goldring, J. P. D., Doerig, C., & Scherf, A. (2007). A novel protein kinase family in *Plasmodium falciparum* is differentially transcribed and secreted to various cellular compartments of the host cell. *Molecular Microbiology*, *63*(2), 391–403. https://doi.org/10.1111/j.1365-2958.2006.05521.x

Nunes, M. C., Okada, M., Scheidig-Benatar, C., Cooke, B. M., & Scherf, A. (2010). Plasmodium falciparum FIKK Kinase Members Target Distinct Components of the Erythrocyte Membrane. *PLoS ONE*, *5*(7), e11747. https://doi.org/10.1371/journal.pone.0011747

Okumu, F., & Finda, M. (2021). Key Characteristics of Residual Malaria Transmission in Two Districts in South-Eastern Tanzania—Implications for Improved Control. *The Journal of Infectious Diseases*, *223*(Supplement_2), S143–S154. https://doi.org/10.1093/infdis/jiaa653

Olivieri, C., Li, G. C., Wang, Y., V.S., M., Walker, C., Kim, J., Camilloni, C., De Simone, A., Vendruscolo, M., Bernlohr, D. A., Taylor, S. S., & Veglia, G. (2022). ATP-competitive inhibitors modulate the substrate binding cooperativity of a kinase by altering its conformational entropy. *Science Advances*, *8*(30). https://doi.org/10.1126/sciadv.abo0696

Ong, H. W., Adderley, J., Tobin, A. B., Drewry, D. H., & Doerig, C. (2023). Parasite and host kinases as targets for antimalarials. *Expert Opinion on Therapeutic Targets*, *27*(2), 151–169. https://doi.org/10.1080/14728222.2023.2185511

Onyeogaziri, F. C., & Papaneophytou, C. (2019). A General Guide for the Optimization of Enzyme Assay Conditions Using the Design of Experiments Approach. *SLAS Discovery*, *24*(5), 587–596. https://doi.org/10.1177/2472555219830084

Oriero, E. C., Amenga-Etego, L., Ishengoma, D. S., & Amambua-Ngwa, A. (2021). *Plasmodium malariae*, current knowledge and future research opportunities on a neglected malaria parasite species. *Critical Reviews in Microbiology*, *47*(1), 44–56. https://doi.org/10.1080/1040841X.2020.1838440

Otto, T. D., Wilinski, D., Assefa, S., Keane, T. M., Sarry, L. R., Böhme, U., Lemieux, J., Barrell, B., Pain, A., Berriman, M., Newbold, C., & Llinás, M. (2010). New insights into the blood-stage transcriptome of *Plasmodium falciparum* using RNA-Seq. *Molecular Microbiology*, *76*(1), 12–24. https://doi.org/10.1111/j.1365-2958.2009.07026.x

Ouji, M., Augereau, J.-M., Paloque, L., & Benoit-Vical, F. (2018). *Plasmodium falciparum* resistance to artemisinin-based combination therapies: A sword of Damocles in the path toward malaria elimination. *Parasite*, *25*, 24. https://doi.org/10.1051/parasite/2018021

Ouologuem, D. T., Dara, A., Kone, A., Ouattara, A., & Djimde, A. A. (2023). Plasmodium falciparum Development from Gametocyte to Oocyst: Insight from Functional Studies. *Microorganisms*, *11*(8), 1966. https://doi.org/10.3390/microorganisms11081966

Pang, K., Wang, W., Qin, J., Shi, Z., Hao, L., Ma, Y., Xu, H., Wu, Z., Pan, D., Chen, Z., & Han, C. (2022). Role of protein phosphorylation in cell signaling, disease, and the intervention therapy. *MedComm*, *3*(4). https://doi.org/10.1002/mco2.175

Paonessa, G., Siciliano, G., Graziani, R., Lalli, C., Cecchetti, O., Alli, C., La Valle, R., Petrocchi, A., Sferrazza, A., Bisbocci, M., Falchi, M., Toniatti, C., Bresciani, A., & Alano, P. (2022). Gametocyte-specific and all-blood-stage transmission-blocking chemotypes discovered from high throughput screening on Plasmodium falciparum gametocytes. *Communications Biology*, *5*(1), 547. https://doi.org/10.1038/s42003-022-03510-w

Patel, P. N., & Tolia, N. (2021). Structural vaccinology of malaria transmission-blocking vaccines. *Expert Review of Vaccines*, *20*(2), 199–214. https://doi.org/10.1080/14760584.2021.1873135

Perrin, A. J., Bisson, C., Faull, P. A., Renshaw, M. J., Lees, R. A., Fleck, R. A., Saibil, H. R., Snijders, A. P., Baker, D. A., & Blackman, M. J. (2021). Malaria Parasite Schizont Egress Antigen-1 Plays an Essential Role in Nuclear Segregation during Schizogony. *MBio*, *12*(2). https://doi.org/10.1128/mBio.03377-20

Philip, N., & Haystead, T. A. (2007). Characterization of a UBC13 kinase in *Plasmodium falciparum*. *Proceedings of the National Academy of Sciences*, *104*(19), 7845–7850. https://doi.org/10.1073/pnas.0611601104

Phillips, M. A., Burrows, J. N., Manyando, C., van Huijsduijnen, R. H., Van Voorhis, W. C., & Wells, T. N. C. (2017). Malaria. *Nature Reviews Disease Primers*, *3*(1), 17050. https://doi.org/10.1038/nrdp.2017.50

Pimenta, P. F., Orfano, A. S., Bahia, A. C., Duarte, A. P., Ríos-Velásquez, C. M., Melo, F. F., Pessoa, F. A., Oliveira, G. A., Campos, K. M., Villegas, L. M., Rodrigues, N. B., Nacif-Pimenta, R., Simões, R. C., Monteiro, W. M., Amino, R., Traub-Cseko, Y. M., Lima, J. B., Barbosa, M. G., Lacerda, M. V., … Secundino, N. F. (2015). An overview of malaria transmission from the perspective of Amazon Anopheles vectors. *Memórias Do Instituto Oswaldo Cruz*, *110*(1), 23–47. https://doi.org/10.1590/0074-02760140266

Pirahmadi, S., Zakeri, S., Afsharpad, M., & Djadid, N. D. (2013). Mutation analysis in pfmdr1 and pfmrp1 as potential candidate genes for artemisinin resistance in Plasmodium falciparum clinical isolates 4years after implementation of artemisinin combination therapy in Iran. *Infection, Genetics and Evolution*, *14*, 327–334. https://doi.org/10.1016/j.meegid.2012.12.014

Poonam, Gupta, Y., Gupta, N., Singh, S., Wu, L., Chhikara, B. S., Rawat, M., & Rathi, B. (2018). Multistage inhibitors of the malaria parasite: Emerging hope for chemoprotection and malaria eradication. *Medicinal Research Reviews*, *38*(5), 1511–1535. https://doi.org/10.1002/med.21486

Radohery, G. F. R., Walz, A., Gumpp, C., Cherkaoui-Rbati, M. H., Gobeau, N., Gower, J., Davenport, M. P., Rottmann, M., McCarthy, J. S., Möhrle, J. J., Rebelo, M., Demarta-Gatsi, C., & Khoury, D. S. (2022). Parasite Viability as a Measure of *In Vivo* Drug Activity in Preclinical and Early Clinical Antimalarial Drug Assessment. *Antimicrobial Agents and Chemotherapy*, *66*(7). https://doi.org/10.1128/aac.00114-22

Radu, M., & Chernoff, J. (2017). Recent advances in methods to assess the activity of the kinome. *F1000Research*, *6*, 1004. https://doi.org/10.12688/f1000research.10962.1

Raja, T. N., Hu, T. H., Kadir, K. A., Mohamad, D. S. A., Rosli, N., Wong, L. L., Hii, K. C., Simon Divis, P. C., & Singh, B. (2020). Naturally Acquired Human *Plasmodium cynomolgi* and *P. knowlesi* Infections, Malaysian Borneo. *Emerging Infectious Diseases*, *26*(8), 1801–1809. https://doi.org/10.3201/eid2608.200343

Ramasamy, R. (2014). Zoonotic Malaria â€“ Global Overview and Research and Policy Needs. *Frontiers in Public Health*, *2*. https://doi.org/10.3389/fpubh.2014.00123

Rauch, J., Volinsky, N., Romano, D., & Kolch, W. (2011). The secret life of kinases: functions beyond catalysis. *Cell Communication and Signaling*, *9*(1), 23. https://doi.org/10.1186/1478-811X-9-23

Reinhardt, R., & Leonard, T. A. (2023). A critical evaluation of protein kinase regulation by activation loop autophosphorylation. *ELife*, *12*. https://doi.org/10.7554/eLife.88210

Rezende Lima, W., Tessarin-Almeida, G., Rozanski, A., Parreira, K. S., Moraes, M. S., Martins, D. C., Hashimoto, R. F., Galante, P. A. F., & Garcia, C. R. S. (2016). Signaling transcript profile of the asexual intraerythrocytic development cycle of

Plasmodium falciparum induced by melatonin and cAMP. *Genes & Cancer*, *7*(9–10), 323–339. https://doi.org/10.18632/genesandcancer.118

Robinson, P. K. (2015). Enzymes: principles and biotechnological applications. *Essays in Biochemistry*, *59*, 1–41. https://doi.org/10.1042/bse0590001

Roncalés, M., Vidal, J., Torres, P. A., & Herreros, E. (2015). In Vitro Culture of Plasmodium falciparum: Obtention of Synchronous Asexual Erythrocytic Stages. *Open Journal of Epidemiology*, *05*(01), 71–80. https://doi.org/10.4236/ojepi.2015.51010

Roques, M., Bindschedler, A., Beyeler, R., & Heussler, V. T. (2023). Same, same but different: Exploring Plasmodium cell division during liver stage development. *PLOS Pathogens*, *19*(3), e1011210. https://doi.org/10.1371/journal.ppat.1011210

Roth, A., Gihring, A., Göser, F., Peifer, C., Knippschild, U., & Bischof, J. (2021). Assessing the Inhibitory Potential of Kinase Inhibitors In Vitro: Major Pitfalls and Suggestions for Improving Comparability of Data Using CK1 Inhibitors as an Example. *Molecules*, *26*(16), 4898. https://doi.org/10.3390/molecules26164898

Roux, A. T., Maharaj, L., Oyegoke, O., Akoniyon, O. P., Adeleke, M. A., Maharaj, R., & Okpeku, M. (2021). Chloroquine and Sulfadoxine–Pyrimethamine Resistance in Sub-Saharan Africa—A Review. *Frontiers in Genetics*, *12*. https://doi.org/10.3389/fgene.2021.668574

Rudolf, A. F., Skovgaard, T., Knapp, S., Jensen, L. J., & Berthelsen, J. (2014). A Comparison of Protein Kinases Inhibitor Screening Methods Using Both Enzymatic Activity and Binding Affinity Determination. *PLoS ONE*, *9*(6), e98800. https://doi.org/10.1371/journal.pone.0098800

Ruecker, A., Mathias, D. K., Straschil, U., Churcher, T. S., Dinglasan, R. R., Leroy, D., Sinden, R. E., & Delves, M. J. (2014). A Male and Female Gametocyte Functional Viability Assay To Identify Biologically Relevant Malaria Transmission-Blocking Drugs. *Antimicrobial Agents and Chemotherapy*, *58*(12), 7292–7302. https://doi.org/10.1128/AAC.03666-14

Ryan, J. R., Stoute, J. A., Amon, J., Dunton, R. F., Mtalib, R., Koros, J., Owour, B., Luckhart, S., Wirtz, R. A., Barnwell, J. W., & Rosenberg, R. (2006). Evidence for transmission of Plasmodium vivax among a duffy antigen negative population in Western Kenya. *The American Journal of Tropical Medicine and Hygiene*, *75*(4), 575–581.

Sager, J. E., Lutz, J. D., Foti, R. S., Davis, C., Kunze, K. L., & Isoherranen, N. (2014). Fluoxetine- and Norfluoxetine-Mediated Complex Drug–Drug Interactions: In Vitro to In Vivo Correlation of Effects on CYP2D6, CYP2C19, and CYP3A4. *Clinical Pharmacology & Therapeutics*, *95*(6), 653–662. https://doi.org/10.1038/clpt.2014.50

Sahu, T., Gehrke, E. J., Flores-Garcia, Y., Mlambo, G., Romano, J. D., & Coppens, I. (2021). Chemoprophylaxis vaccination with a Plasmodium liver stage autophagy mutant affords enhanced and long-lasting protection. *Npj Vaccines*, *6*(1), 98. https://doi.org/10.1038/s41541-021-00360-1

Saldivia, M., Fang, E., Ma, X., Myburgh, E., Carnielli, J. B. T., Bower-Lepts, C., Brown, E., Ritchie, R., Lakshminarayana, S. B., Chen, Y.-L., Patra, D., Ornelas, E., Koh, H. X. Y., Williams, S. L., Supek, F., Paape, D., McCulloch, R., Kaiser, M., Barrett, M. P., … Rao, S. P. S. (2020). Targeting the trypanosome kinetochore with CLK1 protein kinase inhibitors. *Nature Microbiology*, *5*(10), 1207–1216. https://doi.org/10.1038/s41564-020-0745-6

Sato, S. (2021). Plasmodium—a brief introduction to the parasites causing human malaria and their basic biology. *Journal of Physiological Anthropology*, *40*(1), 1. https://doi.org/10.1186/s40101-020-00251-9

Scheiner, M., Burda, P., & Ingmundson, A. (2023). Moving on: How malaria parasites exit the liver. *Molecular Microbiology*. https://doi.org/10.1111/mmi.15141

Schenone, M., Dančík, V., Wagner, B. K., & Clemons, P. A. (2013). Target identification and mechanism of action in chemical biology and drug discovery. *Nature Chemical Biology*, *9*(4), 232–240. https://doi.org/10.1038/nchembio.1199

Scherf, A., Lopez-Rubio, J. J., & Riviere, L. (2008). Antigenic Variation in *Plasmodium falciparum*. *Annual Review of Microbiology*, *62*(1), 445–470. https://doi.org/10.1146/annurev.micro.61.080706.093134

Schröder, M., Bullock, A. N., Fedorov, O., Bracher, F., Chaikuad, A., & Knapp, S. (2020). DFG-1 Residue Controls Inhibitor Binding Mode and Affinity, Providing a Basis for Rational Design of Kinase Inhibitor Selectivity. *Journal of Medicinal Chemistry*, *63*(18), 10224–10234. https://doi.org/10.1021/acs.jmedchem.0c00898

Schussek, S., Trieu, A., Apte, S. H., Sidney, J., Sette, A., & Doolan, D. L. (2017). Novel Plasmodium antigens identified via genome-based antibody screen induce protection associated with polyfunctional T cell responses. *Scientific Reports*, *7*(1), 15053. https://doi.org/10.1038/s41598-017-15354-0

Seeber, F., & Steinfelder, S. (2016). Recent advances in understanding apicomplexan parasites. *F1000Research*, *5*, 1369. https://doi.org/10.12688/f1000research.7924.1

Serafimova, I. M., Pufall, M. A., Krishnan, S., Duda, K., Cohen, M. S., Maglathlin, R. L., McFarland, J. M., Miller, R. M., Frödin, M., & Taunton, J. (2012). Reversible targeting of noncatalytic cysteines with chemically tuned electrophiles. *Nature Chemical Biology*, *8*(5), 471–476. https://doi.org/10.1038/nchembio.925

Sharma, M., Choudhury, H., Roy, R., Michaels, S. A., Ojo, K. K., & Bansal, A. (2021). CDPKs: The critical decoders of calcium signal at various stages of malaria

parasite development. *Computational and Structural Biotechnology Journal*, *19*, 5092–5107. https://doi.org/10.1016/j.csbj.2021.08.054

Sherling, E. S., Perrin, A. J., Knuepfer, E., Russell, M. R. G., Collinson, L. M., Miller, L. H., & Blackman, M. J. (2019). The Plasmodium falciparum rhoptry bulb protein RAMA plays an essential role in rhoptry neck morphogenesis and host red blood cell invasion. *PLOS Pathogens*, *15*(9), e1008049. https://doi.org/10.1371/journal.ppat.1008049

Siddiqui, F. A., Liang, X., & Cui, L. (2021). Plasmodium falciparum resistance to ACTs: Emergence, mechanisms, and outlook. *International Journal for Parasitology: Drugs and Drug Resistance*, *16*, 102–118. https://doi.org/10.1016/j.ijpddr.2021.05.007

Simoiu, M., Codreanu, R., Corlatescu, A.-D., Pauna, A. M., & Cilievici, S. E. (2023). Camillo Golgi's Impact on Malaria Studies. *Cells*, *12*(17), 2156. https://doi.org/10.3390/cells12172156

Singh, B., Sung, L. K., Matusop, A., Radhakrishnan, A., Shamsul, S. S., Cox-Singh, J., Thomas, A., & Conway, D. J. (2004). A large focus of naturally acquired Plasmodium knowlesi infections in human beings. *The Lancet*, *363*(9414), 1017–1024. https://doi.org/10.1016/S0140-6736(04)15836-4

Singh, N., Vayer, P., Tanwar, S., Poyet, J.-L., Tsaioun, K., & Villoutreix, B. O. (2023). Drug discovery and development: introduction to the general public and patient groups. *Frontiers in Drug Discovery*, *3*. https://doi.org/10.3389/fddsv.2023.1201419

Sinka, M. E., Bangs, M. J., Manguin, S., Rubio-Palis, Y., Chareonviriyaphap, T., Coetzee, M., Mbogo, C. M., Hemingway, J., Patil, A. P., Temperley, W. H., Gething, P. W., Kabaria, C. W., Burkot, T. R., Harbach, R. E., & Hay, S. I. (2012). A global map of dominant malaria vectors. *Parasites & Vectors*, *5*(1), 69. https://doi.org/10.1186/1756-3305-5-69

Siqueira-Neto, J. L., Wicht, K. J., Chibale, K., Burrows, J. N., Fidock, D. A., & Winzeler, E. A. (2023). Antimalarial drug discovery: progress and approaches. *Nature Reviews Drug Discovery*, *22*(10), 807–826. https://doi.org/10.1038/s41573-023-00772-9

Smith, R. C., & Barillas-Mury, C. (2016). Plasmodium Oocysts: Overlooked Targets of Mosquito Immunity. *Trends in Parasitology*, *32*(12), 979–990. https://doi.org/10.1016/j.pt.2016.08.012

Solyakov, L., Halbert, J., Alam, M. M., Semblat, J.-P., Dorin-Semblat, D., Reininger, L., Bottrill, A. R., Mistry, S., Abdi, A., Fennell, C., Holland, Z., Demarta, C., Bouza, Y., Sicard, A., Nivez, M.-P., Eschenlauer, S., Lama, T., Thomas, D. C., Sharma, P., … Doerig, C. (2011). Global kinomic and phospho-proteomic analyses of the human malaria parasite Plasmodium falciparum. *Nature Communications*, *2*(1), 565. https://doi.org/10.1038/ncomms1558

Song, M., Pang, L., Zhang, M., Qu, Y., Laster, K. V., & Dong, Z. (2023). Cdc2-like kinases: structure, biological function, and therapeutic targets for diseases. *Signal Transduction and Targeted Therapy*, *8*(1), 148. https://doi.org/10.1038/s41392-023-01409-4

Stanford, S. M., & Bottini, N. (2023). Targeting protein phosphatases in cancer immunotherapy and autoimmune disorders. *Nature Reviews Drug Discovery*, *22*(4), 273–294. https://doi.org/10.1038/s41573-022-00618-w

Stephenson, E. H., & Higgins, J. M. G. (2023). Pharmacological approaches to understanding protein kinase signaling networks. *Frontiers in Pharmacology*, *14*. https://doi.org/10.3389/fphar.2023.1310135

Stroobants, A., Mervin, L. H., Engkvist, O., & Robb, G. R. (2023). An industrial evaluation of proteochemometric modelling: Predicting drug-target affinities for kinases. *Artificial Intelligence in the Life Sciences*, *4*, 100079. https://doi.org/10.1016/j.ailsci.2023.100079

Su, X.-Z., & Miller, L. H. (2015). The discovery of artemisinin and the Nobel Prize in Physiology or Medicine. *Science China Life Sciences*, *58*(11), 1175–1179. https://doi.org/10.1007/s11427-015-4948-7

Sun, D., Gao, W., Hu, H., & Zhou, S. (2022). Why 90% of clinical drug development fails and how to improve it? *Acta Pharmaceutica Sinica B*, *12*(7), 3049–3062. https://doi.org/10.1016/j.apsb.2022.02.002

Sun, M., Jin, Y., Zhang, Y., Gregorich, Z. R., Ren, J., Ge, Y., & Guo, W. (2022). SR Protein Kinases Regulate the Splicing of Cardiomyopathy-Relevant Genes via Phosphorylation of the RSRSP Stretch in RBM20. *Genes*, *13*(9), 1526. https://doi.org/10.3390/genes13091526

Sun, Q.-Z., Lin, G.-F., Li, L.-L., Jin, X.-T., Huang, L.-Y., Zhang, G., Yang, W., Chen, K., Xiang, R., Chen, C., Wei, Y.-Q., Lu, G.-W., & Yang, S.-Y. (2017). Discovery of Potent and Selective Inhibitors of Cdc2-Like Kinase 1 (CLK1) as a New Class of Autophagy Inducers. *Journal of Medicinal Chemistry*, *60*(14), 6337–6352. https://doi.org/10.1021/acs.jmedchem.7b00665

Suresh, N., & Haldar, K. (2018). Mechanisms of artemisinin resistance in Plasmodium falciparum malaria. *Current Opinion in Pharmacology*, *42*, 46–54. https://doi.org/10.1016/j.coph.2018.06.003

Tachibana, M., Ishino, T., Takashima, E., Tsuboi, T., & Torii, M. (2018). A male gametocyte osmiophilic body and microgamete surface protein of the rodent malaria parasite *Plasmodium yoelii* (PyMiGS) plays a critical role in male osmiophilic body formation and exflagellation. *Cellular Microbiology*, *20*(5), e12821. https://doi.org/10.1111/cmi.12821

Tadesse, F. G., Meerstein-Kessel, L., Gonçalves, B. P., Drakeley, C., Ranford-Cartwright, L., & Bousema, T. (2019). Gametocyte Sex Ratio: The Key to

Understanding Plasmodium falciparum Transmission? *Trends in Parasitology*, *35*(3), 226–238. https://doi.org/10.1016/j.pt.2018.12.001

Takashima, E., Otsuki, H., Morita, M., Ito, D., Nagaoka, H., Yuguchi, T., Hassan, I., & Tsuboi, T. (2024). The Need for Novel Asexual Blood-Stage Malaria Vaccine Candidates for Plasmodium falciparum. *Biomolecules*, *14*(1), 100. https://doi.org/10.3390/biom14010100

Takken, W. (2021). The mosquito and malaria. In *Mosquitopia* (pp. 109–122). Routledge. https://doi.org/10.4324/9781003056034-11

Tam, B. Y., Chiu, K., Chung, H., Bossard, C., Nguyen, J. D., Creger, E., Eastman, B. W., Mak, C. C., Ibanez, M., Ghias, A., Cahiwat, J., Do, L., Cho, S., Nguyen, J., Deshmukh, V., Stewart, J., Chen, C.-W., Barroga, C., Dellamary, L., … Yazici, Y. (2020). The CLK inhibitor SM08502 induces anti-tumor activity and reduces Wnt pathway gene expression in gastrointestinal cancer models. *Cancer Letters*, *473*, 186–197. https://doi.org/10.1016/j.canlet.2019.09.009

Tan, M. S. Y., & Blackman, M. J. (2021). Malaria parasite egress at a glance. *Journal of Cell Science*, *134*(5). https://doi.org/10.1242/jcs.257345

Taylor, A. R., Watson, J. A., Chu, C. S., Puaprasert, K., Duanguppama, J., Day, N. P. J., Nosten, F., Neafsey, D. E., Buckee, C. O., Imwong, M., & White, N. J. (2019). Resolving the cause of recurrent Plasmodium vivax malaria probabilistically. *Nature Communications*, *10*(1), 5595. https://doi.org/10.1038/s41467-019-13412-x

Thomas, J. A., Tan, M. S. Y., Bisson, C., Borg, A., Umrekar, T. R., Hackett, F., Hale, V. L., Vizcay-Barrena, G., Fleck, R. A., Snijders, A. P., Saibil, H. R., & Blackman, M. J. (2018). A protease cascade regulates release of the human malaria parasite Plasmodium falciparum from host red blood cells. *Nature Microbiology*, *3*(4), 447–455. https://doi.org/10.1038/s41564-018-0111-0

Thriemer, K., Hong, N. Van, Rosanas-Urgell, A., Phuc, B. Q., Ha, D. M., Pockele, E., Guetens, P., Van, N. Van, Duong, T. T., Amambua-Ngwa, A., D'Alessandro, U., & Erhart, A. (2014). Delayed Parasite Clearance after Treatment with Dihydroartemisinin-Piperaquine in Plasmodium falciparum Malaria Patients in Central Vietnam. *Antimicrobial Agents and Chemotherapy*, *58*(12), 7049–7055. https://doi.org/10.1128/AAC.02746-14

Tizifa, T. A., Kabaghe, A. N., McCann, R. S., van den Berg, H., Van Vugt, M., & Phiri, K. S. (2018). Prevention Efforts for Malaria. *Current Tropical Medicine Reports*, *5*(1), 41–50. https://doi.org/10.1007/s40475-018-0133-y

Tomlinson, L. J., Batchelor, M., Sarsby, J., Byrne, D. P., Brownridge, P. J., Bayliss, R., Eyers, P. A., & Eyers, C. E. (2022). Exploring the Conformational Landscape and Stability of Aurora A Using Ion-Mobility Mass Spectrometry and Molecular Modeling. *Journal of the American Society for Mass Spectrometry*, *33*(3), 420–435. https://doi.org/10.1021/jasms.1c00271

Tse, E. G., Korsik, M., & Todd, M. H. (2019). The past, present and future of anti-malarial medicines. *Malaria Journal*, *18*(1), 93. https://doi.org/10.1186/s12936-019-2724-z

Turnham, R. E., & Scott, J. D. (2016). Protein kinase A catalytic subunit isoform PRKACA; History, function and physiology. *Gene*, *577*(2), 101–108. https://doi.org/10.1016/j.gene.2015.11.052

Tusting, L. S., Bousema, T., Smith, D. L., & Drakeley, C. (2014). *Measuring Changes in Plasmodium falciparum Transmission* (pp. 151–208). https://doi.org/10.1016/B978-0-12-800099-1.00003-X

Umumararungu, T., Nkuranga, J. B., Habarurema, G., Nyandwi, J. B., Mukazayire, M. J., Mukiza, J., Muganga, R., Hahirwa, I., Mpenda, M., Katembezi, A. N., Olawode, E. O., Kayitare, E., & Kayumba, P. C. (2023). Recent developments in antimalarial drug discovery. *Bioorganic & Medicinal Chemistry*, *88–89*, 117339. https://doi.org/10.1016/j.bmc.2023.117339

Usui, M., & Williamson, K. C. (2021). Stressed Out About Plasmodium falciparum Gametocytogenesis. *Frontiers in Cellular and Infection Microbiology*, *11*. https://doi.org/10.3389/fcimb.2021.790067

van de Straat, B., Russell, T. L., Staunton, K. M., Sinka, M. E., & Burkot, T. R. (2021). A global assessment of surveillance methods for dominant malaria vectors. *Scientific Reports*, *11*(1), 15337. https://doi.org/10.1038/s41598-021-94656-w

Vantaux, A., Péneau, J., Cooper, C. A., Kyle, D. E., Witkowski, B., & Maher, S. P. (2022). Liver-stage fate determination in Plasmodium vivax parasites: Characterization of schizont growth and hypnozoite fating from patient isolates. *Frontiers in Microbiology*, *13*. https://doi.org/10.3389/fmicb.2022.976606

Vasta, J. D., Corona, C. R., Wilkinson, J., Zimprich, C. A., Hartnett, J. R., Ingold, M. R., Zimmerman, K., Machleidt, T., Kirkland, T. A., Huwiler, K. G., Ohana, R. F., Slater, M., Otto, P., Cong, M., Wells, C. I., Berger, B.-T., Hanke, T., Glas, C., Ding, K., … Robers, M. B. (2018). Quantitative, Wide-Spectrum Kinase Profiling in Live Cells for Assessing the Effect of Cellular ATP on Target Engagement. *Cell Chemical Biology*, *25*(2), 206-214.e11. https://doi.org/10.1016/j.chembiol.2017.10.010

Venugopal, K., Hentzschel, F., Valkiūnas, G., & Marti, M. (2020). Plasmodium asexual growth and sexual development in the haematopoietic niche of the host. *Nature Reviews Microbiology*, *18*(3), 177–189. https://doi.org/10.1038/s41579-019-0306-2

Vieth, M., Higgs, R. E., Robertson, D. H., Shapiro, M., Gragg, E. A., & Hemmerle, H. (2004). Kinomics—structural biology and chemogenomics of kinase inhibitors and targets. *Biochimica et Biophysica Acta (BBA) - Proteins and Proteomics*, *1697*(1–2), 243–257. https://doi.org/10.1016/j.bbapap.2003.11.028

Vijayan, R. S. K., He, P., Modi, V., Duong-Ly, K. C., Ma, H., Peterson, J. R., Dunbrack, R. L., & Levy, R. M. (2015). Conformational Analysis of the DFG-Out Kinase Motif and Biochemical Profiling of Structurally Validated Type II Inhibitors. *Journal of Medicinal Chemistry*, *58*(1), 466–479. https://doi.org/10.1021/jm501603h

Vlachou, D., Schlegelmilch, T., Runn, E., Mendes, A., & Kafatos, F. C. (2006). The developmental migration of Plasmodium in mosquitoes. *Current Opinion in Genetics & Development*, *16*(4), 384–391. https://doi.org/10.1016/j.gde.2006.06.012

Wall, R. J., Ferguson, D. J. P., Freville, A., Franke-Fayard, B., Brady, D., Zeeshan, M., Bottrill, A. R., Wheatley, S., Fry, A. M., Janse, C. J., Yamano, H., Holder, A. A., Guttery, D. S., & Tewari, R. (2018). Plasmodium APC3 mediates chromosome condensation and cytokinesis during atypical mitosis in male gametogenesis. *Scientific Reports*, *8*(1), 5610. https://doi.org/10.1038/s41598-018-23871-9

Walz, A., Duffey, M., Aljayyoussi, G., Sax, S., Leroy, D., Besson, D., Burrows, J. N., Cherkaoui-Rbati, M. H., Gobeau, N., Westwood, M.-A., Siethoff, C., Gamo, F.-J., Mäser, P., & Wittlin, S. (2023). The Parasite Reduction Ratio (PRR) Assay Version 2: Standardized Assessment of Plasmodium falciparum Viability after Antimalarial Treatment In Vitro. *Pharmaceuticals*, *16*(2), 163. https://doi.org/10.3390/ph16020163

Wan, L., Deng, M., & Zhang, H. (2022). SR Splicing Factors Promote Cancer via Multiple Regulatory Mechanisms. *Genes*, *13*(9), 1659. https://doi.org/10.3390/genes13091659

Wan, R., Yan, C., Bai, R., Wang, L., Huang, M., Wong, C. C. L., & Shi, Y. (2016). The 3.8 Å structure of the U4/U6.U5 tri-snRNP: Insights into spliceosome assembly and catalysis. *Science*, *351*(6272), 466–475. https://doi.org/10.1126/science.aad6466

Ward, P., Equinet, L., Packer, J., & Doerig, C. (2004). Protein kinases of the human malaria parasite Plasmodium falciparum: the kinome of a divergent eukaryote. *BMC Genomics*, *5*(1), 79. https://doi.org/10.1186/1471-2164-5-79

Weiss, D. J., Lucas, T. C. D., Nguyen, M., Nandi, A. K., Bisanzio, D., Battle, K. E., Cameron, E., Twohig, K. A., Pfeffer, D. A., Rozier, J. A., Gibson, H. S., Rao, P. C., Casey, D., Bertozzi-Villa, A., Collins, E. L., Dalrymple, U., Gray, N., Harris, J. R., Howes, R. E., … Gething, P. W. (2019). Mapping the global prevalence, incidence, and mortality of Plasmodium falciparum, 2000–17: a spatial and temporal modelling study. *The Lancet*, *394*(10195), 322–331. https://doi.org/10.1016/S0140-6736(19)31097-9

WHO. (2020). *Global vector control response: progress in planning and implementation*.

Wilder, B. K., Vigdorovich, V., Carbonetti, S., Minkah, N., Hertoghs, N., Raappana, A., Cardamone, H., Oliver, B. G., Trakhimets, O., Kumar, S., Dambrauskas, N.,

Arredondo, S. A., Camargo, N., Seilie, A. M., Murphy, S. C., Kappe, S. H. I., & Sather, D. N. (2022). Anti-TRAP/SSP2 monoclonal antibodies can inhibit sporozoite infection and may enhance protection of anti-CSP monoclonal antibodies. *Npj Vaccines*, *7*(1), 58. https://doi.org/10.1038/s41541-022-00480-2

Woodrow, C. J., & White, N. J. (2017). The clinical impact of artemisinin resistance in Southeast Asia and the potential for future spread. *FEMS Microbiology Reviews*, *41*(1), 34–48. https://doi.org/10.1093/femsre/fuw037

World Health Organization. (2024). *World malaria report 2024: addressing inequity in the global malaria response*.

World Health Organization; 2017. (2017). *Global vector control response 2017–2030*.

Xu, Z., Zhou, H., Li, L., Chen, Z., Zhang, X., Feng, Y., Wang, J., Li, Y., & Wu, Y. (2024). Immunoassay System Based on the Technology of Time-Resolved Fluorescence Resonance Energy Transfer. *Sensors*, *24*(5), 1430. https://doi.org/10.3390/s24051430

Yadav, J., El Hassani, M., Sodhi, J., Lauschke, V. M., Hartman, J. H., & Russell, L. E. (2021). Recent developments in *in vitro* and *in vivo* models for improved translation of preclinical pharmacokinetics and pharmacodynamics data. *Drug Metabolism Reviews*, *53*(2), 207–233. https://doi.org/10.1080/03602532.2021.1922435

Yang, M., Shang, X., Zhou, Y., Wang, C., Wei, G., Tang, J., Zhang, M., Liu, Y., Cao, J., & Zhang, Q. (2021). Full-Length Transcriptome Analysis of Plasmodium falciparum by Single-Molecule Long-Read Sequencing. *Frontiers in Cellular and Infection Microbiology*, *11*. https://doi.org/10.3389/fcimb.2021.631545

Yang, T., Ottilie, S., Istvan, E. S., Godinez-Macias, K. P., Lukens, A. K., Baragaña, B., Campo, B., Walpole, C., Niles, J. C., Chibale, K., Dechering, K. J., Llinás, M., Lee, M. C. S., Kato, N., Wyllie, S., McNamara, C. W., Gamo, F. J., Burrows, J., Fidock, D. A., … Winzeler, E. A. (2021). MalDA, Accelerating Malaria Drug Discovery. *Trends in Parasitology*, *37*(6), 493–507. https://doi.org/10.1016/j.pt.2021.01.009

Yee, D. A., Dean Bermond, C., Reyes-Torres, L. J., Fijman, N. S., Scavo, N. A., Nelsen, J., & Yee, S. H. (2022). Robust network stability of mosquitoes and human pathogens of medical importance. *Parasites & Vectors*, *15*(1), 216. https://doi.org/10.1186/s13071-022-05333-4

Yeoh, L. M., Lee, V. V., McFadden, G. I., & Ralph, S. A. (2019). Alternative Splicing in Apicomplexan Parasites. *MBio*, *10*(1). https://doi.org/10.1128/mBio.02866-18

Yoshimori, A., Miljković, F., & Bajorath, J. (2022). Approach for the Design of Covalent Protein Kinase Inhibitors via Focused Deep Generative Modeling. *Molecules*, *27*(2), 570. https://doi.org/10.3390/molecules27020570

Zaw, M. T., & Lin, Z. (2017). Two sympatric types of Plasmodium ovale and discrimination by molecular methods. *Journal of Microbiology, Immunology and Infection*, *50*(5), 559–564. https://doi.org/10.1016/j.jmii.2016.08.004

Zeeshan, M., Pandey, R., Ferguson, D. J. P., Tromer, E. C., Markus, R., Abel, S., Brady, D., Daniel, E., Limenitakis, R., Bottrill, A. R., Le Roch, K. G., Holder, A. A., Waller, R. F., Guttery, D. S., & Tewari, R. (2020). Real-time dynamics of *Plasmodium* NDC80 reveals unusual modes of chromosome segregation during parasite proliferation. *Journal of Cell Science*. https://doi.org/10.1242/jcs.245753

Zhan, X., Yan, C., Zhang, X., Lei, J., & Shi, Y. (2018). Structures of the human pre-catalytic spliceosome and its precursor spliceosome. *Cell Research*, *28*(12), 1129–1140. https://doi.org/10.1038/s41422-018-0094-7

Zhao, L., Pi, L., Qin, Y., Lu, Y., Zeng, W., Xiang, Z., Qin, P., Chen, X., Li, C., Zhang, Y., Wang, S., Si, Y., Yang, G., Rosenthal, B. M., Huang, Y., & Yang, Z. (2020). Widespread resistance mutations to sulfadoxine-pyrimethamine in malaria parasites imported to China from Central and Western Africa. *International Journal for Parasitology: Drugs and Drug Resistance*, *12*, 1–6. https://doi.org/10.1016/j.ijpddr.2019.11.002

Zheng, H., Lu, X., Li, K., Zhu, F., Zhao, C., Liu, T., Ding, Y., Fu, Y., Zhang, K., Zhou, T., Dai, J., Wu, Y., & Xu, W. (2022). ATG Ubiquitination Is Required for Circumsporozoite Protein to Subvert Host Innate Immunity Against Rodent Malaria Liver Stage. *Frontiers in Immunology*, *13*. https://doi.org/10.3389/fimmu.2022.815936

Zhong, L., Li, Y., Xiong, L., Wang, W., Wu, M., Yuan, T., Yang, W., Tian, C., Miao, Z., Wang, T., & Yang, S. (2021). Small molecules in targeted cancer therapy: advances, challenges, and future perspectives. *Signal Transduction and Targeted Therapy*, *6*(1), 201. https://doi.org/10.1038/s41392-021-00572-w

Zhou, Z., & Fu, X.-D. (2013). Regulation of splicing by SR proteins and SR protein-specific kinases. *Chromosoma*, *122*(3), 191–207. https://doi.org/10.1007/s00412-013-0407-z